

AD-A048 842

CALIFORNIA UNIV BERKELEY DEPT OF MECHANICAL ENGINEERING F/G 13/8
DUCTILE FRACTURE IN AXISYMMETRIC EXTRUSION AND DRAWING. PART 1.--ETC(U)
JUN 77 C C CHEN, S I OH, S KOBAYASHI F33615-75-C-5151

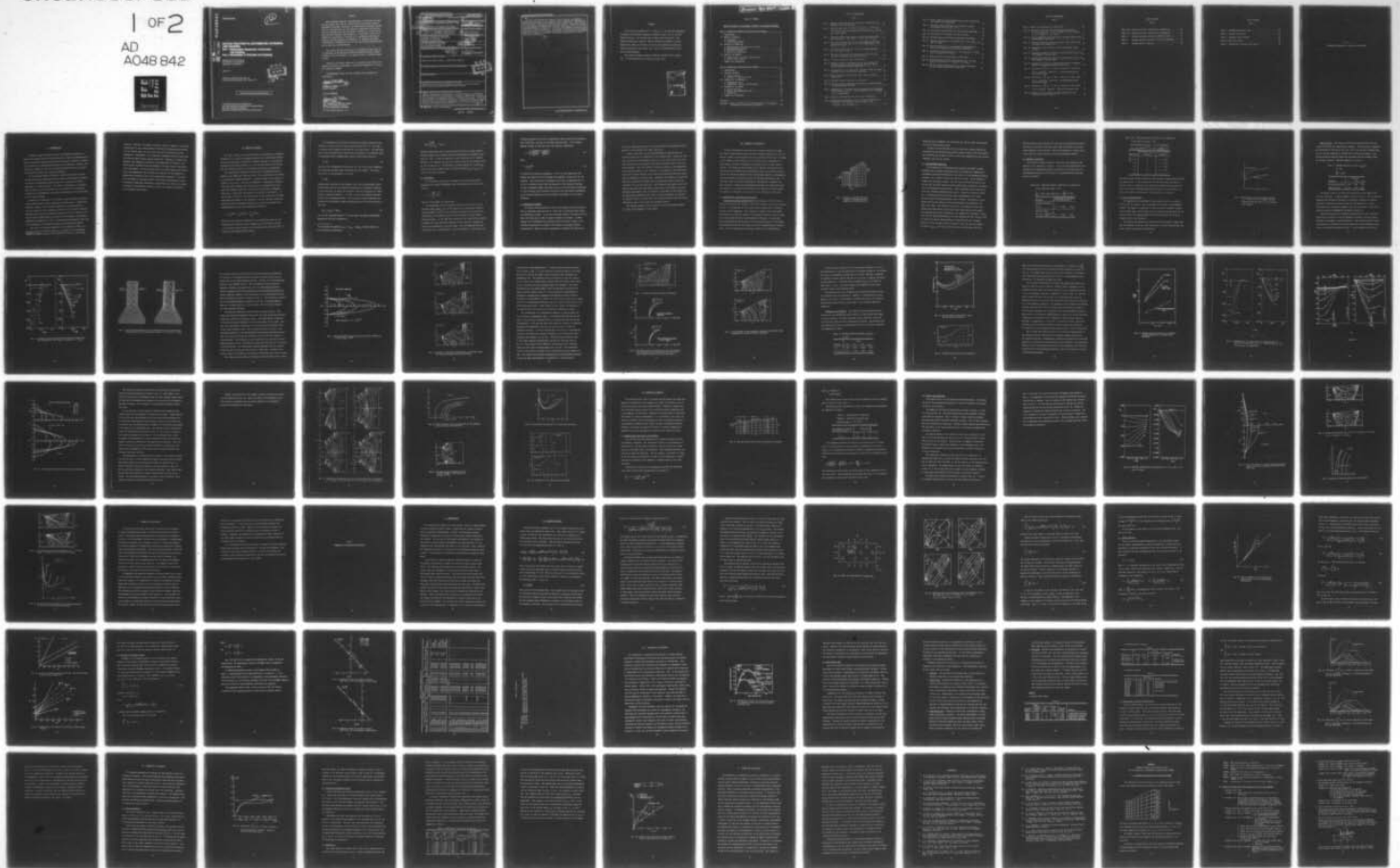
UNCLASSIFIED

AFML-TR-77-96

NL

1 of 2

AD
A048 842



AD A 0 48842

AFML-TR-77-96

12

AJ NO. _____
DDC FILE COPY

**DUCTILE FRACTURE IN AXISYMMETRIC EXTRUSION
AND DRAWING**

**Part 1 Deformation Mechanics of Extrusion
and Drawing**

Part 2 Workability in Extrusion and Drawing

*MECHANICAL ENGINEERING
UNIVERSITY OF CALIFORNIA
BERKELEY, CALIFORNIA*

JUNE 1977

TECHNICAL REPORT AFML-TR-77-96
Final Report for Period March 1976 - March 1977

DDC
JAN 18 1978
RESOLVED
F

Approved for public release; distribution unlimited.

AIR FORCE MATERIALS LABORATORY
AIR FORCE WRIGHT AERONAUTICAL LABORATORIES
AIR FORCE SYSTEMS COMMAND
WRIGHT-PATTERSON AIR FORCE BASE, OHIO 45433

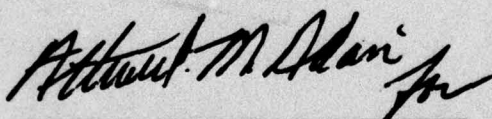
NOTICE

When government drawings, specifications, or other data are used for any purpose other than in connection with a definitely related government procurement operation, the United States government thereby incurs no responsibility nor any obligation whatsoever; and the fact that the government may have formulated, furnished, or in any way supplied the said drawings, specifications, or other data, is not to be regarded by implication or otherwise as in any manner licensing the holder or any other person or corporation, or conveying any rights or permission to manufacture, use, or sell any patented invention that may in any way be related thereto.

This report has been reviewed by the Information Office (IO) and is releasable to the National Technical Information Services (NTIS). At NTIS it will be available to the general public, including foreign nations.

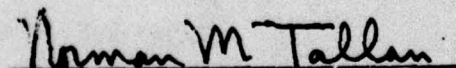
Copies of this report should not be returned unless return is required by security considerations, contractual obligations, or notice on a specific document.

This technical report has been reviewed and is approved for publication.



VINCENT De PIERRE
Project Engineer

FOR THE COMMANDER



NORMAN M. TALLAN
Chief, Processing and
High Temperature Materials Branch
Metals and Ceramics Division
Air Force Materials Laboratory

19 REPORT DOCUMENTATION PAGE		READ INSTRUCTIONS BEFORE COMPLETING FORM
18 1. REPORT NUMBER AFML-TR-77-96	2. GOVT ACCESSION NO.	9 3. RECIPIENT'S CATALOG NUMBER
6 4. TITLE (and Subtitle) DUCTILE FRACTURE IN AXISYMMETRIC EXTRUSION AND DRAWING. Part 1. Mechanics of Extrusion and Drawing Part 2. Workability in Extrusion and Drawing.		5. TYPE OF REPORT & PERIOD COVERED Final Report Mar 1976-Mar 1977
Information 7. AUTHOR(s) C. C./Chen, S. I./Oh and Shiro/Kobayashi		6. PERFORMING ORG. REPORT NUMBER
10 9. PERFORMING ORGANIZATION NAME AND ADDRESS Department of Mechanical Engineering University of California Berkeley, California 94720		8. CONTRACT OR GRANT NUMBER(s) F33615-75-C-5151 ✓
11. CONTROLLING OFFICE NAME AND ADDRESS Air Force Materials Laboratory Air Force Systems Command Wright-Patterson Air Force Base, Ohio 45433	11	10. PROGRAM ELEMENT, PROJECT, TASK AREA & WORK UNIT NUMBERS 62102F 7351 08-20 16 17
14. MONITORING AGENCY NAME & ADDRESS (if different from Controlling Office) 12 126p.		12. REPORT DATE June 1977
		13. NUMBER OF PAGES 115
		15. SECURITY CLASS. (of this report) Unclassified
		15a. DECLASSIFICATION/DOWNGRADING SCHEDULE
16. DISTRIBUTION STATEMENT (of this Report) Approved for public release: distribution unlimited.		
17. DISTRIBUTION STATEMENT (of the abstract entered in Block 20, if different from Report)		
18. SUPPLEMENTARY NOTES		
19. KEY WORDS (Continue on reverse side if necessary and identify by block number) Workability, fracture, plastic deformation processes, void growth, matrix method, extrusion, drawing, mechanics, central bursting		
20. ABSTRACT (Continue on reverse side if necessary and identify by block number) This investigation applies theories on flow and fracture in metalworking processes to prediction of workability of materials in axisymmetric bar extrusion and drawing, with special reference to central bursting. Part 1 deals with the determination of deformation mechanics in extrusion and drawing. The matrix method is used as the method of analysis and is shown to be an efficient numerical method which provides useful information on the detailed deformation characteristics for various process variables. (over)		

DDC
RESOLVED
JAN 18 1978
F

mt

In Part 2 the validity of a theory on ductile fracture was examined by experimental data found in the literature. Then, combining the formulation of fracture criteria with the deformation mechanics found in Part 1, the workability of materials in extrusion and drawing was determined. Workability in extrusion was examined for aluminum alloy 2024-T351, using data found in the literature, and experiments of workability in drawing were attempted for SAE 1144 cold-drawn steel to test the prediction. The results of validation were inconclusive. Conclusive validation of the present workability theory in extrusion and drawing awaits more extensive and systematic experimental investigations, as well as theoretical calculations.

D D C
RECEIVED
JAN 18 1964
F

FOREWORD

This report was prepared by C. C. Chen, S. I. Oh, and Shiro Kobayashi, University of California, Berkeley, California, under U.S.A.F. Contract F33615-75-C-5151. The contract was initiated under Project No. 7351, "Metallic Materials," Task No. 735108, "Processing of Metals," and was administered under the direction of the Air Force Materials Laboratory, Wright-Patterson Air Force Base, Ohio, with Mr. Vincent DePierre as Air Force Project Engineer.

This report discusses research conducted from March 1976 to March 1977. It was submitted by the authors in April 1977.

ACCESSION for	
N+PS	White Section <input checked="" type="checkbox"/>
DOC	B.l.f Section <input type="checkbox"/>
UNANNOUNCED	<input type="checkbox"/>
J. S. T. I. C. A. T. I. O. N	
BY	
DISTRIBUTION/AVAILABILITY CODES	
SPECIAL	
A	

TABLE OF CONTENTS

DUCTILE FRACTURE IN AXISYMMETRIC EXTRUSION AND DRAWING PROCESSES

Part 1 Deformation Mechanics of Extrusion and Drawing

I	INTRODUCTION.	2
II	METHOD OF ANALYSIS.	4
	A. Convergence.	6
	B. Rigid-body treatment	7
III	ANALYSIS OF EXTRUSION	9
	A. Computational conditions and procedures.	9
	B. Work-hardening material	11
	C. Extrusion condition.	12
	D. Results and discussion	13
IV	ANALYSIS OF DRAWING	36
	A. Computational conditions and procedures.	36
	B. Results and discussion	39
V	SUMMARY AND CONCLUSIONS	45

Part 2 Workability in Extrusion and Drawing

I	INTRODUCTION.	48
II	FRACTURE CRITERIA	49
	A. Surface fracture	55
	B. Fracture in uniaxial tension	59
III	WORKABILITY IN EXTRUSION.	64
	A. Experimental data.	66
	B. Computation, results, and discussion	69
IV	WORKABILITY IN DRAWING.	73
	A. Process mechanics.	73
	B. Tension and compression tests.	75
	C. Workability.	75
V	SUMMARY AND DISCUSSION.	79

References	81
----------------------	----

Appendix: Computer Program of the Matrix Method for the Analysis of Axisymmetric Extrusion and Drawing	83
---	----

LIST OF ILLUSTRATIONS

Part 1

Fig. 1	Boundary conditions and mesh system for steady-state axisymmetric extrusion analysis.	10
Fig. 2	Stress-strain curves for SAE 1112 steel ($Y_0 = 79,800$ psi; 550.21 MN/m^2) and for aluminum alloy 2024-T351 ($Y_0 = 47,778$ psi; 329.42 MN/m^2).	14
Fig. 3	Computed velocity distributions for SAE 1112 steel under the conditions $\alpha = 30^\circ$, $R_i/R_0 = 2.366$, and $f = 0.2Y_0$	16
Fig. 4	Grid distortion patterns for non-work-hardening and work-hardening materials with (a) die frictional stress $f = 0$, and (b) $f = 0.4Y_0$	17
Fig. 5	Total grid distortions for various friction conditions; $\alpha = 30^\circ$, $R_i/R_0 = 2.366$	19
Fig. 6	Effective strain-rate distributions for SAE 1112 steel for various interface friction conditions	20
Fig. 7	A typical effective strain distribution	22
Fig. 8	Effective strain distributions at the exit sections for work-hardening and non-work-hardening materials under various interface friction conditions	22
Fig. 9	Distributions of the hydrostatic pressure in SAE 1112 steel extrusion for the two friction conditions	23
Fig. 10	The die pressure distributions under various friction conditions.	25
Fig. 11	Principal stress directions in extrusion.	25
Fig. 12	Average extrusion pressures as functions of area reduction for aluminum alloy 2024-T351.	27
Fig. 13	Comparison of (a) computer and (b) experimental [11] velocity distributions; $R_i/R_0 = 2$, semi-die angle $\alpha = 45^\circ$ (frictionless in computation).	28
Fig. 14	Total grid distortions for various area reductions.	30
Fig. 15	Strain-rate distributions for two friction conditions at reductions of (a) $R_i/R_0 = 1.25$, (b) $R_i/R_0 = 1.6$, (c) $R_i/R_0 = 1.8$, (d) $R_i/R_0 = 2$	33

Fig. 16	Total effective strain distributions in the extruded bar for various area reductions.	34
Fig. 17	The mean stress distribution in extrusion through a frictionless die at $R_1/R_0 = 1.25$	34
Fig. 18	Die pressure distributions for various area reductions	35
Fig. 19	Directions of the largest principal stresses	35
Fig. 20	The mesh system and boundary conditions for drawing.	37
Fig. 21	Velocity distributions in drawing with $\alpha = 6^\circ$, $R_1/R_0 = 1.2$ and $f = 0.25Y_0$	41
Fig. 22	Total distortion of a line originally perpendicular to the axis of drawing for various area reductions.	42
Fig. 23	Strain-rate distributions for $\alpha = 6^\circ$ and $R_1/R_0 = 1.2$ with (a) $f = 0$ and (b) $f = 0.25Y_0$	43
Fig. 24	Effective strain distributions in drawn bars	43
Fig. 25	The hydrostatic pressure distributions for $\alpha = 6^\circ$ and $R_1/R_0 = 1.2$ with (a) $f = 0$ and (b) $f = 0.25Y_0$	44
Fig. 26	The die pressure distributions for various reductions and for the two die-friction conditions.	44

LIST OF ILLUSTRATIONS

Part 2

Fig. 27 Model for distribution of large voids. 52

Fig. 28 Effective stress and effective strain distributions
in the unit section. (a) $e_2 = 0.00525$; (b) $e_2 = 0.0423$;
(c) $e_2 = 0.0699$; (d) $e_2 = 0.1163$ 53

Fig. 29 Plot of hyperbolic sine function for various values of the
work-hardening coefficient 56

Fig. 30 Fracture conditions predicted from Eqs. (20) and (21) and
by Cockroft and Latham [16]. 58

Fig. 31 Comparison of two fracture criteria for various values
of $\sigma_e/\bar{\sigma}$ 58

Fig. 32 Comparison between the fracture criterion given by Eq. (23)
and Bridgman's fracture data 61

Fig. 33 Comparison between the fracture criterion given by Eq. (24)
and Bridgman's fracture data 61

Fig. 34 Workability criteria for center burst based on a maximum
tensile stress-strain energy criterion [23]. 65

Fig. 35 Variations of $\int_0^{\bar{E}} (F_1 + 1) d\bar{E}$ as a function of area reduc-
tion in extrusion. Materials: non-work-hardening and
al alloy 2024-T351 71

Fig. 36 Variations of $\int_0^{\bar{E}} (F_2 + 1) d\bar{E}$ as a function of area reduc-
tion in extrusion. Materials: non-work-hardening and
al alloy 2024-T351 71

Fig. 37 Variations of $\int_0^{\bar{E}} (F_2 + 1) d\bar{E}$ as a function of area reduc-
tion in drawing. Material: SAE 1144 cold-drawn steel . . 74

Fig. 38 Computed and experimental average drawing stress as
functions of area reduction. 78

LIST OF TABLES

Part 1

Table 1(a)	Extrusion process conditions for computation.	12
Table 1(b)	Extrusion process conditions for computation.	13
Table 2	Average extrusion pressure for SAE 1112 steel	15
Table 3	Average extrusion pressure for al alloy 2024-T351	24
Table 4	Drawing process conditions.	38

LIST OF TABLES

Part 2

Table 5	Bridgman experimental data.	62
Table 6	Tension test results.	68
Table 7	Compression test results.	69
Table 8	Extrusion results	69
Table 9	Experimental conditions and results	76

In order to apply successfully to metalworking processes, we must first establish the and theoretical theories. Then, by conducting the detailed information on mechanics and the ductile fracture criterion, workability of materials in metalworking processes can be predicted. Based on this prediction, workability control for preventing fracture can be achieved.

Part 1

DEFORMATION MECHANICS OF EXTRUSION AND DRAWING

In the previous report [1], theories on flow and fracture in metalworking processes were developed with an emphasis on applying the workability theory to metalworking processes where the occurrence of fracture is concerned. The present investigation is concerned with the application of these theories to the prediction of workability of materials in extrusion and drawing, with special reference to cold-chamber die casting.

Workability of materials in the extent to which materials can deform without forming cracks during mechanical working processes, workability, therefore, depends on the conditions imposed by the working process. Critical stress and strain conditions involved in the mechanical working processes must be known and should be specified in terms of process variables, such as strain rate, friction at the interface, and workpiece geometry and dimensions. Part I of the present investigation deals with the description of deformation mechanics in extrusion and drawing.

The role of the detailed mechanics in the workability theory is to provide the stress and strain paths at a critical site of a deforming workpiece in practice refer to the references at the end of this report.

I. INTRODUCTION

In order to apply workability theory to metalworking processes, we must first establish flow and fracture theories. Then, by combining the detailed information on mechanics and the ductile fracture criterion, workability of materials in metalworking processes can be predicted. Based on this prediction, workability control for preventing fracturing can be achieved by selecting the proper set of process parameters.

In the previous report [1]*, theories on flow and fracture in metalworking processes were developed with an emphasis on applying the workability theory to metalworking processes where the occurrence of internal fracturing is a limiting factor. The present investigation is concerned with the application of these theories to the prediction of workability of materials in axisymmetric bar extrusion and drawing, with special reference to center bursting.

Workability of materials is the extent to which materials can deform without forming cracks during a mechanical working process. Workability, therefore, depends on the conditions imposed by the working process. Critical stress and strain conditions involved in the mechanical working processes must be known and should be specified in terms of process variables, such as height reduction, friction at the interface, and workpiece geometries and dimensions. Part I of the present investigation deals with the determination of deformation mechanics in extrusion and drawing.

The role of the detailed mechanics in the workability study is to provide the stress and strain paths at a critical site of a deforming

*Numbers in brackets refer to the references at the end of this report.

material. Therefore, the method of analysis should be capable of accurately determining not only overall quantities involved in metalworking processes, such as forming loads, but also stress and strain distributions during deformation. Furthermore, it is required to determine the stress and strain distributions under various process conditions. Therefore, to justify the approach, the computation involved in the method must be efficient. The matrix method developed by Lee and Kobayashi [2] comes close to fulfilling these requirements. In the previous report, this matrix method was refined and it was demonstrated that the method is effective for the analysis of steady-state processes as well as non-steady-state processes. In the present investigation, the matrix method, with further improvements, is used to determine steady-state deformation characteristics as functions of material property, die-workpiece interface friction, die angle, and reduction in bar extrusion and drawing.

II. METHOD OF ANALYSIS

The basic concepts of the matrix method for rigid-plastic deformation problems are the use of the Lagrange multiplier in a variational formulation and linearization of nonlinear stiffness equations. In the present formulation the dynamic effects, i.e., the inertia effects on the forces and the strain-rate effects on the material properties, are neglected.

For rigid-plastic materials the condition of incompressibility is imposed on the admissible velocity fields. This constraint can be removed by introducing a Lagrange multiplier. Consider a body V whose surface S , consists of S_U and S_T . The body is composed of a rigid-plastic material that obeys the von Mises yield criterion and its associated flow rule, under the boundary conditions, such that the entire body is deforming plastically. Body forces are assumed to be absent in the region V . It can be shown [3] that for the actual solution, the functional (1) becomes stationary with respect to the multiplier λ and the velocity fields that satisfy the velocity boundary conditions on S_U but not necessarily the incompressibility condition (kinematically complete):

$$\Phi = \int_V \bar{\sigma} \dot{\bar{\epsilon}} \, dV + \int_V \lambda \underline{C}^T \dot{\bar{\epsilon}} \, dV - \int_{S_T} \underline{T}^T \underline{U} \, dS, \quad (1)$$

where $\dot{\bar{\epsilon}}$ is the effective strain-rate; $\bar{\sigma}$, the effective stress; \underline{T} , the traction vector specified on the boundary S_T ; \underline{U} , the velocity vector; \underline{C} is the proper vector notation of the Kronecker delta such that $\underline{C}^T \dot{\bar{\epsilon}} = 0$ implies the incompressibility condition.

The formulation of the discrete variational problem follows the same procedure as that used in the finite-element method [4], [5]. The body V is divided into M elements interconnected at N nodal points. The approximation of the functional Φ by a function $\tilde{\phi}$ is performed on the elemental level by replacing U with a kinematically complete distribution, given by

$$\underline{U} \approx \underline{G}u, \quad (2)$$

where \underline{G} is the interpolation function and u is the vector whose components are velocities at nodal points associated with the element. The strain-rate vector is then derivable in the form

$$\dot{\underline{\epsilon}} = \underline{B}u. \quad (3)$$

Assembling the function at the elemental level into an approximate finite-element model over all the elements and applying the stationary condition to the function $\tilde{\phi}$, we obtain the stiffness relations consisting of a large system of nonlinear equations. In order to solve the stiffness equations, we adopt the following procedure. The nonlinear stiffness equations were linearized by considering a small perturbation Δu in the velocity vector u , such that

$$u_{(n)} = u_{(n-1)} + \Delta u_{(n)}, \quad (4)$$

for the n -th iteration process.[†] We then obtain the global perturbation equation for the n -th iteration as

[†]In the actual calculations, $u_{(n)} = u_{(n-1)} + \alpha \Delta u_{(n)}$ is used, where α is the deceleration coefficient.

$$\underline{S}_{(n-1)} \left\{ \frac{\Delta u}{\lambda} \right\}_{(n)} = \underline{R}_{(n-1)}. \quad (5)$$

Specific formulations for the matrix \underline{S} and the vector \underline{R} , using a quadrilateral element with a bilinear velocity distribution, are presented elsewhere [1], [6]. It must be noted that, since the method is an iterative process, it is necessary to provide an initial guess for the velocity field u_0 (but no need for λ). The solution of linear equation (5) yields $\Delta u_{(n)}$ close to zero and a proper value of the mean stresses $\lambda_{(n)}$, if $u_{(n-1)}$ is close to the actual solution.

A. Convergence

In the previous studies the convergence of the solution has been measured by the quantity $\|\Delta u\|/\|u\|$, where the Euclidean vector norm is defined by

$$u = \sqrt{\sum_{i=1}^N |u_i|^2}, \quad (6)$$

where N = total number of nodal points.

The convergence criterion requires that the error norm at the n -th iteration ($\|\Delta u_{(n)}\|/\|u_{(n-1)}\|$) be less than that at the previous iteration. This convergence criterion, with suitable selections of the deceleration coefficient α , has worked out well for the solutions of various metal-working problems. At the same time, however, it was realized that solution divergence has been indicated according to this criterion, although the solution was converging in its true sense. This can apparently be seen, particularly for a function which is not well behaved. In this case, the

criterion resulted in the use of unnecessarily small values of the deceleration coefficient, and thus in increased computing time. In the present program, instead of the error norm, the quantity f defined by

$$f = \sqrt{\sum_m \left\{ \left(\frac{\partial \tilde{\phi}^{(m)}}{\partial u^{(m)}} \right)^2 + \left(\frac{\partial \tilde{\phi}^{(m)}}{\partial \lambda^{(m)}} \right)^2 \right\}} \quad (7)$$

where

$$\phi \cong \sum_m \tilde{\phi}^{(m)} \quad (8)$$

is utilized for solution convergence. In Eq. (7), the superscript (m) denotes the values of the m -th element and summation is made over all the elements. The criterion for convergence now is that the magnitude of f at the n -th iteration be less than the magnitude at the previous iteration. In this convergence scheme, the proper value of the deceleration coefficient at each iteration can be selected efficiently from the previous information on the function behavior and the convergence requirement at the current iteration.

B. Rigid-body treatment

The matrix method described in this section applies only if the entire body is deforming plastically and no rigid zone or unloading exists during the deformation process. In practical problems, however, situations do arise where the rigid zone as well as rigid unloading are involved. If these regions of no deformation are contained within the control volume V , the extremum principles do not apply to the problem of obtaining internal distributions. There are several approaches to handling this difficulty,

but a most effective technique is one which involves the approximate determination of the boundary of a nearly rigid zone.

A nearly rigid zone can be characterized by its very low value of effective strain rate in comparison to the deforming body. During the iteration process for an incremental solution over the entire body, the effective strain-rate in the possible rigid region approaches zero as the solution converges. Since the effective strain-rate appears in the denominator of the stiffness matrix S , the component of the normalized stiffness matrix will tend to become infinity if the nodal point associated with this component is contained in the rigid zone. Therefore, the elements for which the effective strain-rate is smaller than a certain value (say, 0.0001) are considered to be in the rigid zone. The effective strain-rates of the elements lying inside the rigid zone are then kept at this value in the perturbation relationship, and the iteration is continued for the solution in the plastically deforming region until a desired convergence is achieved. It should be noted, of course, that the converged solution gives the stress distribution only in the plastically deforming region.

The complete program of this improved version of the matrix method is listed in the appendix of this report.

III. ANALYSIS OF EXTRUSION

Several investigators have analyzed the extrusion process by using the finite-element method, mostly by elastic-plastic analysis [7], [8], [9]. However, almost all the analyses have been performed for the case of loading of the workpiece that fits the die and container and of extruding it a small amount, instead of extruding the workpiece until a steady state is reached. The exceptions are the work by Lee, Mallett, and Yang [10] for the plane-strain extrusion with frictionless curved dies using the elastic-plastic finite-element method and the rigid-plastic analysis of axisymmetric extrusion through frictionless conical dies by Shah and Kobayashi [6]. In the latter work, the authors investigated a possibility of applying the matrix method to steady-state metalworking processes and demonstrated that the analysis of a steady-state extrusion can be made by the matrix method. The analysis of extrusion in this section is an extension of this work.

A. Computational conditions and procedures

Boundary conditions and mesh system The boundary conditions and the mesh system used for the analysis of extrusion through conical dies are shown in Fig. 1. The material in the container moves axially with the uniform velocity of unit magnitude. The container is assumed to be frictionless, and along the conical die surfaces, the tangential traction, which is equal to the frictional stress at the die-workpiece interface, is prescribed. The extruded material moves axially with the uniform velocity of the magnitude determined from the area reduction and the incompressibility relationship. Also, no traction acts along the surfaces of the extruded part.

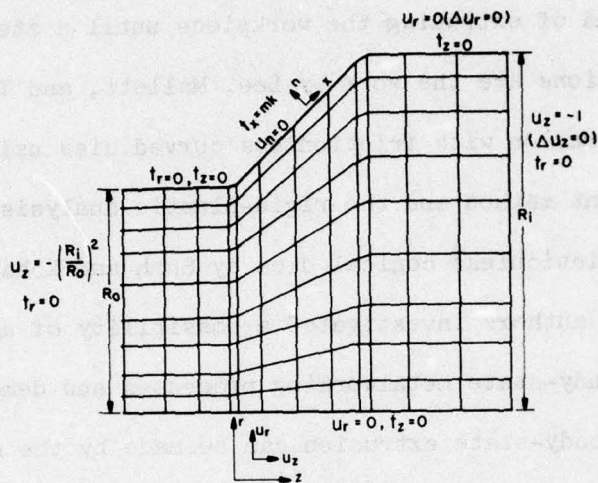


Fig. 1 Boundary conditions and mesh system for steady-state axisymmetric extrusion analysis.

Along the axis of symmetry, the conditions are that the shear traction and the radial velocity must vanish.

It must be noted here that the die corners were slightly modified by connecting the two material nodal points located closest to the die corners. This modification was made in order to avoid high singularity of the velocity components near the die corners.

B. Work-hardening materials

In the analysis of a non-steady-state process, the effect of work-hardening can be readily incorporated into the analysis by computing the incremental strains and modifying the flow stress at each deformation step according to the increase in the total effective strain. In the analysis of steady-state processes, however, the flow stress distribution must be consistent with the final effective strain distribution according to the material's work-hardening characteristics. This requirement can be achieved by using the following computational procedure. During the iteration process for a converging solution, the flow lines corresponding to the latest velocity field are constructed after each iteration. The network of grid distortions and the effective strain distributions are determined from these flow lines. The effective strains for all elements are then interpolated from these values, and using a given stress-strain relationship, corresponding flow stress distributions for elements are determined. Using this new flow stress distribution, the next iteration for the velocity field is carried out and the same procedure is repeated until the converged solution for the velocity field is obtained. Since the solution depends not only on $u_{(n-1)}$, but also on the flow stress distribution, when the

velocity solution has converged, the flow stress distribution and effective strain distribution also match each other according to the stress-strain behavior of the material. Thus the convergence of velocity solutions gives the correct solution for the work-hardening material.

C. Extrusion conditions

The extrusion process conditions under which the computation was carried out are summarized in Table 1. Since the final solution for the extrusion with nonhardening material was used as the initial guess for work-hardening materials, the results for non-work-hardening materials are also presented.

Table 1(a): Extrusion process conditions for computation.

α (die semi-cone angle) = 30°

$\frac{R_i}{R_0} = 2.366$, area reduction $1 - \left(\frac{R_0}{R_i}\right)^2 = 0.82$

Material	Die-workpiece interface frictional stress f
Non-work-hardening $\bar{\sigma} = Y_0$	0, 0.2Y ₀ , 0.4Y ₀
SAE 1112 steel $\bar{\sigma} = Y_0 \left(1 + \frac{\bar{\epsilon}}{0.3}\right)^{0.25}$	0, 0.2Y ₀ , 0.4Y ₀

Table 1(b): Extrusion process conditions for computation.

$$\alpha \text{ (die semi-cone angle)} = 45^\circ$$

Work-hardening material: al alloy 2024-T351

$$\bar{\sigma} = Y_0 \cdot 2.202(\bar{\epsilon})^{0.1675} \text{ or } Y_0 \left(1 + \frac{\bar{\epsilon}}{0.01021}\right)^{0.171}$$

Reduction	Non-work-hardening friction f	Work-hardening friction f
$\frac{R_i}{R_0} = 1.25$	0	0 , 0.4Y ₀
1.6	0	0 , 0.4Y ₀
1.8	-	0 , 0.4Y ₀
2.0	0	0 , 0.4Y ₀
2.4	0	- , -

The stress-strain curves for SAE 1112 steel and for aluminum alloy 2024-T351 are shown in Fig. 2. The calculations for SAE 1112 steels are mainly to find the effect of friction on the deformation characteristics, while the cases for al alloy 2024-T351 emphasized the effect of area reduction, as well as the effect of friction, on the deformation in extrusion.

D. Results and discussion

The computation was performed for each solution until the accuracy of $r^2 = 10^{-5}$ was reached. This corresponds to the error norm of $\|\Delta y\|/\|y\| = 0.00008$. The number of iterations to reach the above convergence depends on the initial guess, but by using the best available initial guess for the velocity field, the average number of iterations required for the final solution was 25 ~ 30 iterations.

The results were obtained for average extrusion pressure, normal pressure distribution on the die, grid distortions, velocity distributions, and stress, strain, strain-rate distributions.

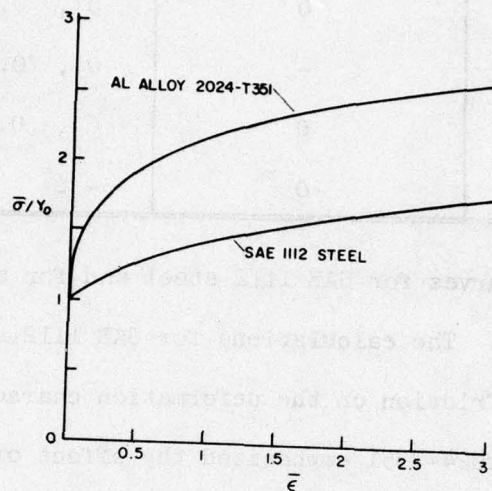


Fig. 2 Stress-strain curves for SAE 1112 steel ($Y_0 = 79,800$ psi; 550.21 MN/m²) and for aluminum alloy 2024-T351 ($Y_0 = 47,778$ psi; 329.42 MN/m²).

SAE 1112 steel The stress distributions computed differs from the actual distribution by a hydrostatic component. This hydrostatic component was determined by setting the net axial force along the exit boundary equal to zero, and the magnitude of stresses were corrected accordingly. The average extrusion pressures were then determined from the stresses along the entrance boundary. They are summarized in Table 2.

Table 2: Average extrusion pressure, p_{ave}/Y_0 .

$$\alpha = 30^\circ$$

$$\frac{R_i}{R_0} = 2.366$$

Material	Friction		
	0	$0.2Y_0$	$0.4Y_0$
Non-work-hardening	1.755	2.292	2.784
SAE 1112 steel	2.425	3.148	3.665

The general trend of the velocity distributions is the same for all friction conditions. A typical example is given in Fig. 3. The two velocity components are plotted as functions of the radial coordinate at various locations in the axial direction within the deformation zone. These distributions are in general agreement with the measurements in the visio-plasticity study of axisymmetric extrusion of lead [11].

Detailed differences of deformation characteristics, due to material properties and friction at the die-workpiece interface, are more clearly indicated, for example, in grid distortions. The steady-state grid distortion patterns are compared for non-work-hardening and work-hardening cases for the two friction conditions in Fig. 4. With reference to Fig. 4(a),

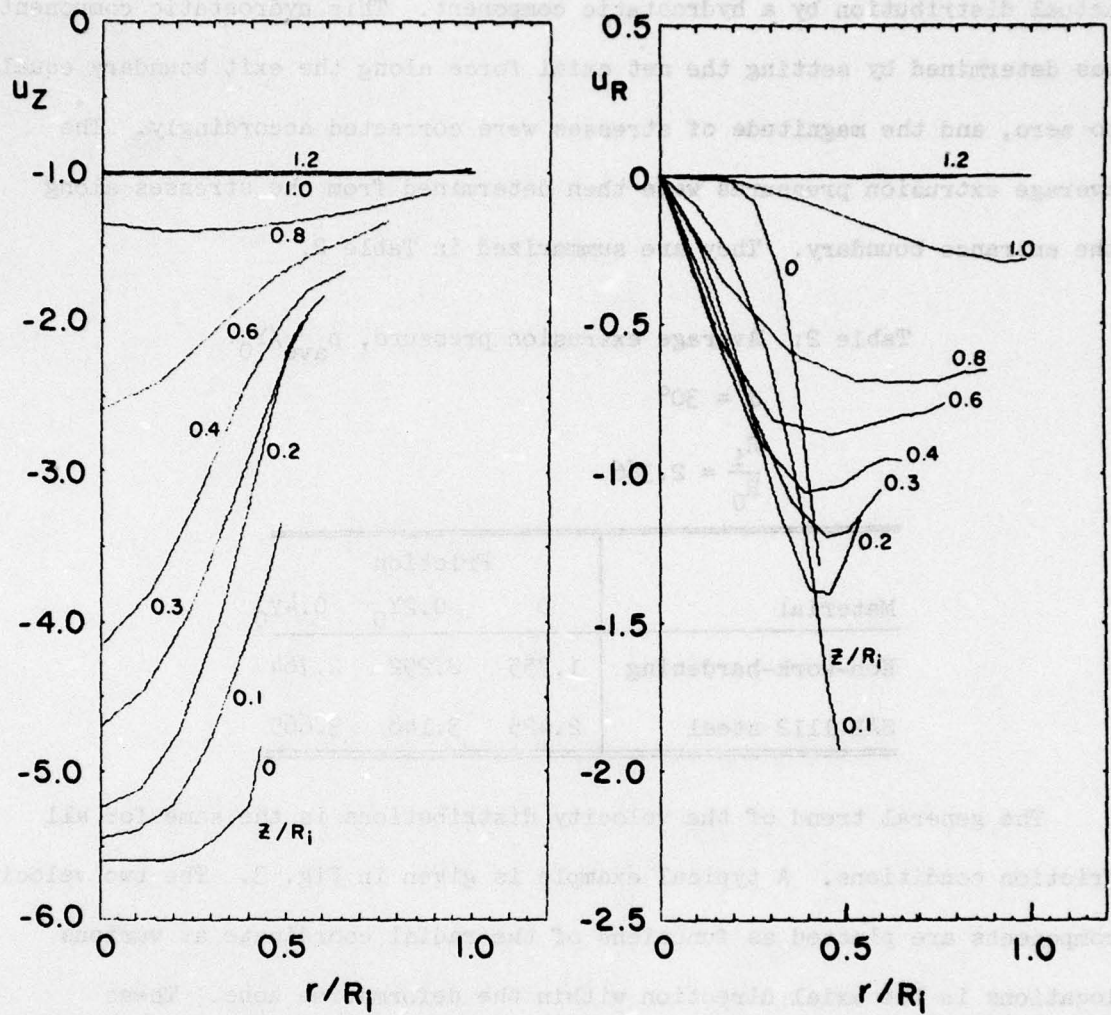


Fig. 3 Computed velocity distributions for SAE 1112 steel under the conditions $\alpha = 30^\circ$, $R_1/R_0 = 2.366$, and $f = 0.2Y_0$.

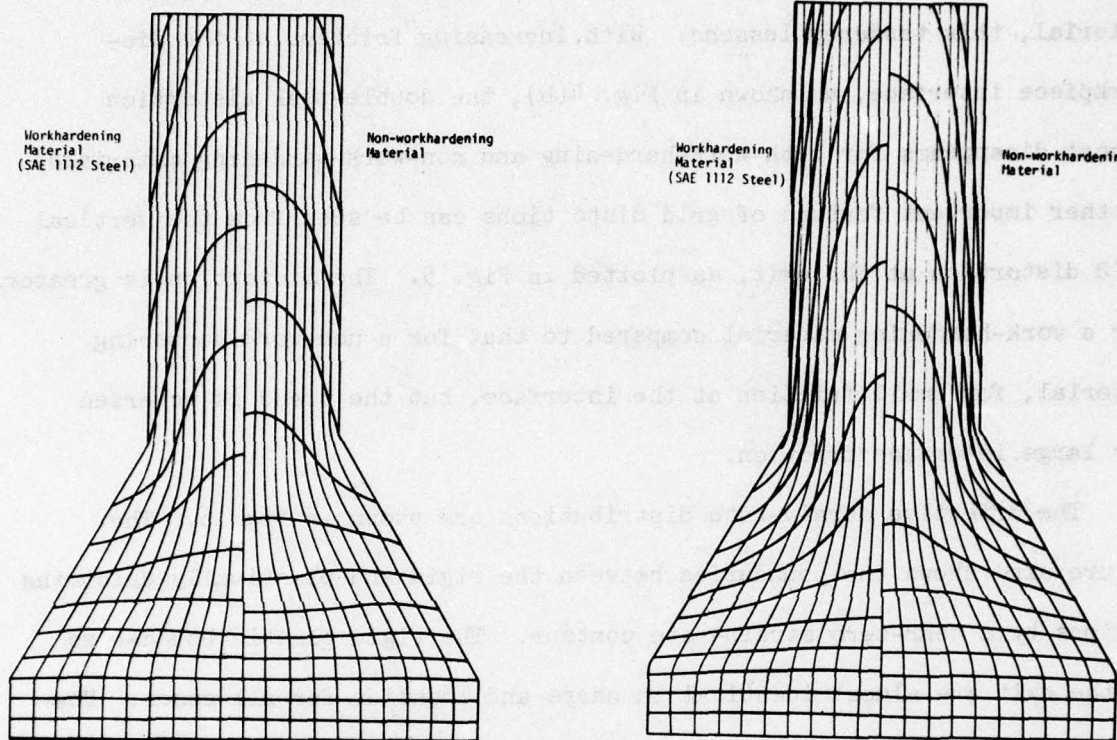


Fig. 4 Grid distortion patterns for non-workhardening and workhardening materials with (a) die frictional stress $f = 0$, and (b) $f = 0.4Y_0$.

it is clearly seen that the grid lines that are originally perpendicular to the axis of the workpiece distort and show the double peak in the extruded part for non-work-hardening material. However, for a work-hardening material, this tendency lessens. With increasing friction at the die-workpiece interface, as shown in Fig. 4(b), the double-peak distortion almost disappears for both work-hardening and non-work-hardening materials. Another important feature of grid distortions can be seen from the vertical grid distortion at the exit, as plotted in Fig. 5. The distortion is greater for a work-hardening material compared to that for a non-work-hardening material, for small friction at the interface, but the trend is reversed for large interface friction.

The effective strain-rate distributions are shown in Fig. 6. The figure also shows the boundaries between the rigid and plastically deforming regions by a near-zero strain-rate contour. The rigid plastic boundaries at the exit are almost identical in shape and location for all cases. However, the rigid-plastic boundaries at the entrance moves backwards, indicating larger deforming zones, with increasing interface friction. This observation applies to both work-hardening and non-work-hardening materials. Also, the results show that the deformation zone size becomes larger for work-hardening. The difference is more pronounced with increasing friction. Neglecting small details, the effective strain-rate distribution is identical for both materials. The strain-rate increases gradually from the entrance toward the exit and near the exit there is a sharp drop. As might be expected, there is some degree of strain-rate concentration near the die corner.

The effective strain-rates are integrated along the flow lines to yield

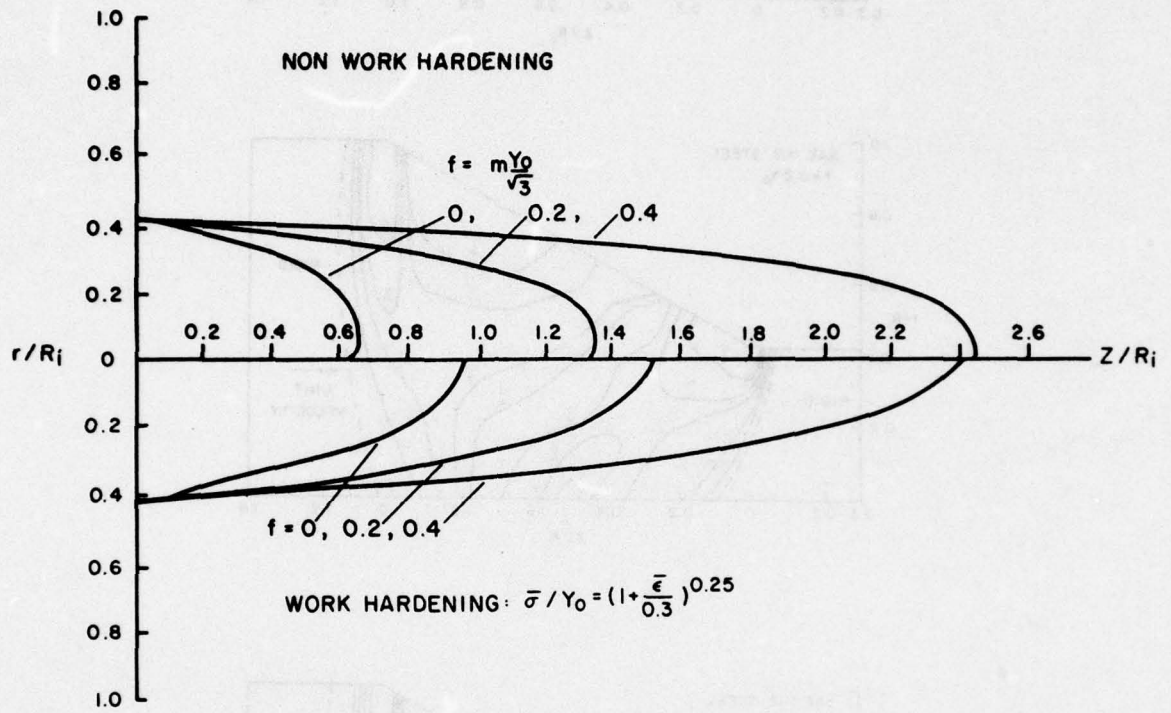


Fig. 5 Total grid distortions for various friction conditions;
 $\alpha = 30^\circ$, $R_i/R_0 = 2.366$.

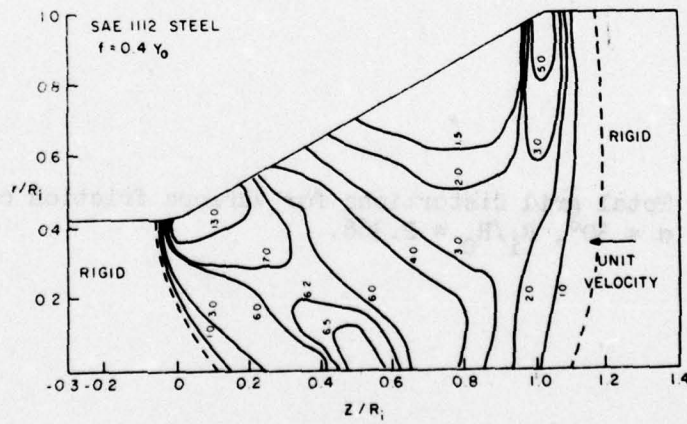
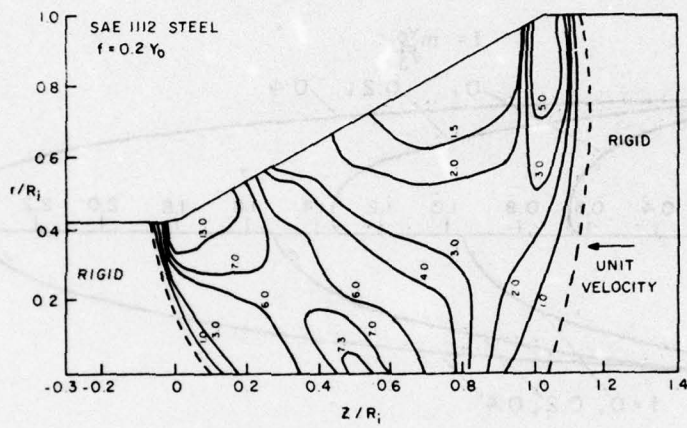
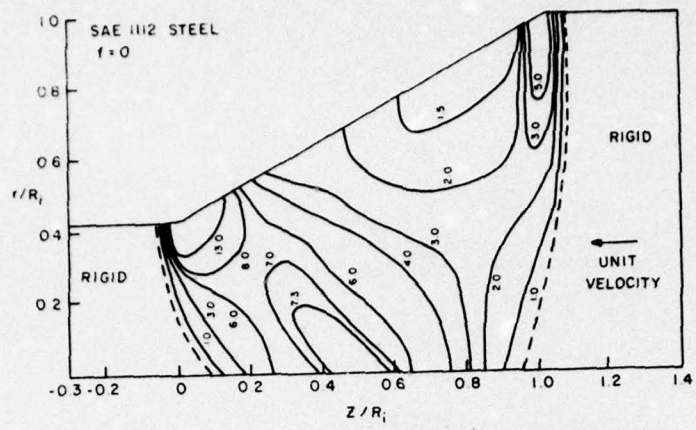


Fig. 6 Effective strain-rate distributions for SAE 1112 steel for various interface friction conditions.

the effective strain distributions. A typical effective strain distribution is given in Fig. 7. As for vertical sections, the strain is the highest near the die and the lowest near the extrusion axis throughout the deformation zone. The effective strain distribution at the exit section is also shown in the figure, which indicates that the strain is the lowest near the extrusion axis and increases toward the periphery. The strain distributions in the final product of the two materials are plotted for several friction values in Fig. 8. For both materials nonuniformity of deformation increases with increasing die-workpiece interface friction. The degree of nonuniformity is greater for small friction and less for large friction in work-hardening materials, while the opposite holds true for non-work-hardening materials. These results reflect exactly the findings in the vertical grid line distortion discussed with reference to Fig. 5.

The distributions of the hydrostatic pressure ($-\sigma_m/\bar{\sigma}$) are shown for the two friction conditions in Fig. 9. The distribution patterns are the same for both friction conditions and for both materials with and without work-hardening. Note that the hydrostatic pressure increases its magnitude throughout the deformation zone with increasing friction at the die-workpiece interface. It can be observed also that along the die-workpiece interface, the hydrostatic pressure is largest at the entrance and shows a minimum at some distance from the exit. This particular feature is seen in the normal pressure distributions along the die interface shown in Fig. 10. The pressure is the highest at the entrance and it decreases toward the exit, then increasing again near the exit. With increasing friction, the pressure increases but the distribution pattern remains the same. The trend of the curves for nonhardening and work-hardening materials is also the same with difference in magnitude of a constant amount.

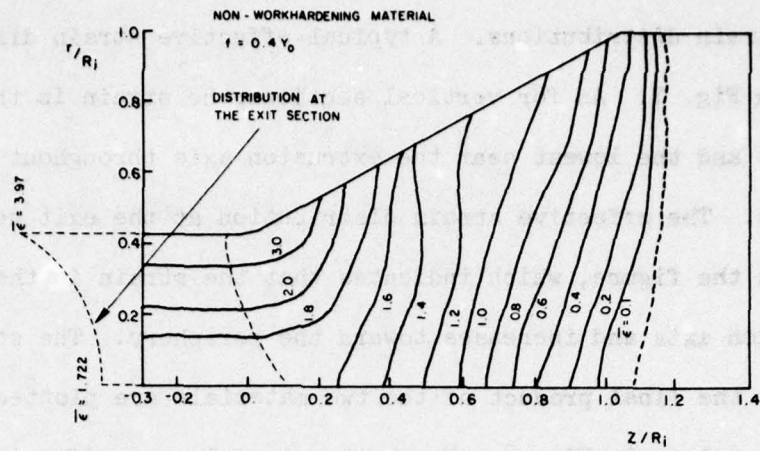


Fig. 7 A typical effective strain distribution.

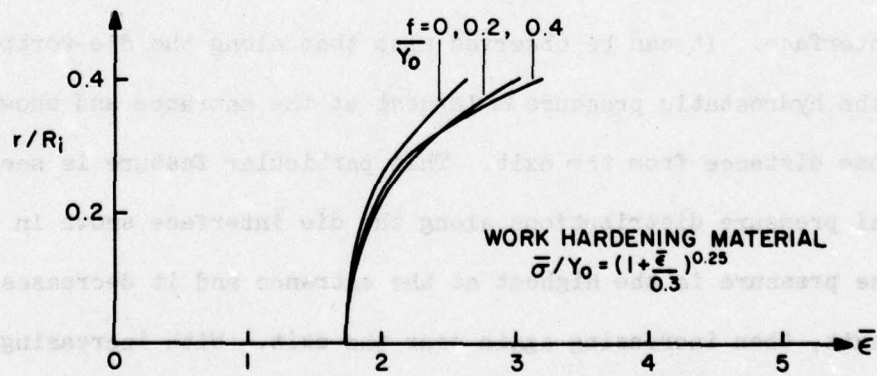
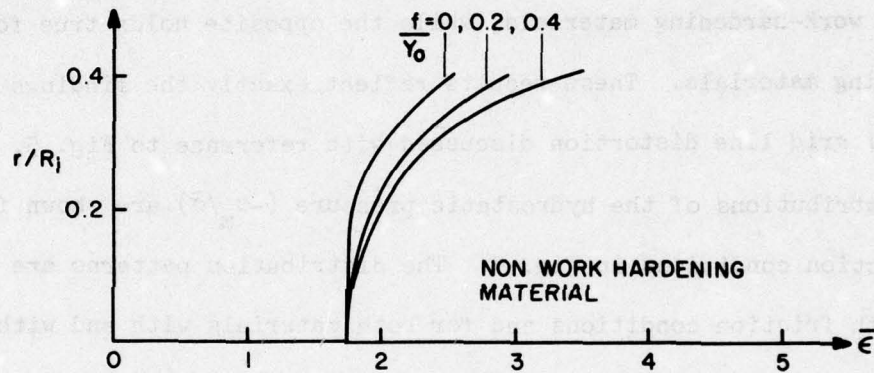


Fig. 8 Effective strain distributions at the exit sections for workhardening and non-workhardening materials under various interface friction conditions.

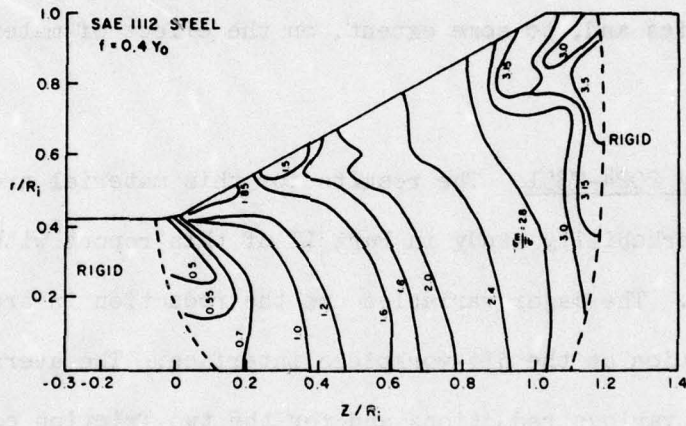
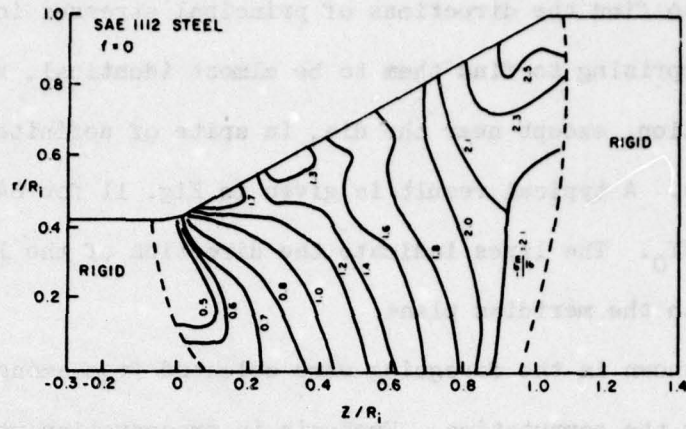


Fig. 9 Distributions of the hydrostatic pressure in SAE 1112 steel extrusion for the two friction conditions.

In other results obtained by the finite-element analysis, it is not only interesting to find the directions of principal stresses in the deformation zone, but surprising to find them to be almost identical, regardless of interface friction, except near the die, in spite of definite deviations of some quantities. A typical result is given in Fig. 11 for SAE 1112 steel with $f = 0.4Y_0$. The lines indicate the direction of the larger principal stress in the meridian plane.

The results shown in the foregoing were selected from among information obtained from the computation. Emphasis in presentation was placed mainly on the effect of die-workpiece interface friction on the detailed deformation mechanics and, to some extent, on the effect of materials properties.

Aluminum alloy 2024-T351 The results for this material are also utilized for the workability study in Part II of this report with regard to center bursting. The major variables are the reduction in area and the friction condition at the die-workpiece interface. The average extrusion pressures for various reductions and for the two friction conditions are summarized in Table 3.

Table 3: Average extrusion pressure, p_{ave}/Y_0 .
 $\alpha = 45^\circ$

Friction	R_1/R_0			
	1.25	1.6	1.8	2.0
$f = 0$	2.102	2.913	3.289	3.567
$f = 0.4Y_0$	2.310	3.408	3.826	4.202

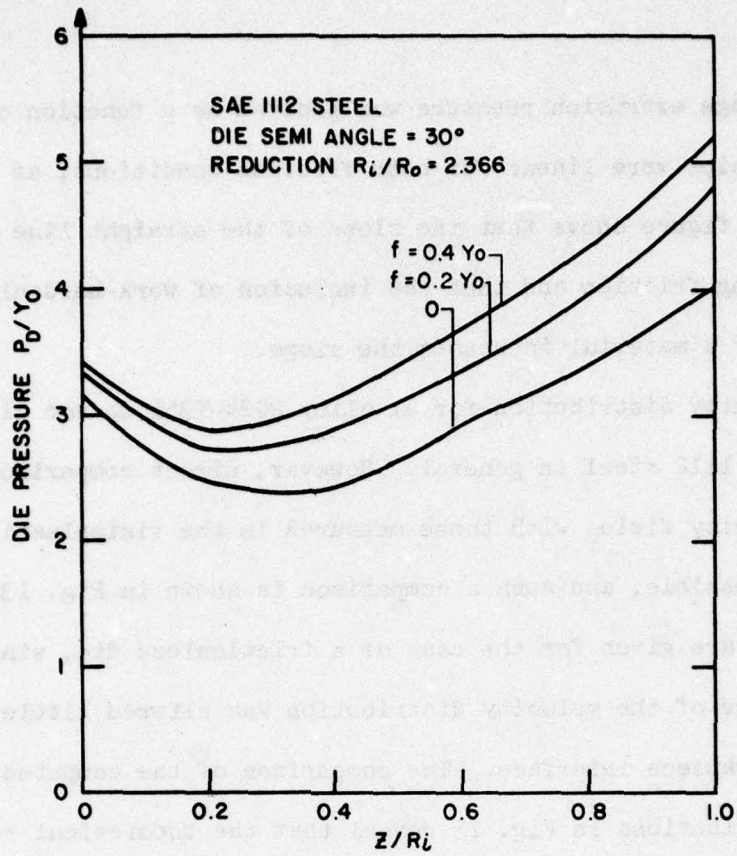


Fig. 10 The die pressure distributions under various friction conditions.

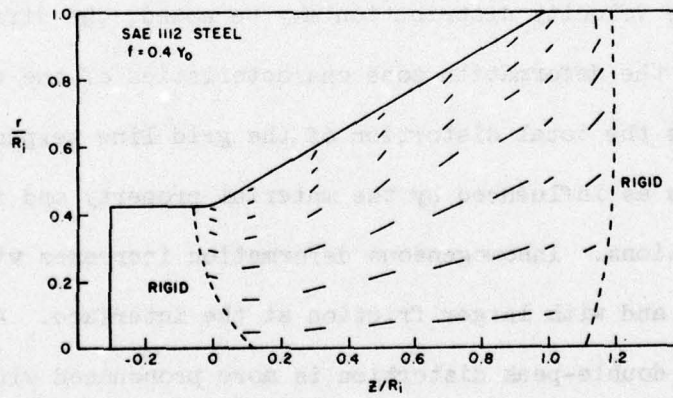


Fig. 11 Principal stress directions in extrusion.

When the average extrusion pressure was plotted as a function of $\ln\left(\frac{R_1}{R_0}\right)$, the relationships were linear for both friction conditions, as shown in Fig. 12. The figure shows that the slope of the straight line increases with increasing friction and that the inclusion of work-hardening characteristics of a material increases the slope.

The velocity distribution for all alloy 2024-T351 do not differ from those for SAE 1112 steel in general. However, direct comparison of the computed velocity fields with those measured in the viscoplasticity study [11] is now possible, and such a comparison is shown in Fig. 13. The computed results are given for the case of a frictionless die, since the general picture of the velocity distribution was altered little by friction at the die-workpiece interface. The comparison of the computed and measured velocity distributions in Fig. 13 reveal that the theoretical results in both velocity components are in agreement with the experimental results in every detail of distribution characteristics. This is one of the convincing evidences of the accuracy of the rigid-plastic finite-element analysis. Although in comparing Fig. 13 with Fig. 3 for SAE 1112 steel, some minor differences in the velocity distribution may be noted, the differences are mainly due to the deformation zone characteristics of the two materials.

Fig. 14 shows the total distortion of the grid line perpendicular to the extrusion axis as influenced by the material property and friction for several reductions. Inhomogeneous deformation increases with increasing reduction in area and with larger friction at the interface. An interesting feature is that a double-peak distortion is more pronounced with increasing reduction for a non-work-hardening material, while the contrary is true for a work-hardening material.

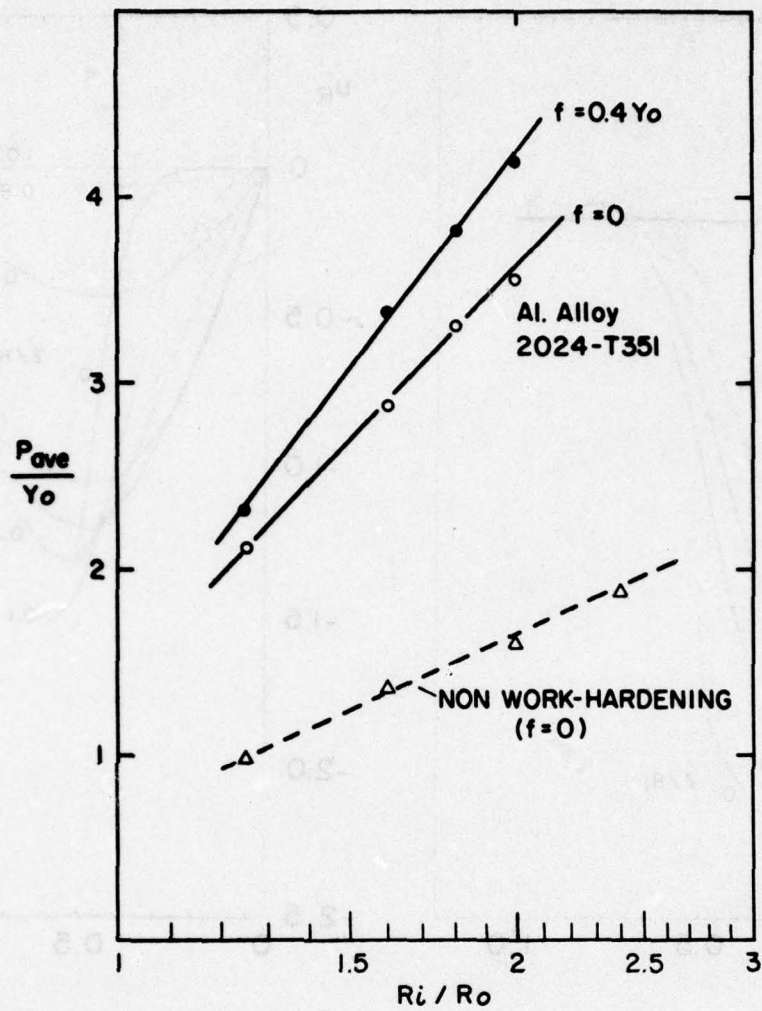
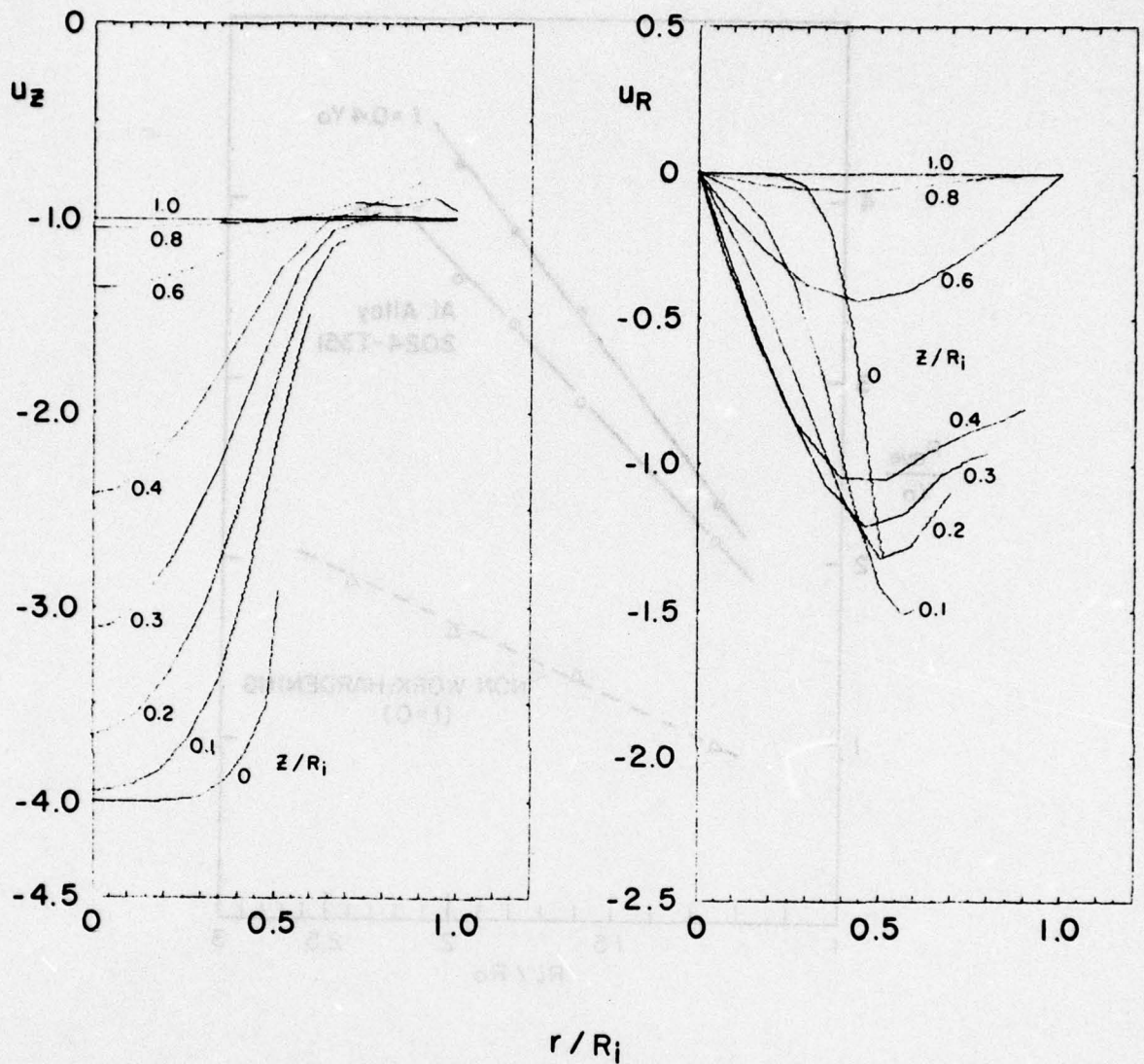
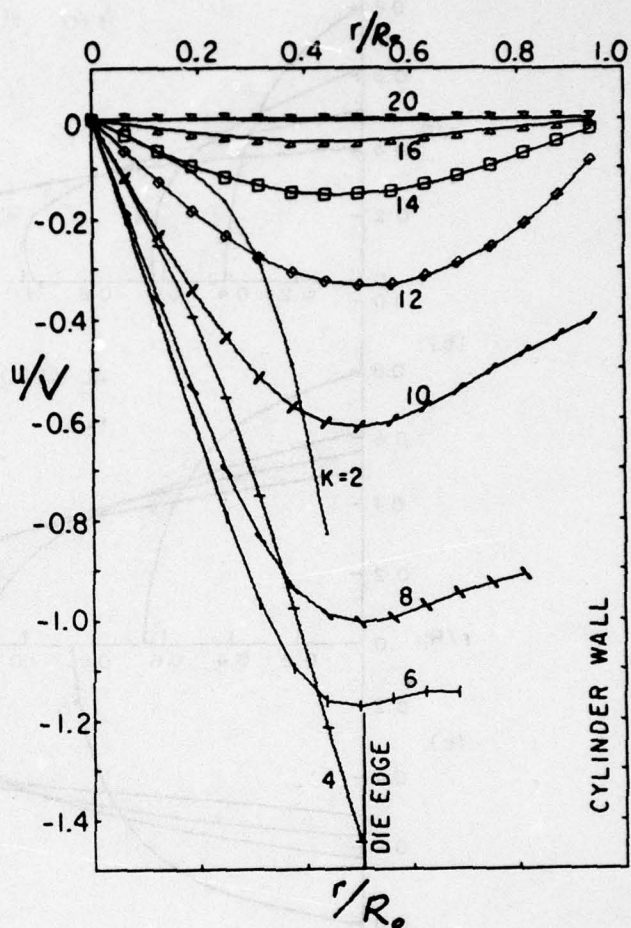
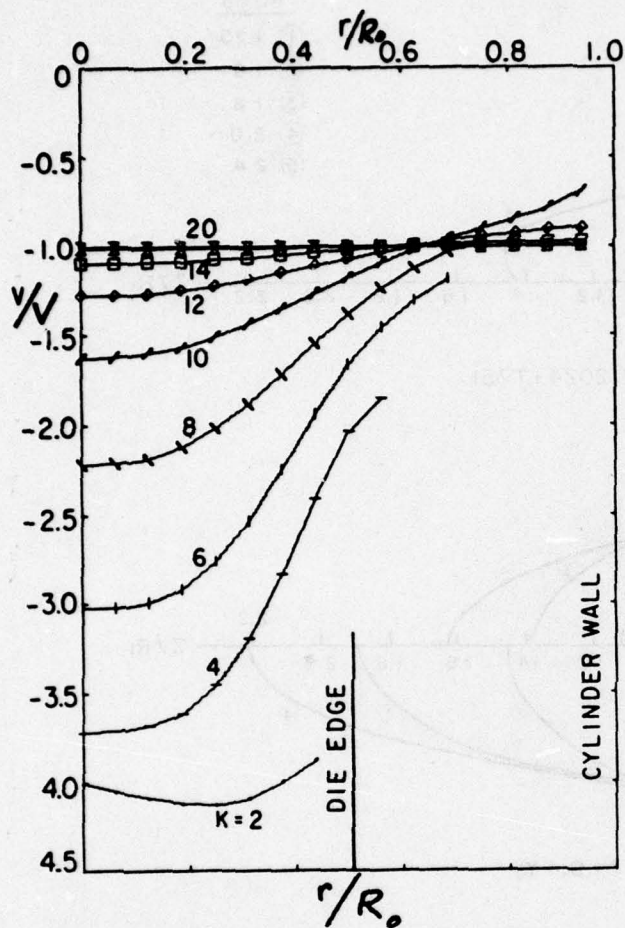


Fig. 12 Average extrusion pressures as functions of area reduction for aluminum alloy 2024-T351.



(a)

Fig. 13 Comparison of (a) computed and (b) experimental [11] velocity distributions; $R_1/R_0 = 2$, semi-die angle $\alpha = 45^\circ$ (frictionless in computation).



(b)

Figure 13

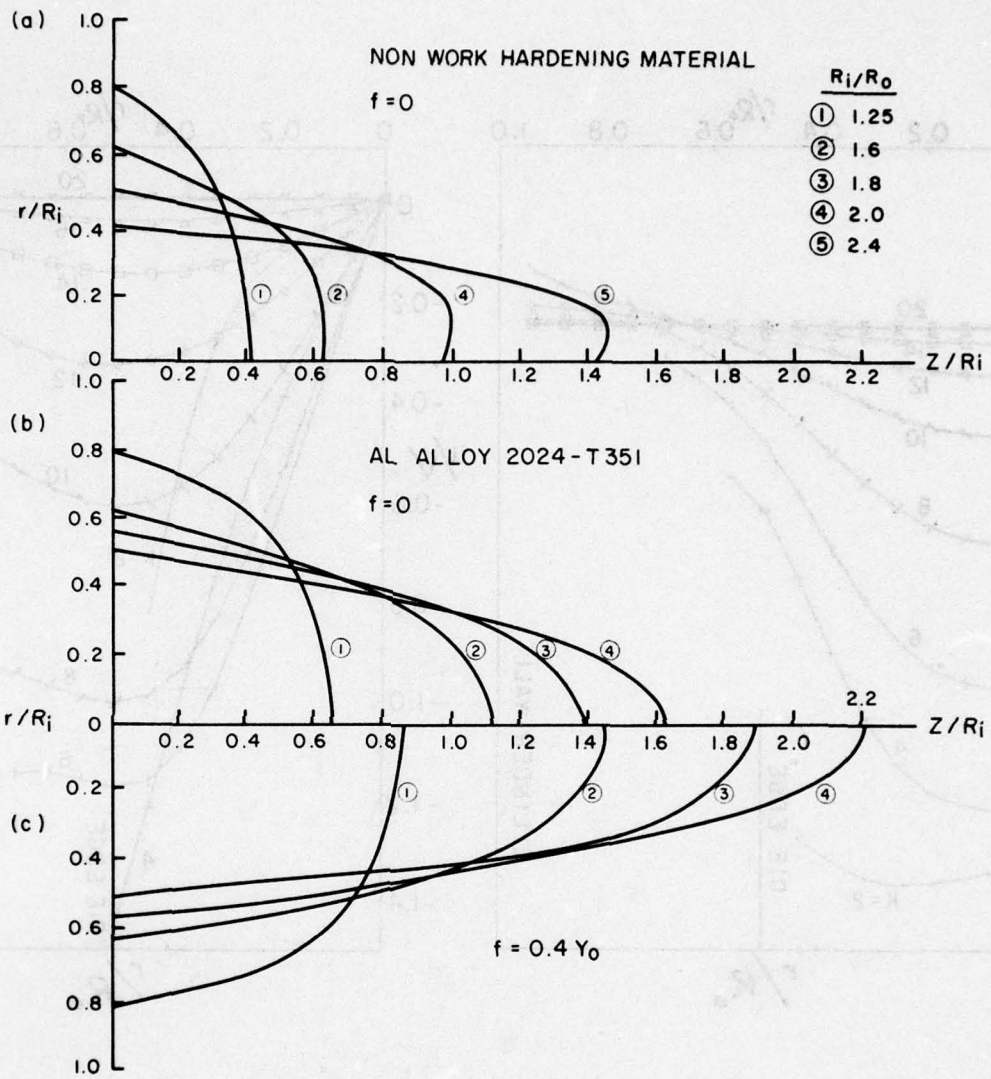


Fig. 14 Total grid distortions for various area reductions.

The effective strain-rate distributions for various area reductions, with two friction conditions, are shown in Fig. 15. With regard to the effect of friction on the deformation zone, the exit boundary remains about the same but the deformation zone expands as friction at the die-workpiece interface increases. This conclusion is the same as that drawn for SAE 1112 steel.

As the reduction in area increases, naturally the deformation zone becomes larger and the magnitude of strain-rate increases. Common features of the strain-rate distributions for all the reductions investigated are: (1) strain-rate concentrations occur near the corners at the entrance and at the exit, and (2) along the axis of symmetry the strain-rate peak appears in the middle of the deformation zone. The effective strain distributions across the extruded bar are plotted in Fig. 16. The strain is largest at the surface and smallest at the center. An interesting result is that the degree of nonuniformity in strain (difference between the largest and smallest strains) is greatest for the smallest area reduction. Also, the effect of friction on the final strain distribution is practically none, except that the magnitude of the surface strain increases slightly with increasing interface friction.

The distribution of the mean stress is similar to the pattern obtained for SAE 1112 steel. As the reduction decreases, the mean stress increases and becomes tensile in the zone near the center, as shown in Fig. 17. Another finding is seen, with respect to the die pressure, in Fig. 18. The die pressure is highest for the smallest reduction. This implies that the pressure distributions for smaller reductions are critical for die design. The distribution pattern is the same as that for SAE 1112 steel showing a minimum at some distance from the die exit.

Finally, the directions of the largest principal stresses are plotted for two reductions in Fig. 19. Again, the effect of die-workpiece interface friction is negligible and the pattern appears to be determined solely by the geometrical constraints.

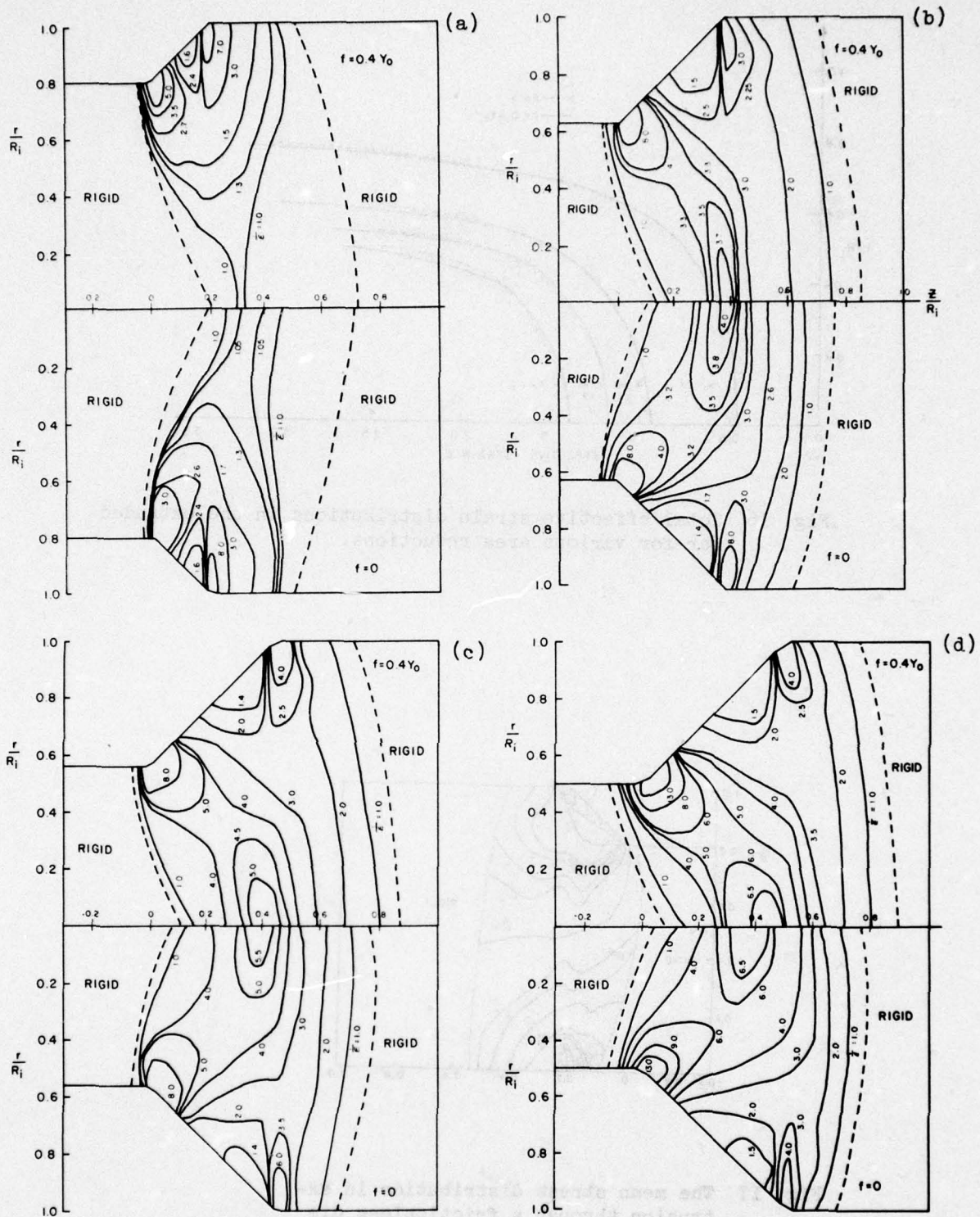


Fig. 15 Strain-rate distributions for two friction conditions at reductions of (a) $R_1/R_0 = 1.25$; (b) $R_1/R_0 = 1.6$; (c) $R_1/R_0 = 1.8$; (d) $R_1/R_0 = 2$.

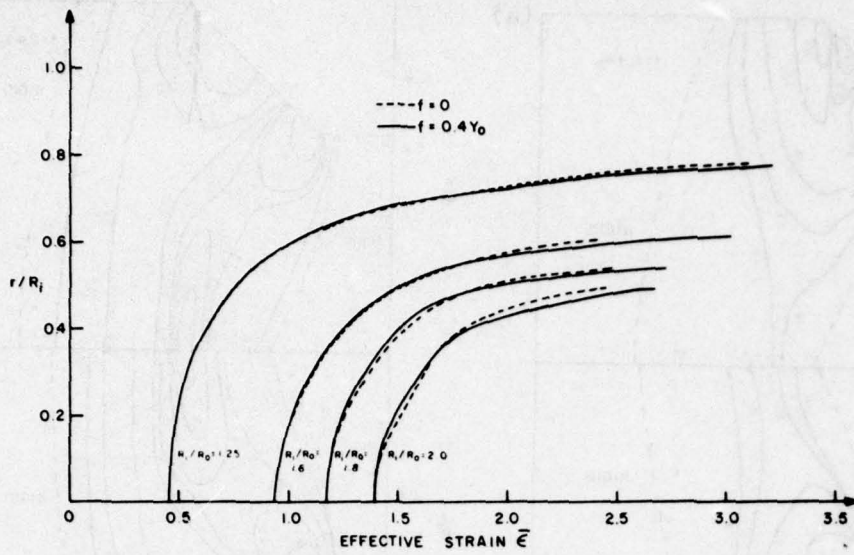


Fig. 16 Total effective strain distributions in the extruded bar for various area reductions.

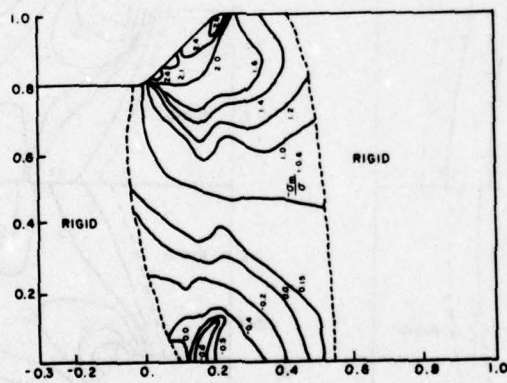


Fig. 17 The mean stress distribution in extrusion through a frictionless die at $R_1/R_0 = 1.25$.

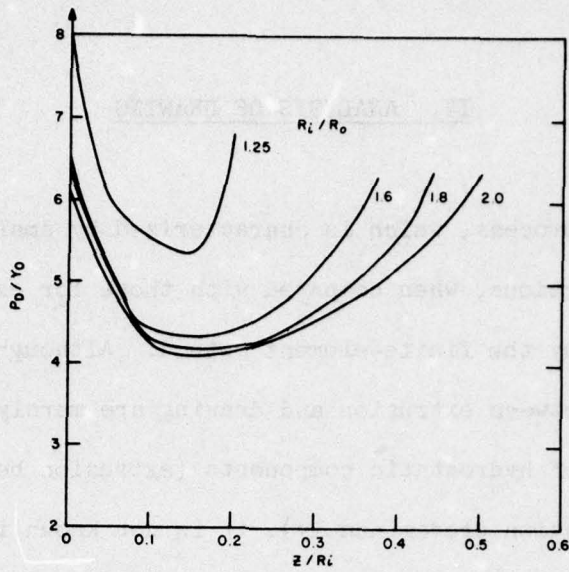


Fig. 18 Die pressure distributions for various area reductions.

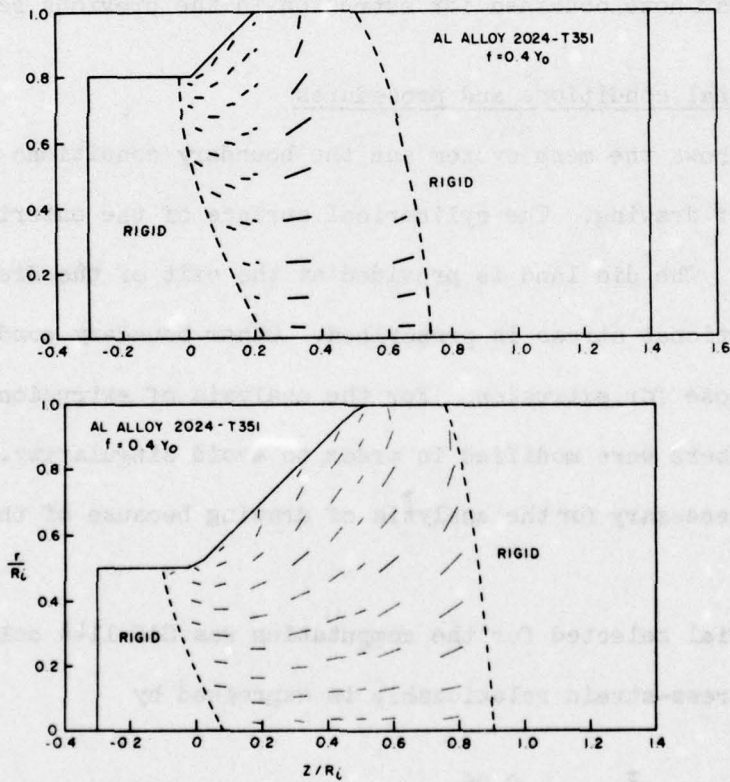


Fig. 19 Directions of the largest principal stresses.

IV. ANALYSIS OF DRAWING

The drawing process, which is characterized by smaller die angles and smaller area reductions, when compared with those for extrusion, has not yet been treated by the finite-element method. Although it appears that the differences between extrusion and drawing are merely geometrical and in the magnitude of hydrostatic components (extrusion being in compression and drawing in tension predominantly), it is not known if the results obtained in extrusion can be extrapolated to those in drawing according to the geometrical conditions and a simple concept of pushing and pulling. Therefore, we discuss the analytical results in drawing, emphasizing a comparison with those obtained for extrusion in the previous section.

A. Computational conditions and procedures

Fig. 20 shows the mesh system and the boundary conditions used for the analysis of drawing. The cylindrical surface of the entering bar is traction-free. The die land is provided at the exit of the die, along which the frictional stress is prescribed. Other boundary conditions are the same as those for extrusion. For the analysis of extrusion the shape of the die corners were modified in order to avoid singularity. However, this was not necessary for the analysis of drawing because of the small die angle.

The material selected for the computation was SAE 1144 cold-drawn steel whose stress-strain relationship is expressed by

$$\frac{\bar{\sigma}}{Y_0} = \left(1 + \frac{\bar{\epsilon}}{0.262 \times 10^{-4}}\right)^{0.06}$$

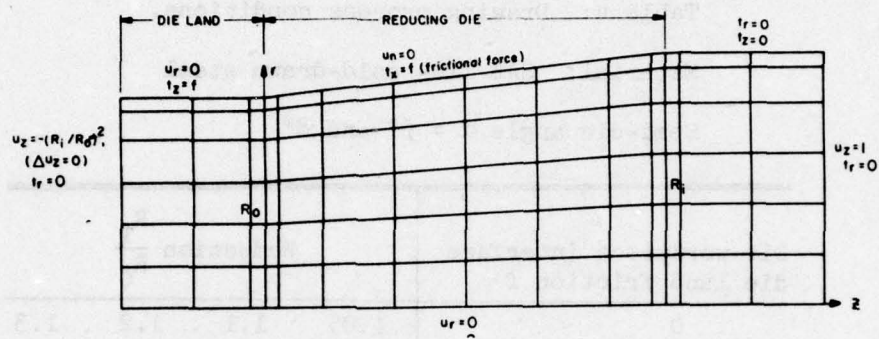


Fig. 20 The mesh system and boundary conditions for drawing.

with $Y_0 = 84,800$ psi
 $= 584.68$ MN/m².

This material was selected mainly for the workability study in drawing given in Part 2 of this report.

The drawing process conditions for which the computation was performed are summarized in Table 4.

Table 4: Drawing process conditions.

Material: SAE 1144 cold-drawn steel

Semi-die angle $\alpha = 6^\circ$ and 8°

Die-workpiece interface die land friction f	Reduction $\frac{R_i}{R_0}$			
0	1.05	1.1	1.2	1.3
0.25 Y_0	1.05	1.1	1.2	-

For computation purposes the solution of extrusion for $\alpha = 45^\circ$ and $R_i/R_0 = 1.25$ was used as an initial guess for drawing with $\alpha = 6^\circ$ and $R_i/R_0 = 1.2$ by modifying the solution according to geometrical proportions. Thirty-four (34) iterations were required to achieve the converged solution with

$$\sum_m \left\{ \left(\frac{\partial \tilde{\phi}^{(m)}}{\partial u^{(m)}} \right)^2 + \left(\frac{\partial \tilde{\phi}^{(m)}}{\partial \lambda^{(m)}} \right)^2 \right\} = 10^{-6}, \quad \left(\frac{\|\Delta u\|}{\|u\|} \sim 4 \times 10^{-6} \right).$$

This solution was then used as an initial guess for the computation of all the other cases. The convergence was excellent and only 6 to 10 iterations were necessary to obtain the solutions in most cases.

B. Results and discussion

The results for $\alpha = 6^\circ$ are presented and discussed here. The results for $\alpha = 8^\circ$ are presented and discussed in terms of workability in drawing in Part 2 of this report.

An example of the velocity distribution is shown for $R_1/R_0 = 1.2$ and $f = 0.25Y_0$ in Fig. 21. The distribution pattern looks somewhat different from those for extrusion. This is because of small reduction and small die angle and because the total distortion is small. Fig. 22 shows vertical grid line distortion in drawn bars. Greater friction produces more distortion. The difference in the total distortion due to die friction increases with increasing reductions.

The general pattern of the effective strain-rate distribution is the same as that for extrusion, as seen in Fig. 23. Concentrations of strain rate occur at the die corners. Along the axis of symmetry, strain-rate distribution shows a peak at the midpoint of the deformation zone. The deformation zone expands with larger die-workpiece interface friction as it did for extrusion.

The variation of effective strain distribution in drawn bars is comparatively small due to a small die angle and small reductions (Fig. 24). Fig. 24 shows also that the effect of the die friction on the strain distribution is negligible. By comparing Fig. 24 with the results of extrusion in Fig. 16, it can be seen that the die angle is a most important variable in controlling nonuniformity of the extruded or drawn bar properties.

The hydrostatic pressure distribution is shown in Fig. 25. It shows the combined characteristics of those for small reductions similar to

Fig. 17 and those for relatively extended deformation zone similar to Fig. 9. The magnitude of the hydrostatic component increases with larger die friction in drawing. This is contrary to the results with extrusion shown in Fig. 9. The die pressure distribution is plotted for various reductions and for two die friction conditions in Fig. 26. Higher die pressure is obtained for smaller reduction as it was for extrusion. However, contrary to the case of extrusion, the die pressure is higher with frictionless dies than those with friction. These findings on die pressure are in agreement with experimental results [12], although empirical values are average die pressures.

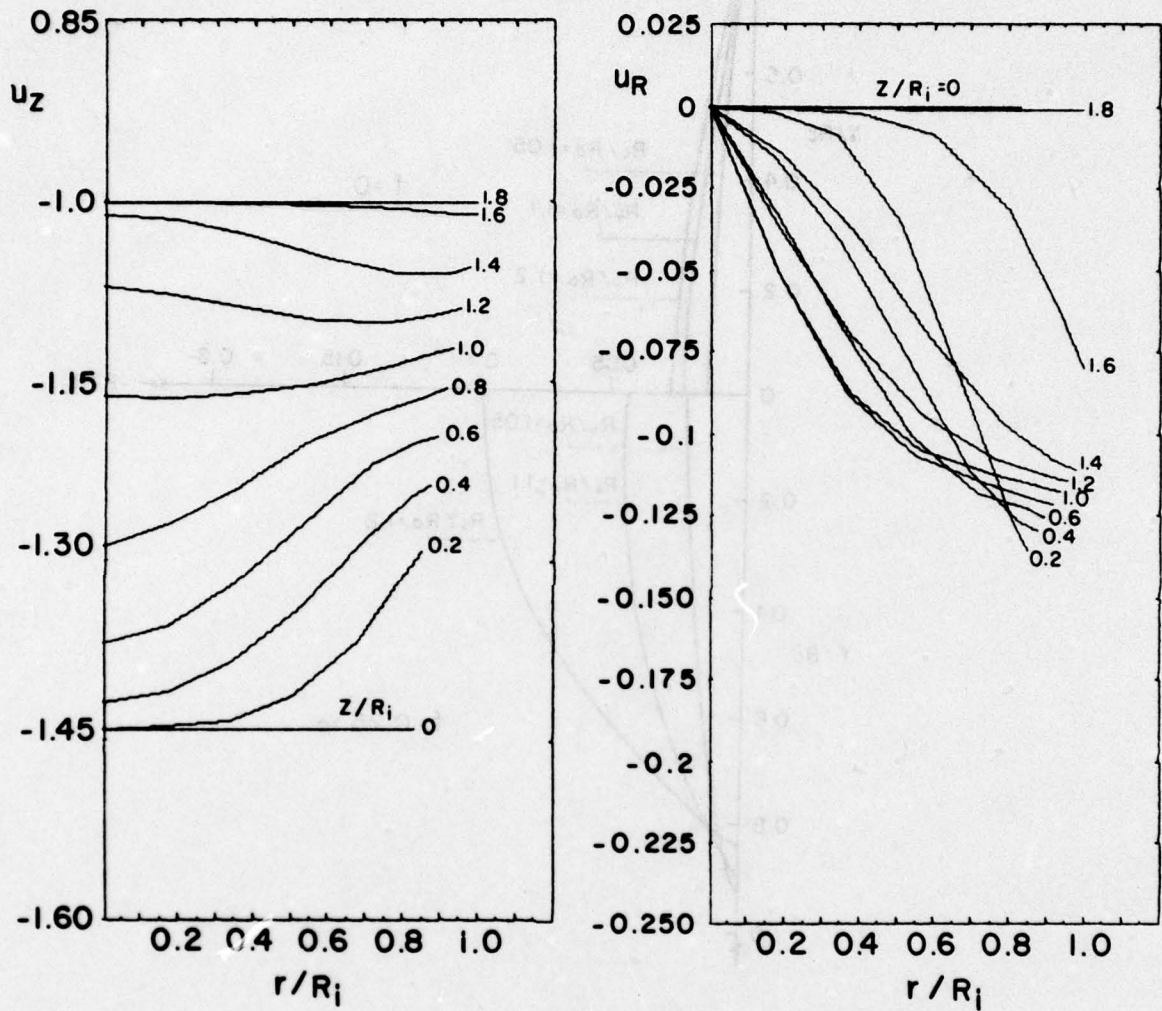


Fig. 21 Velocity distributions in drawing with $\alpha = 6^\circ$, $R_1/R_0 = 1.2$, and $f = 0.25Y_0$.

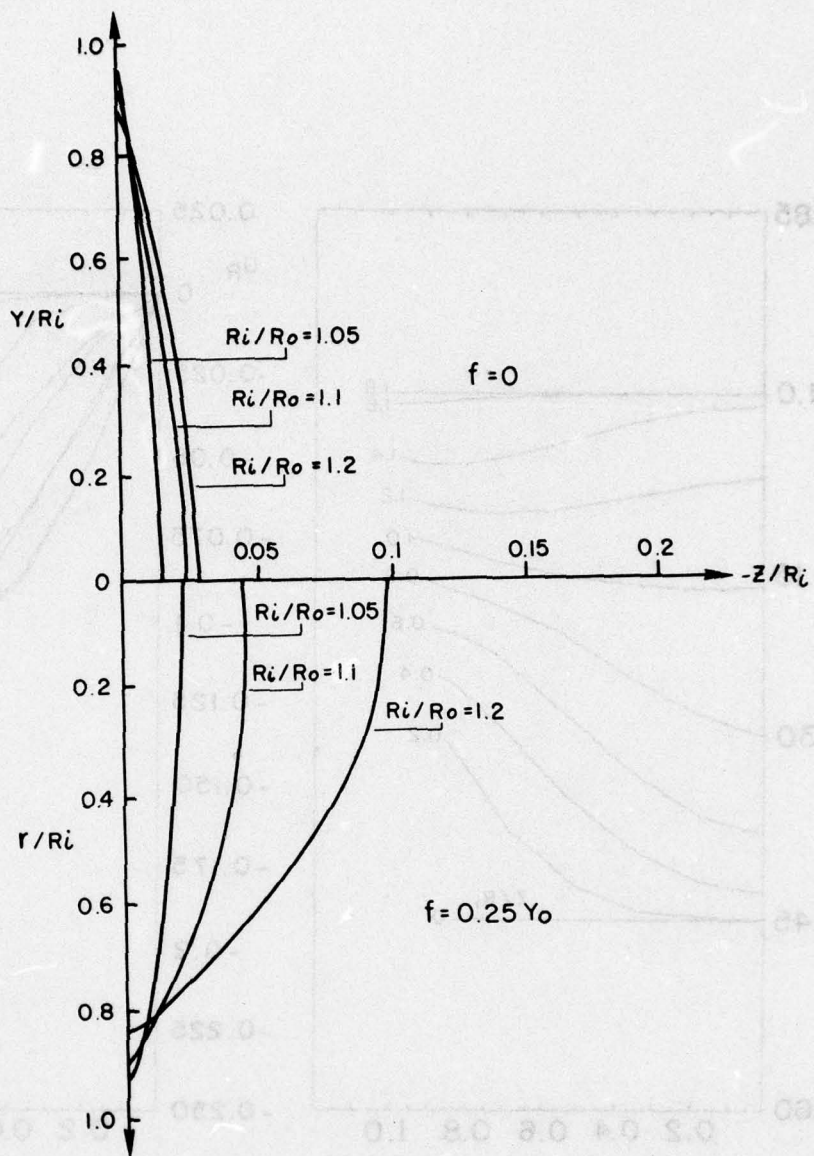


Fig. 22 Total distortion of a line originally perpendicular to the axis of drawing for various area reductions.

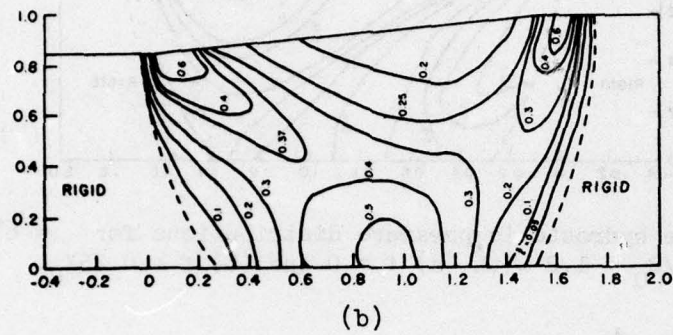
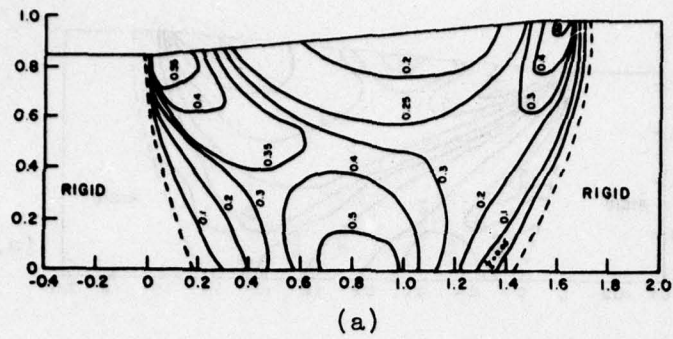


Fig. 23 Strain-rate distributions for $\alpha = 6^\circ$ and $R_i/R_0 = 1.2$ with
 (a) $f = 0$ and (b) $f = 0.25Y_0$.

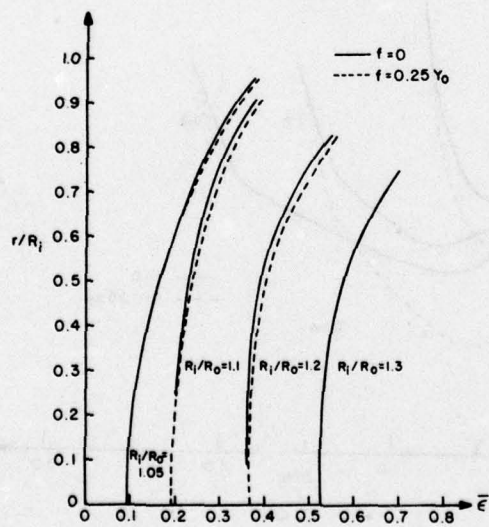


Fig. 24 Effective strain distributions in drawn bars.

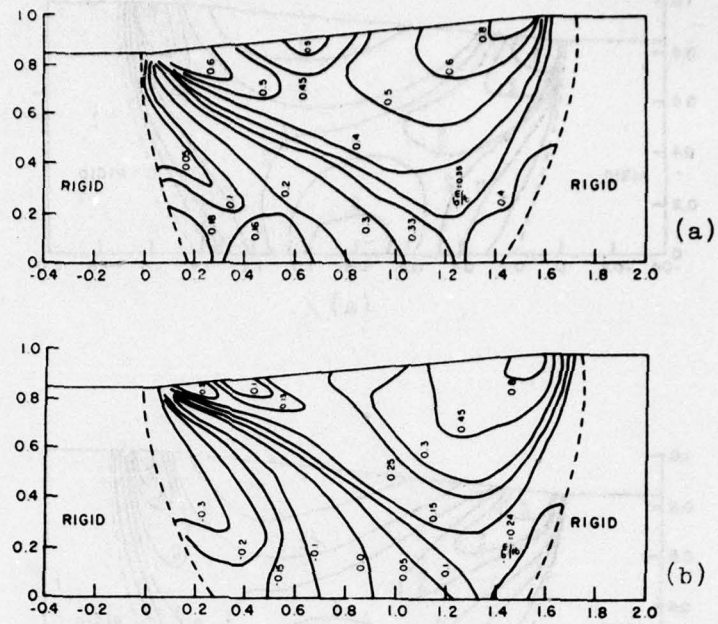


Fig. 25 The hydrostatic pressure distributions for $\alpha = 6^\circ$ and $R_1/R_0 = 1.2$ with (a) $f = 0$ and (b) $f = 0.25Y_0$.

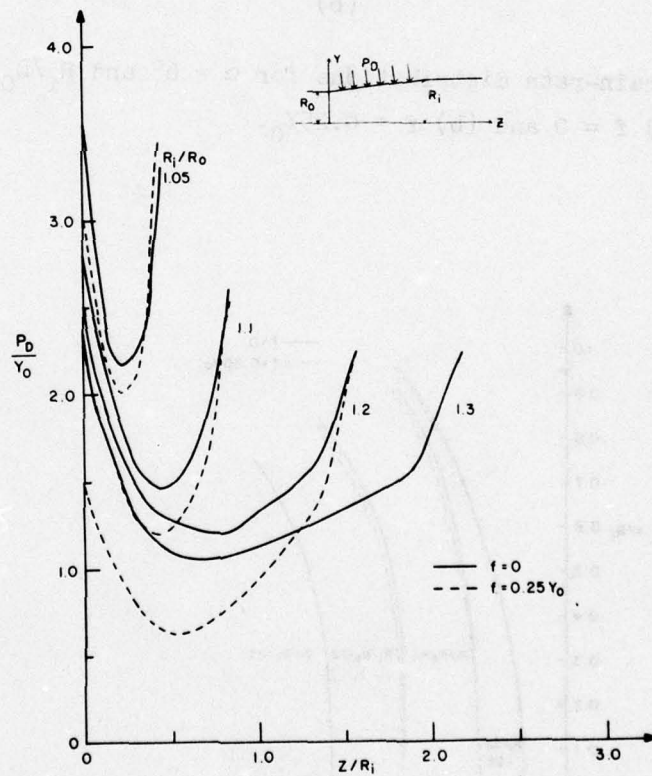


Fig. 26 The die pressure distributions for various reductions and for the two die-friction conditions.

V. SUMMARY AND CONCLUSIONS

In recent years the matrix method has been applied to the analysis of various metalworking processes, including the steady-state extrusion process. The present matrix method program incorporates the treatment of friction at the die-workpiece interface and an improvement of computational efficiency by adopting a new convergence criterion. Using this program, the detailed mechanics of steady-state extrusion and drawing were obtained under various process conditions. The stress-strain properties of SAE 1112 steel and aluminum alloy 2024-T351 were used for extrusion and the stress-strain curve of SAE 1144 cold-drawn steel was used for drawing. The variables included for the computation were the die angle, die-workpiece interface friction, and the area reduction. The computed results were presented in terms of velocity distribution, grid distortion, strain-rate distribution, and stress and strain distributions.

Although materials properties apparently influence metal flow, as seen in grid distortion patterns, their effects on the overall deformation characteristics appear to be insignificant in extrusion and drawing processes. Among other variables, friction at the die-workpiece interface plays an important role in determining the detailed mechanics in these processes. With increasing friction the degree of grid distortion becomes larger and the deformation zone size expands in both processes. But the effect of friction on nonuniformity of product properties is less significant, while the die angle is an important variable in controlling this nonuniformity. The contrast between the extrusion process and the drawing process can be

found in the die pressure distribution and the distribution of hydrostatic stress components. In both processes, the die pressure decreases with increasing reduction in area. However, the die pressure is greater for larger interface friction in extrusion, while the reverse is true in drawing. Similarly, the magnitude of the hydrostatic stress component is less with larger interface friction in extrusion, but increases with increasing friction in drawing.

It is concluded that the matrix method is indeed an efficient numerical method which provides useful information on the detailed deformation characteristics for various process variables. In order to ascertain the accuracy of the solutions presented here, however, an extensive theoretical and experimental investigation is still needed.

I. INTRODUCTION

For purposes of choice at the first surface, such as in the case of
in sheet rolling and surface cracks in upsetting, the fracture criterion
can be considered experimentally. However, the preceding internal
fracture, formation of fracture voids under certain deformation
was required. In this part of the investigation, the validity of
the theory of voids

Part 2

WORKABILITY IN EXTRUSION AND DRAWING

examined by the experimental data found in the literature. When analyzing
the formation of fracture criterion with an deformation process found
in Part 1, the workability of materials in extrusion and drawing was deter-
mined.

In an attempt to develop a general fracture criterion, a model for
void growth was proposed to examine the stress and strain fields around
voids. The solutions were obtained by the finite-difference method. The
results show that deformation is concentrated along the narrow band in
the maximum shear stress direction. The fracture criterion assumed that

voids of critical size are smaller than the primary voids are distributed
throughout and that fracture occurred when the small voids grow and
touch each other along the band connecting the large voids. The Hollomon
analysis was used for predicting the growth and coalescence of small voids.
Based on this concept, the fracture strain formulation by Hollomon was

modified. Then the modified form, along with the formulation by Cockcroft
and Latham, was tested by the experiments on various steels and by the
tension data by Bridgman. Its validity was further examined by applying the
criterion to the determination of workability in bar extrusion and drawing.

I. INTRODUCTION

For occurrence of cracks at the free surface, such as in edge-cracking in sheet rolling and surface cracks in upsetting, the fracture criterion can be constructed experimentally. However, for predicting internal fracturing, formulations of fracture criteria under general deformation are required. In this part of the present investigation, the validity of the theory on ductile fracture developed in the previous report [1] was examined by the experimental data found in the literature. Then, combining the formulation of fracture criterion with the deformation mechanics found in Part 1, the workability of materials in extrusion and drawing was determined.

In an attempt to develop a general fracture criterion, a model for void growth was proposed to examine the stress and strain fields around voids. The solutions were obtained by the finite-element method. The results show that deformation is concentrated along the narrow band in the maximum shear stress direction. The fracture criterion assumed that voids of orders of magnitude smaller than the primary voids are distributed throughout and that fracturing occurred when the small voids grow and touch each other along the band connecting the large voids. The McClintock analysis was used for predicting the growth and coalescence of small voids. Based on this concept, the fracture strain formulation by McClintock was modified. Then the modified form, along with the formulation by Cockcroft and Latham, was tested by the experiments on surface cracks and by the tension data by Bridgman. Its validity was further examined by applying the criterion to the determination of workability in bar extrusion and drawing.

II. FRACTURE CRITERIA

McClintock and his coworkers [13], [14] developed solutions for void growth under the transverse stress state. Their model consists of a single elliptic cylindrical void extending in one direction and imbedded in a rigid plastic media. The major and minor axes of the void coincide with the principal stress directions. They derived an approximate solution for the rigid work-hardening materials, $\bar{\sigma} = K\bar{\epsilon}^n$, as

$$\log_e \left(\frac{R}{R_0} \right) = \frac{\sqrt{3} \bar{\epsilon}}{2(1-n)} \sinh \left[\frac{\sqrt{3}(1-n)}{2} \frac{\sigma_a + \sigma_b}{\bar{\sigma}} \right] + \left(\frac{\epsilon_a + \epsilon_b}{2} \right); \quad (9)$$

$$m = \left(\frac{\sigma_a - \sigma_b}{\sigma_a + \sigma_b} \right) + \left[m_0 - \left(\frac{\sigma_a - \sigma_b}{\sigma_a + \sigma_b} \right) \right] \exp \left[-\frac{\sqrt{3} \bar{\epsilon}}{(1-n)} \sinh \left\{ \frac{\sqrt{3}(1-n)}{2} \left(\frac{\sigma_a + \sigma_b}{\bar{\sigma}} \right) \right\} \right] \quad (10)$$

where R and R_0 are the current and initial mean radii of the hole, respectively; σ_a and σ_b , principal stress components along the major and minor axes, respectively; $\bar{\sigma}$ is the effective stress and $\bar{\epsilon}$ is the effective strain; m is the eccentricity of the ellipse defined in terms of the semi-major and semi-minor axes a and b , as

$$m = \frac{a - b}{a + b}, \quad (11)$$

and m_0 is the initial eccentricity. They assumed that the cylindrical hole is contained in the cell and that the material is composed of these cells. Fracturing was assumed to occur at the point where a growing void touches the cell boundary whose deformation is assumed to be the same as that of the boundary at infinity. The fracture strain, neglecting the void inter-

action, is then expressed (dropping a transient term) by

$$\bar{\epsilon}_f = \frac{\log_e \left(\frac{l_a^0}{2a_0} \right)}{\left\{ \frac{\sqrt{3}}{2(1-n)} \sinh \left[\frac{\sqrt{3}(1-n)}{2} \left(\frac{\sigma_a + \sigma_b}{\bar{\sigma}} \right) \right] + \frac{3}{4} \left(\frac{\sigma_b - \sigma_a}{\bar{\sigma}} \right) \right\}} \quad (12)$$

where l_a^0 and a_0 are the initial values of hole spacing l_a and a , respectively. The above derivation was given for generalized plane strain as an approximation for three-dimensional deformations. In three-dimensional configurations, there are six modes of fracture, two in each of the three perpendicular planes. Whichever one of these six modes gives the smallest fracture strain is the actual mode.

The model considers only the case where holes form at zero strain by complete separation of the particle-matrix interface. The review of the investigations on ductile fracture revealed that void nucleation is a complex process and that the nucleation pattern depends on particle size, particle composition, and possibly, particle distribution. The general observation is that void nucleation occurs at the large particles first. If a number of voids form and grow, then these voids may act as a stress raiser in the matrix and cause further void nucleation at other particle sites. Also, there are many indications that, during deformation, shear bands between large voids develop and that voids form at small particles in these bands, while the particles outside the bands remain relatively inactive. Thus, the formation of shear bands between large voids and growth and coalescence of small voids in the shear band may be a mechanism of eventual fracture.

Assuming this mechanism for fracture, a model for the growth of large voids has been proposed. Fig. 27 shows an assumed distribution of large voids, extending in arrays to infinity. The plane-strain condition is assumed in the direction perpendicular to the (x_a, x_b) plane. The minimum and maximum principal stresses act along the boundary at infinity in the directions of coordinate axes $(\sigma_a^\infty, \sigma_b^\infty)$. The solutions of this void growth model were obtained by the elastic-plastic finite-element model [1]. A result of the computation is shown in Fig. 28. As Fig. 28 indicates, deformation is concentrated along the narrow band in the maximum shear stress direction, and the concentration of strain along the band is about $2 \sim 3$ times the overall strain for most of the band and about $4 \sim 5$ greater near a large void. This implies that the band is the most favorable place for small voids to nucleate and grow.

The modified form of fracture criterion was obtained by assuming that voids of orders of magnitude smaller than the primary voids are distributed throughout and that fracturing occurred when the small voids grow and touch each other along the band connecting the large voids. When the McClintock analysis is applied locally under the condition prevailing within the shear band, we obtain

$$\bar{\epsilon}^f = \frac{K}{\frac{2}{\sqrt{3}(1-n)} \sinh\left\{\frac{\sqrt{3}(1-n)}{2} \frac{\sigma_a + \sigma_b}{\bar{\sigma}}\right\} + \frac{\sigma_b - \sigma_a}{\bar{\sigma}}} \quad (13)$$

where $K = \frac{4}{3f} \log_e \left(\frac{l_a^0}{2a_0}\right)$ and f is a factor indicating the strain concentration along the shear band.

Assuming this mechanism for fracture, a model for the growth of large voids has been proposed. Fig. 27 shows an assumed distribution of large voids, extending always in the direction of the maximum strain. The minimum strain in the direction perpendicular to the x_a plane. The minimum and maximum principal stresses are along the boundary as indicated in the directions of coordinate axes. The solutions of this void growth model were obtained by elastic-plastic finite element model [1]. A result of the computation is shown in Fig. 28. As the x_b indicates deformation concentration along the x_a axis, the maximum shear stress direction and the maximum strain direction are about 45° to the x_a axis. The maximum strain is about $2 \sim 3$ times the initial strain. The maximum shear stress is about 2 times the initial shear stress. The maximum principal stress is about 1.5 times the initial principal stress. The maximum shear stress is about 1.5 times the initial shear stress. The maximum strain is about 2 times the initial strain. The maximum shear stress is about 2 times the initial shear stress. The maximum principal stress is about 1.5 times the initial principal stress. The maximum shear stress is about 1.5 times the initial shear stress.

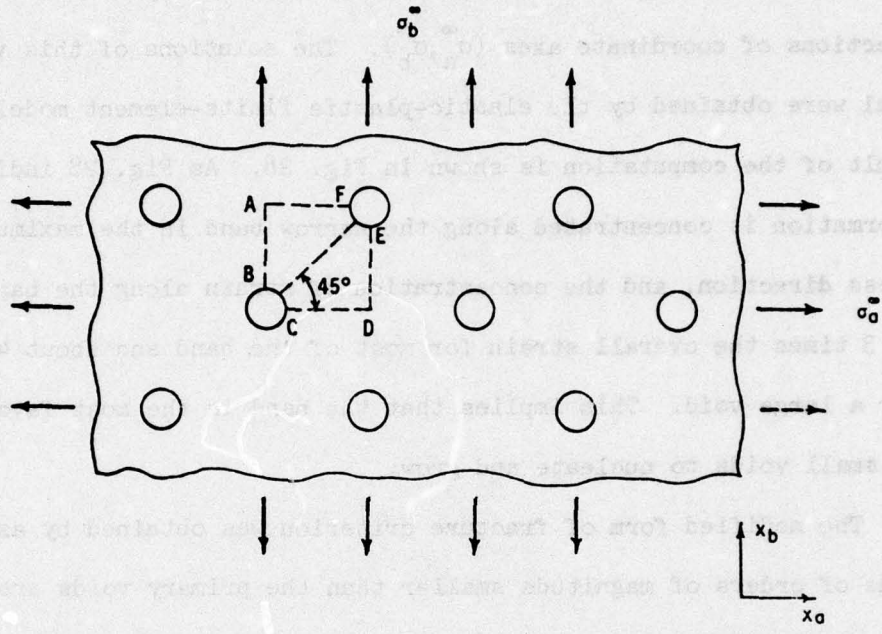
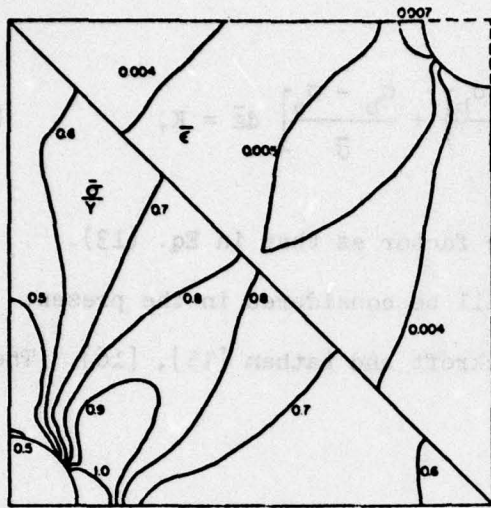
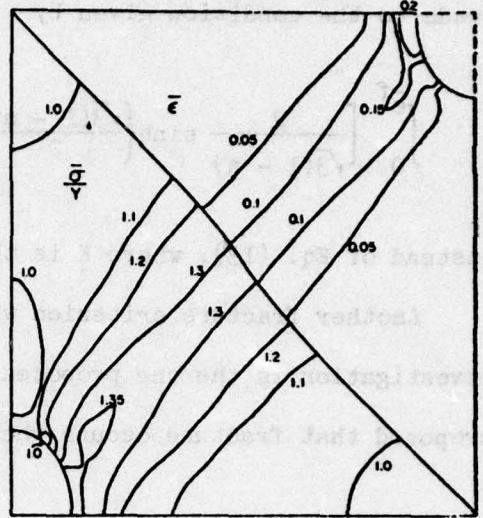


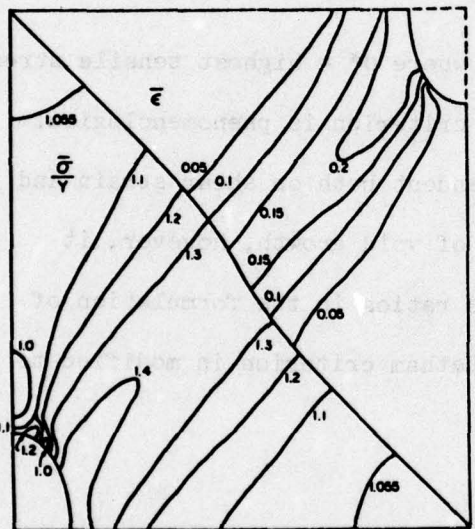
Fig. 27 Model for distribution of large voids.



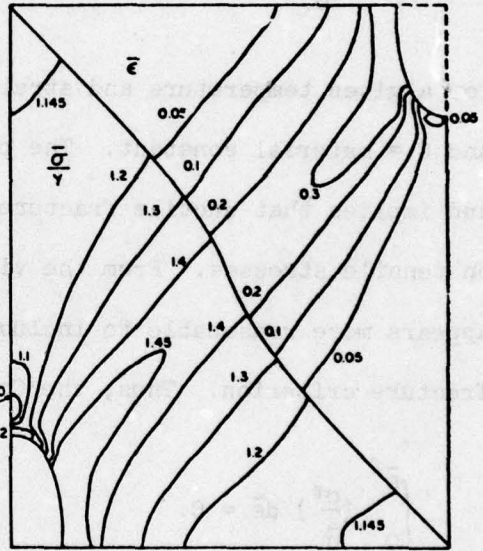
(a)



(b)



(c)



(d)

Fig. 28 Effective stress and effective strain distributions in the unit section. (a) $e_2 = 0.00525$; (b) $e_2 = 0.0423$; (c) $e_2 = 0.0699$; (d) $e_2 = 0.1163$.

When the stress ratios vary during deformation, McClintock's model leads to the condition given by

$$\int_0^{\bar{\epsilon}^f} \left[\frac{2}{\sqrt{3}(1-n)} \sinh\left\{ \frac{\sqrt{3}(1-n)}{2} \frac{\sigma_a + \sigma_b}{\bar{\sigma}} \right\} + \frac{\sigma_b - \sigma_a}{\bar{\sigma}} \right] d\bar{\epsilon} = K, \quad (14)$$

instead of Eq. (13), where K is the same factor as that in Eq. (13).

Another fracture criterion which will be considered in the present investigation is the one proposed by Cockcroft and Latham [15], [16]. They proposed that fracture occurs when

$$\int_0^{\bar{\epsilon}^f} \bar{\sigma} \left(\frac{\sigma^*}{\bar{\sigma}} \right) d\bar{\epsilon} = C \quad (15)$$

for a given temperature and strain-rate, where σ^* = highest tensile stress and C = material constant. The proposed criterion is phenomenological and implies that ductile fracture is dependent both on shear strain and on tensile stresses. From the viewpoint of void growth, however, it appears more reasonable to include stress ratios in the formulation of fracture criterion. Thus, the Cockcroft-Latham criterion is modified to

$$\int_0^{\bar{\epsilon}^f} \left(\frac{\sigma^*}{\bar{\sigma}} \right) d\bar{\epsilon} = C. \quad (16)$$

It may be of interest to note that Eq. (14) reduces to Eq. (16) with $K = 2C$, if the argument of sinh is small so that the hyperbolic sine function is approximated by a linear function. The magnitude of the argument of sinh depends on the stress state as well as on the work-hardening coefficient. When $n = 1$, Eqs. (14) and (16) are identical. For other values

of the work-hardening coefficient, the difference between the two criteria is small if $\frac{\sigma_a + \sigma_b}{\bar{\sigma}} < 1$, but increases with increasing values of $\frac{\sigma_a + \sigma_b}{\bar{\sigma}}$, as shown in Fig. 29.

We now examine in more detail the two criteria expressed by Eq. (14) and by Eq. (16).

A. Surface fracture

Since the fracture condition applicable to the free-surface cracks can be observed experimentally, several investigators [17]-[20] have used upsetting of cylindrical specimens for the study of ductile fractures. It was concluded from these investigations that the fracture criterion is expressed by

$$\epsilon_1 = a - \frac{1}{2} \epsilon_2, \quad (17)$$

where a is a material constant and ϵ_1 and ϵ_2 are the circumferential strain and the axial strain at the equatorial free surface, respectively. The two principal stresses in the surface, σ_1 and σ_2 ($\sigma_1 > \sigma_2$), during plastic deformation, are expressed by

$$\sigma_1 = \frac{\bar{\sigma}}{\sqrt{3}} \frac{2 + \alpha}{\sqrt{1 + \alpha + \alpha^2}} + \sigma_e, \quad \sigma_2 = \frac{\bar{\sigma}}{\sqrt{3}} \frac{1 + 2\alpha}{\sqrt{1 + \alpha + \alpha^2}} + \sigma_e, \quad (18)$$

where $\alpha = \frac{d\epsilon_2}{d\epsilon_1}$ and σ_e is a hydrostatic stress acting on the surface. The incremental effective strain $d\bar{\epsilon}$ is given by

$$d\bar{\epsilon} = \frac{2}{\sqrt{3}} \sqrt{1 + \alpha + \alpha^2} d\epsilon_1, \quad (19)$$

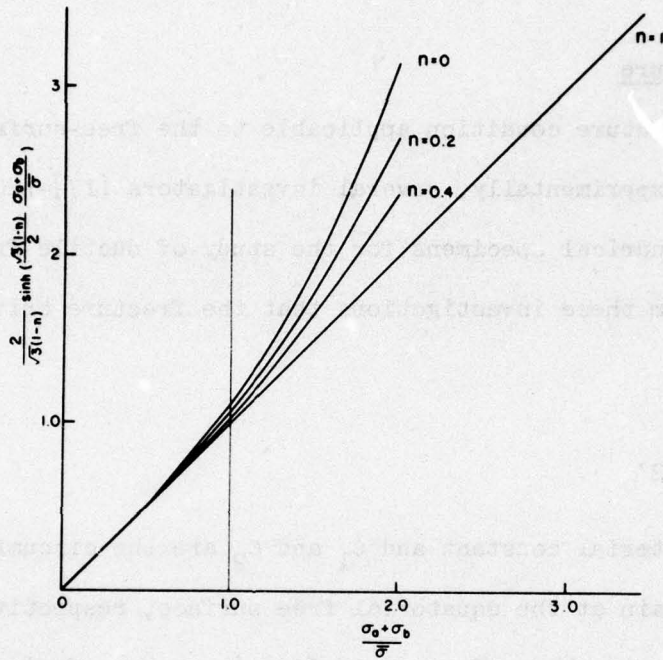


Fig. 29 Plot of hyperbolic sine function for various values of the work-hardening coefficient.

Under these conditions, the fracture criteria given by Eqs. (14) and (16) are both path-dependent, except when Eq. (16) becomes path-independent for $\sigma_e = 0$. Taking linear strain paths under $\sigma_e/\bar{\sigma} = \text{const.}$, and noting that σ_a and σ_b are the minimum and maximum stresses, respectively, Eq. (14) gives, for non-work-hardening materials ($n = 0$), the fracture strain as

$$\epsilon_1^f = \frac{\sqrt{3}}{2\sqrt{1 + \alpha + \alpha^2}} \left[\frac{K}{\frac{2}{\sqrt{3}} \sinh\left(\frac{\sqrt{3}}{2} \frac{\sigma_1 + \sigma_2}{\bar{\sigma}}\right) + \frac{\sigma_1 - \sigma_2}{\bar{\sigma}}} \right] \quad (20)$$

for $\alpha \leq -\frac{1}{2}$, and

$$\epsilon_1^f = \frac{\sqrt{3}}{2\sqrt{1 + \alpha + \alpha^2}} \left[\frac{K}{\frac{2}{\sqrt{3}} \sinh\left(\frac{\sqrt{3}}{2} \frac{\sigma_1 + \sigma_e}{\bar{\sigma}}\right) + \frac{\sigma_1 - \sigma_e}{\bar{\sigma}}} \right] \quad (21)$$

for $-\frac{1}{2} \leq \alpha \leq 0$. The criterion given by Eq. (16) becomes

$$\int_0^{\bar{\epsilon}^f} \frac{\sigma^*}{\bar{\sigma}} d\epsilon = \int_0^{\bar{\epsilon}^f} \frac{\sigma_1}{\bar{\sigma}} d\bar{\epsilon}$$

from which

$$\epsilon_1^f = \frac{\sqrt{3}}{2\sqrt{1 + \alpha + \alpha^2}} \left(\frac{C}{\sigma_1/\bar{\sigma}} \right) = \frac{C}{\frac{2}{3}(2 + \alpha) + \frac{2}{\sqrt{3}}(\sqrt{1 + \alpha + \alpha^2}) \left(\frac{\sigma_e}{\bar{\sigma}} \right)}. \quad (22)$$

Eqs. (20), (21), and (22), with $\sigma_e/\bar{\sigma} = 0$ are plotted for $K = 0.5$ and $C = 0.25$ in Fig. 30.

It can be seen in Fig. 30 that the fracture line given by Eq. (22) has a slope of $-\frac{1}{2}$ for $\sigma_e/\bar{\sigma} = 0$ (free-surface cracks), and Eqs. (20) and

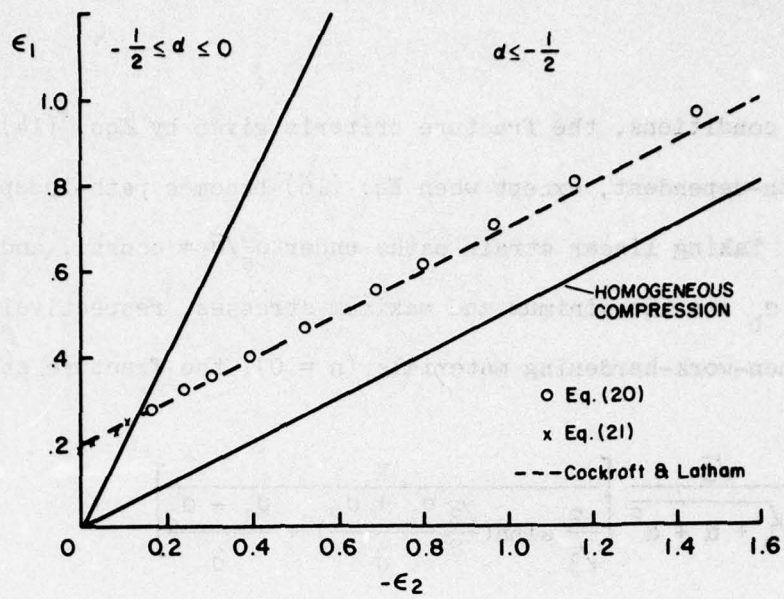


Fig. 30 Fracture conditions predicted from Eqs. (20) and (21) and by Cockroft and Latham [16].

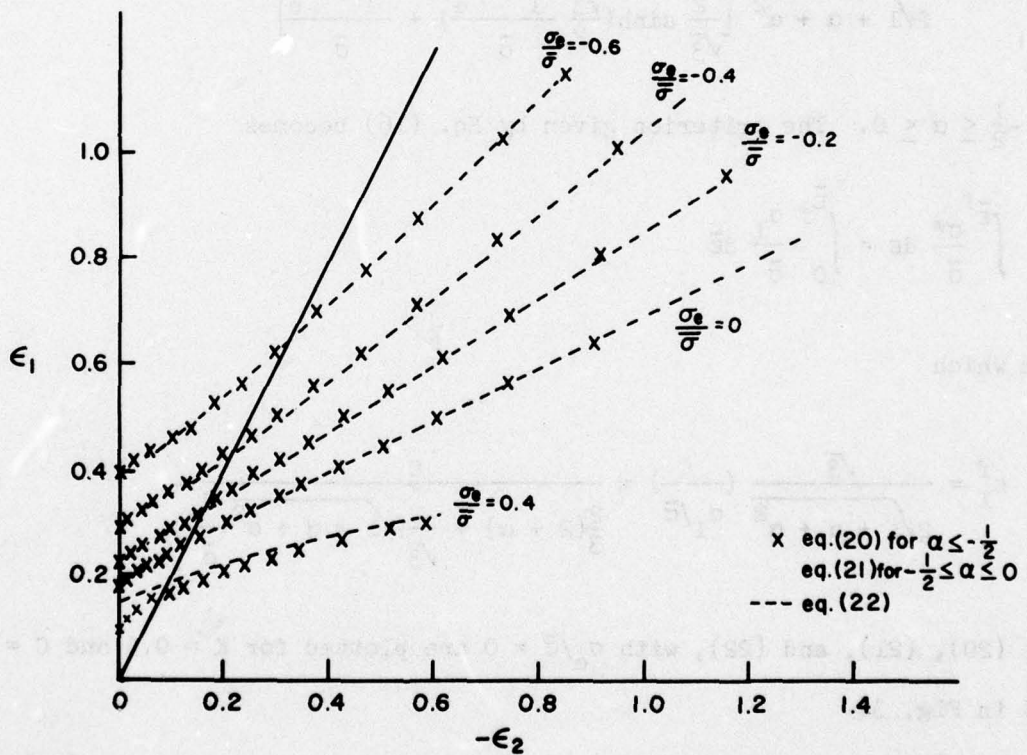


Fig. 31 Comparison of two fracture criteria for various values of $\sigma_e/\bar{\sigma}$.

(21) result in almost the same fracture strains as those according to Eq. (22) if the relationship $K = 2C$ is maintained. Similar plots of Eqs. (20), (21), and (22) for various values of $\sigma_e/\bar{\sigma}$ are given in Fig. 31.

B. Fracture in uniaxial tension

Bridgman [21] investigated plastic flow and fracture with special emphasis on the effects of hydrostatic pressure, using uniaxial tension. The two criteria given by Eqs. (14) and (16) are examined for internal fracturing, using the Bridgman experimental results. In uniaxial tension of a bar, the critical site for fracture is at the axis of symmetry in the neck section where $\epsilon_1 = \epsilon_z$ and $\alpha = \frac{1}{2}$. Therefore, $\sigma_a = \sigma_r = \sigma_e$ and $\sigma_b = \sigma_z = \bar{\sigma} + \sigma_r$. Then, Eq. (14) is expressed by

$$\int_0^{\bar{\epsilon}^f} (F_1 + 1) d\bar{\epsilon} = K, \quad (23)$$

where $F_1 = h$ when $h > -1$,

$$F_1 = -1 \text{ when } h \leq -1$$

and

$$h = \frac{2}{\sqrt{3}(1-n)} \sinh\left\{\frac{\sqrt{3}(1-n)}{2}\left(1 + 2\frac{\sigma_r}{\bar{\sigma}}\right)\right\},$$

assuming that the negative damage rate is not permitted.

The criterion given by Eq. (16) becomes

$$\int_0^{\bar{\epsilon}^f} (F_2 + 1) d\bar{\epsilon} = C, \quad (24)$$

where

$$F_2 = \frac{\sigma_r}{\bar{\sigma}} \quad \text{for } \frac{\sigma_r}{\bar{\sigma}} > -1$$

and

$$F_2 = -1 \quad \text{for } \frac{\sigma_r}{\bar{\sigma}} \leq -1.$$

Eqs. (23) and (24) are compared with experiments in Figs. 32 and 33, respectively. The experimental results by Bridgman used for comparison are summarized in Table 5.

In deducing experimental points in the figures from the data in Table 5, several assumptions and approximations are introduced: (1) the effective stress $\bar{\sigma}$ was assumed to be independent of the hydrostatic pressure, (2) the stress σ_r at the neck was estimated according to the Bridgman analysis, and (3) the effect of work-hardening coefficients was neglected.

The comparison shown in Figs. 32 and 33 reveals that the fracture criteria are both reasonably good for predicting the fracture strains.

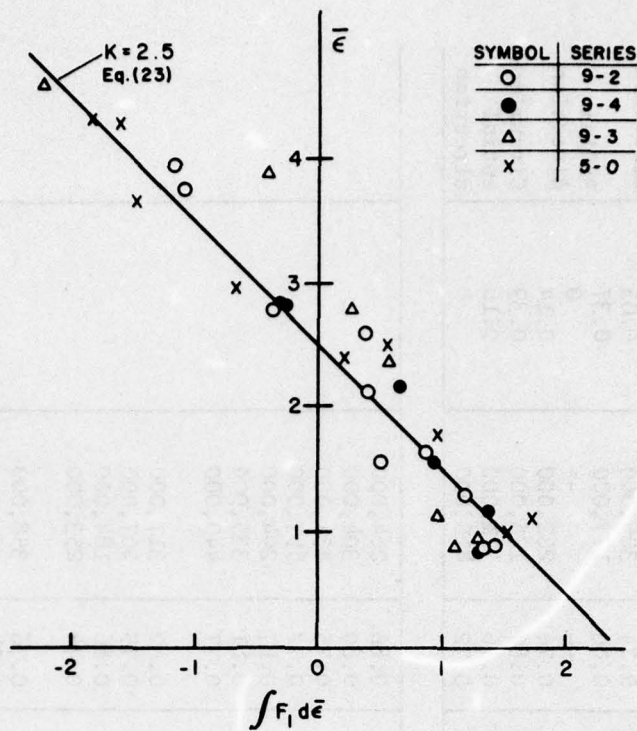


Fig. 32 Comparison between the fracture criterion given by Eq. (23) and Bridgman's fracture data.

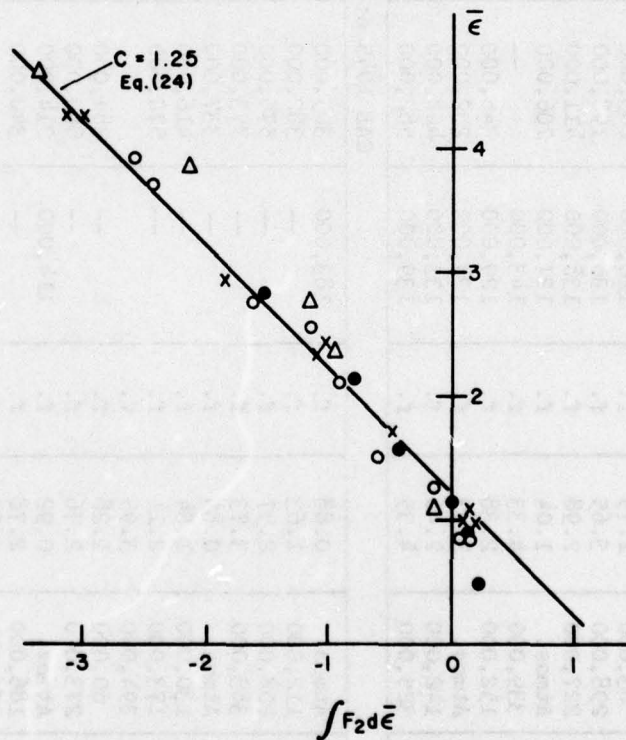


Fig. 33 Comparison between the fracture criterion given by Eq. (24) and Bridgman's fracture data.

Table 5 Bridgman experimental data.

Specimen	Pressure psi	Strain $\log A_1/A$	Fract. or not	Ave. stress at max. load psi	Ave. final stress, psi	a/R	Corr. factor	Final flow stress F, psi	Ratio of areas in fracture	Remarks
Navy Gun Steel, as received										
5-0-1	Atmos.	1.12	f.	125,000	214,000	(0.74)	0.86	184,000	0.38	Longi-
5-0-2	83,000	1.75	f.	126,000	265,000	(1.19)	0.80	213,000	0.25	tudinal
5-0-3	298,000	3.65	f.	136,000	198,000	(1.96)	0.73	143,000	0	direction
5-0-5	227,000	2.98	f.	138,000	411,000	(1.78)	0.74	305,000	0.03	
5-0-6	Atmos.	1.04	f.	127,000	206,000	(0.70)	0.86	177,000	0.37	Radial
5-0-8	339,000	4.33	f.	143,000	--	--	--	--	0	direction
5-0-9	152,000	2.38	f.	129,000	345,000	(1.53)	0.76	262,000	0.14	
5-0-10	Atmos.	1.03	f.	124,000	202,000	(0.69)	0.87	175,000	0.39	Circumfer-
5-0-11	142,000	2.46	f.	133,000	408,000	(1.56)	0.76	311,000	0.16	ential
5-0-13	325,000	4.35	f.	139,000	582,000	(2.10)	0.72	415,000	0	direction
SAE 1045 steel [†]										
9-2-1	Atmos.	0.88	f.	183,000	305,000	--	0.86	264,000		
9-2-6	112,000	1.63	f.	--	382,000	--	0.80	304,000		
9-2-7	208,000	2.57	f.	--	575,000	--	0.75	431,000		
9-2-8	383,000	3.73	f.	--	773,000	--	0.72	557,000		
9-2-18	Atmos.	0.85	f.	--	337,000	--	0.87	294,000		
9-2-20	130,000	1.54	f.	--	416,000	--	0.81	335,000		
9-2-22	173,000	2.11	f.	--	570,000	--	0.77	440,000		
9-2-23	394,000	3.95	f.	--	--	--	0.82	317,000		
9-2-24	60,000	1.28	f.	--	384,000	--	0.75	507,000		
9-2-26	273,000	2.76	f.	114,000	680,000	--	0.86	184,000		
9-3-1	Atmos.	0.92	f.	--	214,000	--	0.74	253,000		
9-3-5	186,000	2.78	f.	--	340,000	--	0.74	253,000		
9-3-6	269,000	3.87	f.	--	--	--	0.76	358,000		
9-3-7	145,000	2.37	f.	--	474,000	--	0.84	210,000		
9-3-9	34,000	1.10	f.	--	250,000	--	0.87	180,000		
9-3-10	387,000	4.61	f.	--	206,000	--	0.86	163,000		
9-3-11	Atmos.	0.81	f.	105,000	189,000	--	0.84	125,000		
9-4-1	Atmos.	0.89	f.	--	149,000	--	0.77	240,000		
9-4-7	18,000	1.13	f.	--	313,000	--	0.86	163,000		
9-4-9	116,000	2.14	f.	--	189,000	--	0.80	180,000		
9-4-12	Atmos.	0.90	f.	--	225,000	--	0.74	295,000		
9-4-13	74,000	1.56	f.	--	396,000	--				
9-4-14	182,000	2.83	f.	--	--	--				
9-4-15	389,000	4.80	f.	--	--	--				

Table 5 (continued)

† SAE 1045 steel	Quenched into water from 1575°F; drawn to 800°F
9-2 series:	Quenched into salt at 800°F from 1575°F
9-3 series:	Quenched into salt at 1100°F from 1575°F
9-4 series:	Quenched into salt at 1100°F from 1575°F

III. WORKABILITY IN EXTRUSION

For workability in extrusion with reference to center bursting, experimental observations are limited and information about the stresses developed in metal being deformed by extrusion is insufficient. Thus, Latham and Cockroft [15] speculated the conditions in axisymmetric extrusion by assuming that the slip-line theory can be applied even though this is appropriate only to plane-strain conditions. Also, it was assumed that lubrication during cold extrusion is sufficiently good for the calculations to be based on zero friction. Based on the tensile plastic work density, they determined a damage factor for a range of extrusion conditions for several metals. Avitzur [22], [23] investigated theoretically center bursting in extrusion, using the upper-bound approach. Because the fracture condition was not incorporated in the approach, some objections may be raised regarding the validity of the results. However, the study led to defining the range of successful extrusions in terms of die angle, friction conditions, and the reduction.

Hoffmanner [24] also performed slip-line analysis for extrusion and compared with viscoplasticity results for axisymmetric extrusion. He found that the calculated maximum center line principal stresses were in good agreement with viscoplasticity results when the plane strain and axisymmetric results were compared on the basis of equal cross-sections. Combining the slip-line analysis for deformation and the fracture criterion proposed by Cockroft and Latham [16], Hoffmanner examined workability in extrusion. In Fig. 34, the three parabolic curves represent the process-

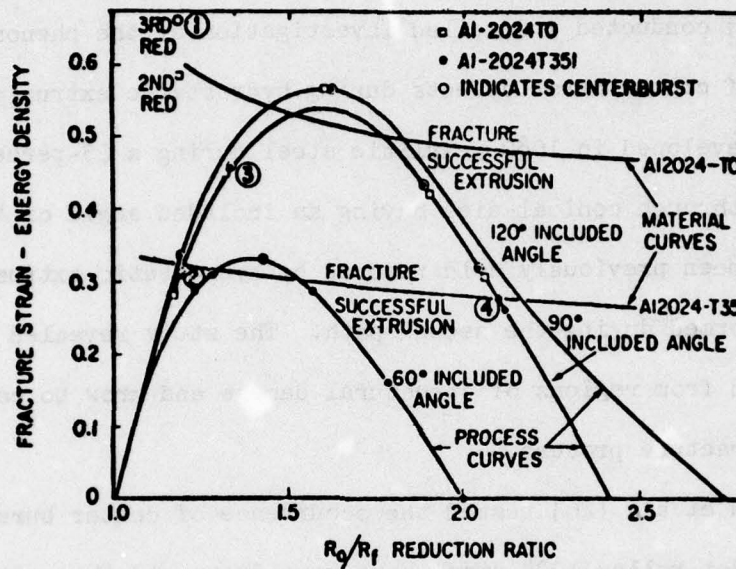


Fig. 34 Workability criteria for center burst based on a maximum tensile stress-strain energy criterion [23].

required strain energy as a function of the reduction ratio for three die angles. Whenever the process-required energy exceeds the energy available for successful deformation of the material, center burst should be observed. The extrusion observations are superimposed on these curves and demonstrate the near-perfect agreement between practice and prediction.

A. Experimental data

Pepe [25] conducted a detailed investigation of the phenomenological development of center burst defects during hydrostatic extrusion. Central bursts were developed in 1080 pearlitic steel during a 25-percent reduction in area pass through conical dies having an included angle of 45° . The material had been previously cold reduced by hydrostatic extrusion. Central bursts were formed during the second pass. The study revealed that central bursts develop from regions of structural damage and grow to completion by a two-stage fracture process.

Zimmerman et al. [26] tested the occurrence of center bursting using 1024 steel. Hot-rolled 1024 steel bars were drawn and then extruded in three steps. The final extrusion step was utilized to examine, through a variety of die semi-angles, whether central bursting was produced or not. They found that among 4000 (1000 shafts from each of the four heats) shafts, center bursting was detected in about 45 shafts from one of the heats.

The above observations of center bursting in extrusion, as some other experimental studies show, were all made in material which has been pre-deformed. Although the present theoretical method is applicable to the determination of stress and strain distributions in extrusion for the material which has distributed strength and is capable of following the

previous deformation history, the experimental observation of center bursting during a single pass of deformation has been sought because the process condition in the computation can then be specified more faithfully according to the experimental procedure. In the present investigation, experiments reported by Hoffmann [24] were used for examining the validity of the workability theory.

Hoffmann observed center bursting in a single-step extrusion for aluminum alloy 2024-T351 at room temperature. The experimental conditions and the results were as follows:

1. Material: The specimens were obtained from a 3-inch diameter of aluminum alloy 2024 in as-received T351 condition.
2. Tensile test: Testing was performed at room temperature on an Instron testing machine at a nominal strain rate of 0.1 in/in/min. Measurements of extension were performed continuously until fracture with an extensometer exhibiting a strain sensitivity of at least 0.0005 in/in. Measurements of the minimum cross-sectional radius (a) and neck radius of curvature (R) were performed in two directions at 90° to each other either continuously by photographing the specimen or discontinuously by removing the specimen from the test fixtures and performing these measurements on an optical comparator.
3. Compression test: Compression testing was investigated by using simple upsetting of cylinders. For strain measurements, an orthogonal array of Vickers diamond pyramid impressions was accurately placed at 0.050-inch separations about the exact center of the specimens along subsequent directions of principal normal stress. These directions corresponded to the direction of loading and

the direction normal to it through the center of the specimen.

Eight impressions were placed in each of the two directions.

4. Extrusion: Extrusion was performed at a ram speed of 12 in/min with dies of (60°), 90°, and (120°) included angles with anhydrous lanolin as a lubricant. Both the billets and the container were lubricated prior to extrusion and load-time curves were recorded on an oscillograph during deformation. The billets were machined with one end contoured to match the die and approximately 0.005 inch under the container diameter. A surface finish in the 20 to 30 microinch rms range was specified. Initial billet diameters of 1.780, 1.412, and 0.812 were used. The two larger diameters were used in extrusion through 90° dies to study single- and multiple-pass extrusion and the 0.812 diameter billets were used in single-pass reductions through all three die angles.

Results

1. Tension test results

Table 6

Specimen number	Gauge section diameter (inch)	Initial a/R ratio	Final a/R ratio	Fracture strain	Remarks
TNLH1	0.250	0	0.294	0.382	Longitudinal specimen
TNLH2	0.250	0	0.342	0.354	Longitudinal specimen
TNTH1	0.250	0	0	0.146	Transverse specimen
TNTH2	0.250	0	0	0.156	Transverse specimen

2. Compression test results

Table 7

Specimen no.	-		Initial height/diameter ratio	Fracture strain	Remarks
	Initial	Final			
UHN-1(upset)	0.50	1.61	1.145	0.265	Teflon lub., sheared over
UHN-2(upset)	0.50	-	2.24	-	
UHN-3(upset)	0.50	1.58	1.145	0.281	

3. Extrusion results

Table 8

Specimen no.	R_o/R_f	Included die angle	Remarks
HN-101A	1.245	90°	Unlubricated, billet stuck
HN-101B	1.326	90°	Centerburst
HN-101C	1.249	90°	Centerburst
HN-451	1.157	90°	Centerburst
HN-452	2.328	90°	
HN-990	1.988	90°	Centerburst
HN-999	1.089	90°	
HN-90B	2.132	90°	

B. Computation, results, and discussion

Using the matrix method, the extrusion process was analyzed for the material, al alloy 2024-T351, and the detailed mechanics were presented in Part 1 of this report. The process conditions were: semi-cone angle $\alpha = 45^\circ$, area reduction $R_i/R_0 = 1.25, 1.6, 1.8, \text{ and } 2.0$ for the two friction conditions, $f = 0$ and $0.4Y_0$. The critical site for occurrence of center bursting is along the axis of extrusion. The stress and strain states along the axis of extrusion resulted from the computation described in Part 1. Because the strain system along the axis of extrusion is identical

to that in uniaxial tension, the quantities necessary for workability are

$$\int_0^{\bar{\epsilon}} (F_1 + 1) d\bar{\epsilon} \quad \text{from Eq. (23) for one criterion}$$

and

$$\int_0^{\bar{\epsilon}} (F_2 + 1) d\bar{\epsilon} \quad \text{from Eq. (24) for another.}$$

These quantities are plotted as functions of area reduction in Figs. 35 and 36. From the figures, some conclusions immediately follow. The two quantities are almost identical, with a factor of 2. The magnitudes decreased greatly when work-hardening of materials was included. The magnitudes decreased further with friction at the die-workpiece interface. Note that the curve for non-work-hardening materials in Fig. 36 is in good agreement with the Hoffmann result given in Fig. 34 for 90° included angle. This is somewhat surprising because the curve by Hoffmann was obtained by approximations based on the slip-line analysis.

The critical values of these quantities (K in Eq. (23) and C in Eq. (24)) above which fracturing is predicted can be obtained from the fracture data in tension or compression tests. Hoffmann estimated $C \approx 0.3$ ($K = 2C$) from the tension test results. On the other hand, another estimate of $C \approx 0.08$ was obtained from the compression test results. If we apply the critical value of $C = 0.3$ to the results in Fig. 36, fracturing should not occur in all the reductions. If we assume $C = 0.08$ to be a critical value, then center bursting would be observed over the range $1.08 < R_1/R_0 < 1.86$ with frictionless die and $1.16 < R_1/R_0 < 1.60$ with friction $f = 0.4Y_0$.

Although the prediction of workability with a critical value, $C = 0.08$, appears to be in good agreement with the experimental results in Table 8,

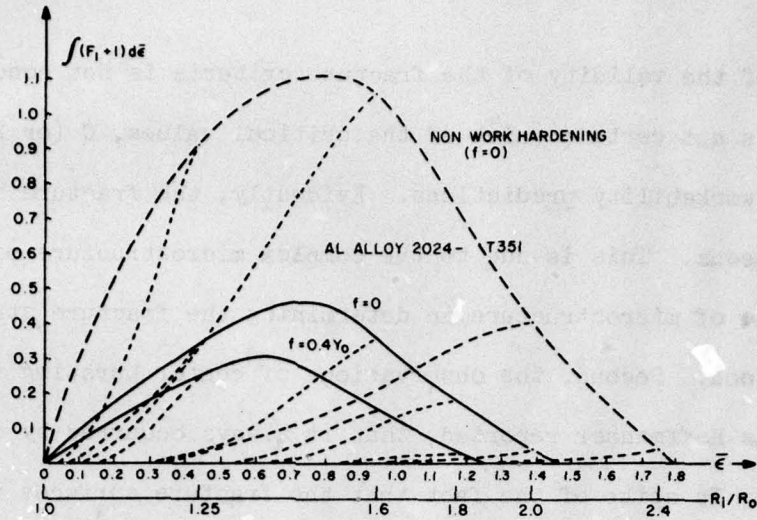


Fig. 35 Variations of $\int_0^{\bar{\epsilon}} (F_1 + 1) d\bar{\epsilon}$ as a function of area reduction in extrusion. Materials: non-work-hardening and al alloy 2024-T351.

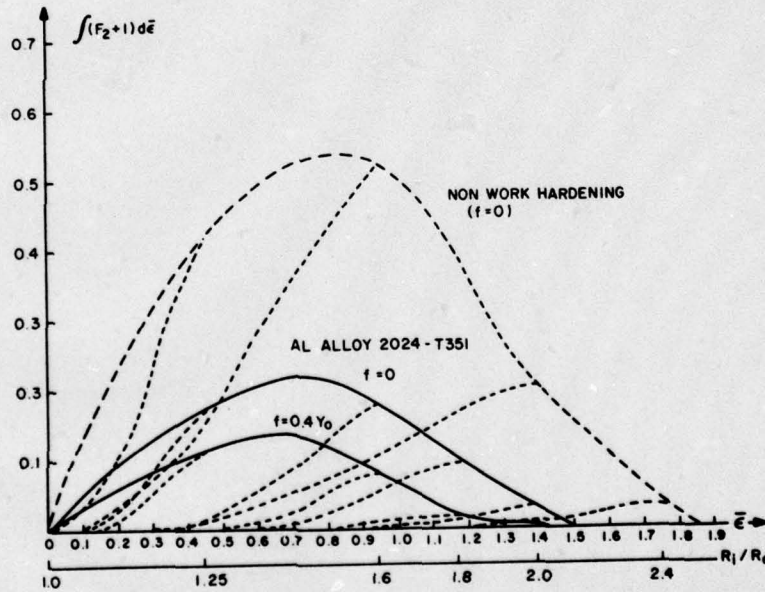
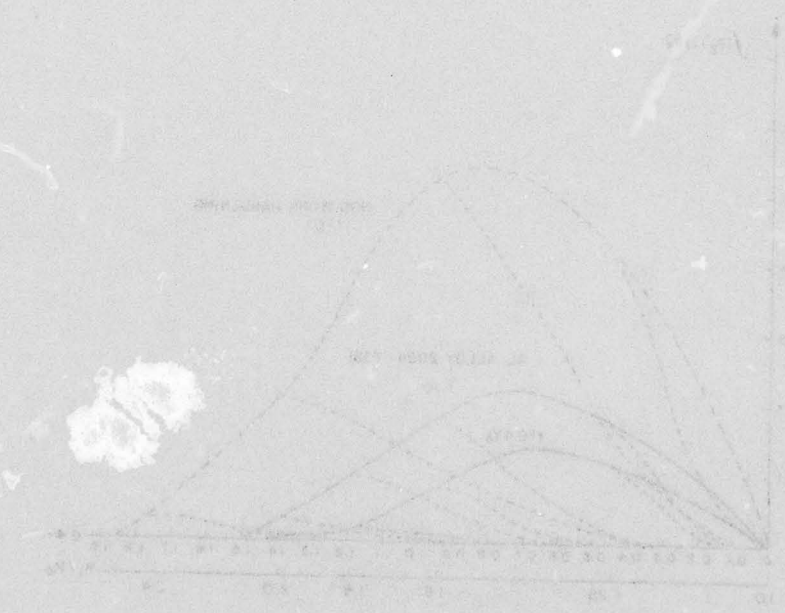


Fig. 36 Variations of $\int_0^{\bar{\epsilon}} (F_2 + 1) d\bar{\epsilon}$ as a function of area reduction in extrusion. Materials: non-work-hardening and al alloy 2024-T351.

the proof of the validity of the fracture criteria is not conclusive. First, it is not certain which of the critical values, C (or K), is proper to use for workability predictions. Evidently, the fracture behavior is not homogeneous. This is due to the complex microstructure of the material and the role of microstructure in determining the fracture strains is not yet understood. Second, the observations of center bursting in Table 8 revealed, as Hoffmann reported, that it always occurred by complete separation. In spite of the fact that the fracture surfaces always possessed the centrally located conical cavity typical of the center burst, whether fracturing initiated at the center is in doubt.



IV. WORKABILITY IN DRAWING

To determine workability in drawing, the same approach as that for extrusion was applied. The process mechanics were analyzed by the matrix method and the stress and strain distributions along the axis of drawing were computed for various reductions of area. The tension and compression tests were performed to obtain the stress and strain property of the material and to determine the critical value for fracturing. Combining these data, the workability in drawing was predicted. The drawing experiments were conducted at room temperature to examine the predictions. The material was SAE 1144 cold-drawn steel. The stress-strain property of the material is given in Part 1.

A. Process mechanics

The process conditions were: semi-die angle $\alpha = 8^\circ$; area reduction $R_i/R_0 = 1.05, 1.10, 1.2, 1.3$; and friction $f = 0, 0.25Y_0$. The stress and strain distributions were obtained and the significant quantities for fracturing were determined for each area reduction.

Because the two fracture criteria discussed in the previous sections resulted in almost identical predictions of fracture conditions, only the quantities (normalized energy density) defined by $\int_0^{\bar{\epsilon}} (F_2 + 1) d\bar{\epsilon}$ was shown as a function of the area reduction in Fig. 37. In calculating the energy density, the stress components were determined by correcting the hydrostatic part of the stress components from the total force balance. It is seen in Fig. 37 that the energy densities for the critical path along the axis of drawing increased monotonically with increasing area reduction.

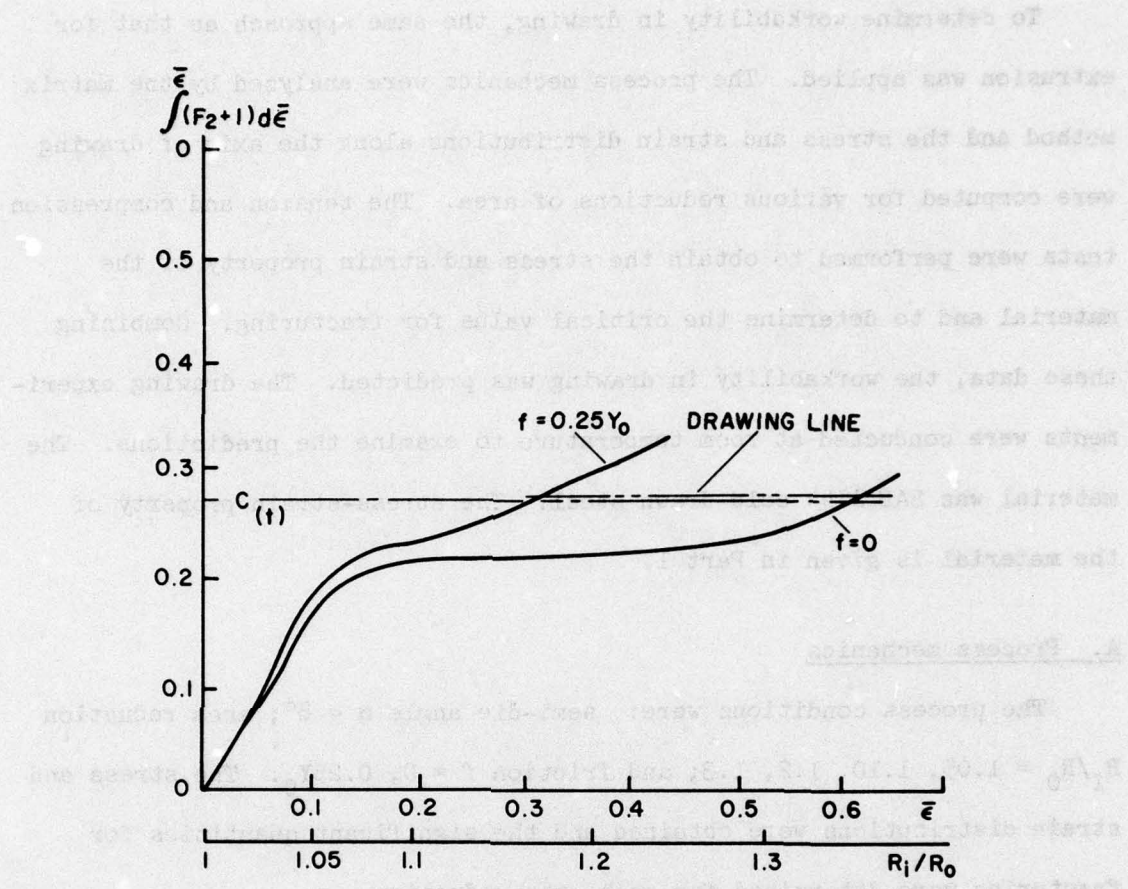


Fig. 37 Variations of $\int_0^{\epsilon} (F_2 + 1) d\epsilon$ as a function of area reduction in drawing. Material: SAE 1144 cold-drawn steel.

They were larger for larger die-workpiece interface friction. This is contrary to the extrusion results shown in Figs. 35 and 36. To determine workability, this energy density level must be compared with the critical value C for fracturing, estimated from the fracture data in tension and compression tests.

B. Tension and compression tests

Tension specimens were machined longitudinally from a 0.5-in. diameter bar. Testing was performed on an Instron machine with a plate speed of 0.02 in/min. The load-displacement curve was recorded and the instantaneous neck radii, as well as neck diameter, was measured until fracture. The critical energy density was estimated from the tension test as $C_{(t)} = 0.271$. The Bridgman analysis was used for an approximate stress analysis during neck formation.

Compression specimens were machined from the same bar of 0.5-in. diameter. The height and the diameter of the specimens were 0.50 in. and 0.49 in., respectively. The grid lines were printed on the cylindrical surface of the specimens, and the strains at fracture were determined from the grid distortion of the deformed specimens. The critical value C was estimated from the fracture strains according to Eq. (22) and was given by $C_{(c)} = 0.093$. It is to be noted that the fracture behavior is different in tension and in compression.

C. Workability

The energy density in drawing shown in Fig. 37 is compared with the critical value for fracturing in order to predict workability of SAE 1144

steel in drawing. It is seen again that the prediction is drastically different depending upon which critical value of tension and compression is applied. With the critical value of 0.09 which was estimated from the compression tests, center bursting would occur in all drawing with the area reduction larger than $R_1/R_0 = 1.03$, with very little effect of die-workpiece interface. On the other hand, if $C_{(t)}$ is taken as the critical value, the prediction is that for frictionless dies no center burst would occur up to $R_1/R_0 = 1.36$, and that this limiting value decreases with increasing die friction; for example, for friction $f = 0.25Y_0$, center burst would not be observed for R_1/R_0 less than 1.16.

In order to examine the workability predictions, bar drawing experiments were performed. The bar specimen configuration is shown in Fig. 38. A threaded grip was used for drawing. This scheme, however, sets the drawing limit according to the maximum drawing force which can be sustained by the threaded part of the specimen. Commercially available carbide drawing dies with 8° semi-included die angle were used. The steady-state drawing force was measured, and the occurrence of center bursting was checked with drawn bars. The experimental conditions and results are summarized in Table 9.

Table 9 Experimental conditions and results.

Specimen no.	(Outlet diam.) $2R_0$	(Inlet diam.) $2R_1$	(Reduc. ratio) R_1/R_0	Lubrication	Ave. drawing pressure $(L/\pi R_0^2 Y_0)$	Center bursting
4	0.388"	0.485"	1.25	White lead in oil	0.907	} No
8	0.388"	0.465"	1.198	"	0.713	
5	0.4195"	0.485"	1.156	"	0.691	
16	0.4195"	0.465"	1.108	"	0.361	
1	0.451"	0.485"	1.075	"	0.435	
9	0.451"	0.465"	1.031	"	0.428	
21	0.451"	0.5"	1.109	Dry	0.664	
7	0.465"	0.465"	1.198	Dry	0.997	

In Fig. 38 the experimental and theoretical average drawing stresses were plotted as functions of the reduction ratio R_i/R_0 . Theoretical curves were for frictionless dies ($f = 0$) and for the frictional stress $f = 0.25Y_0$. The experimental values with and without lubrication fell between these two theoretical curves. The drawing limit due to the present experimental scheme is also shown in Fig. 38. Under the lubricated condition, drawing over the reduction range of $R_i/R_0 = 1.031 \sim 1.25$ produced no center bursting. This suggests that the use of the critical value $C_{(c)}$, estimated from the compression fracture data for workability prediction, was not appropriate. With regard to the critical value of $C_{(t)} = 0.271$, it was found that the drawing limit set by the present experimental scheme was very close to the critical value $C_{(t)}$, as shown in Fig. 37. In fact, drawing was not possible for three cases of drawing under the dry condition. As a result, it was not possible to determine the applicability of $C_{(t)}$ as a fracture criterion to the occurrence of center bursting in bar drawing.

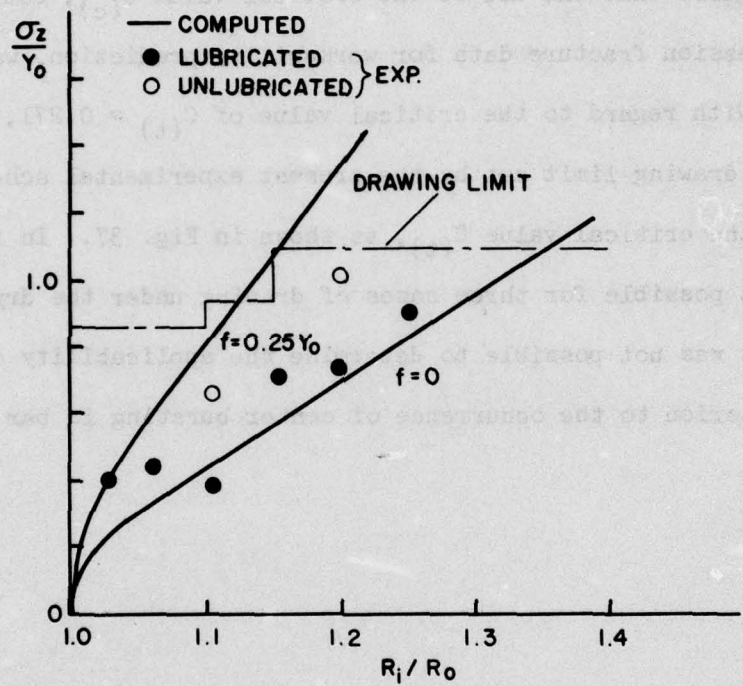
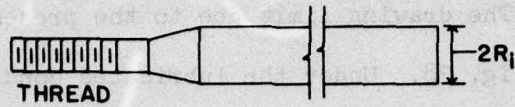


Fig. 38 Computed and experimental average drawing stress as functions of area reduction.

V. SUMMARY AND DISCUSSION

For workability in metalworking processes, formulation of a ductile fracture criterion must be simple (or in the form of easy applicability) and yet reflect physical mechanisms of fracture so that the predicted fracture behavior is close to the one of real materials within reasonable accuracy. With a two-size voids model a modified interpretation to the McClintock formulation of fracture strains was given. It was shown then that this formulation and the one by Cockcroft and Latham resulted in almost identical fracture strains for occurrence of free-surface cracks and for fracturing in uniaxial tension. It was demonstrated further that these formulations predicted reasonably well the experimentally observed fracture strains. In examining the validity of the prediction by experiments, the stress-strain histories at a critical site were determined by using the continuous experimental observations on distortion in the case of surface cracks and by the Bridgman analysis combined with experimental measurements of load and neck geometry in the case of uniaxial tension. In applying the criteria to occurrence of center bursting in axisymmetric extrusion and drawing, the determination of stress and strain paths at a critical site was provided theoretically by the matrix method of analysis. The critical value of the material's capability against fracturing was obtained by tension and compression experiments. Workability in extrusion was examined for aluminum alloy 2024-T351 using the data found in the literature and the experiments of workability in drawing was attempted for SAE 1144 cold-drawn steel to test the predictions. The results of

validation were inconclusive. This is attributed to the fact that the fracture behavior has directionality as evidenced from the tension and compression fracture data. Furthermore, most of the previous investigations on center bursting in extrusion and drawing have reported observations of center bursting in pre-deformed materials. Although alloy 2024-T351 was reported to have produced center bursting in a single extrusion path at room temperature, it occurred always by complete separation. With regard to bar drawing of SAE 1144 steel, the drawing limit set by the present experimental scheme was very close to the limiting energy density level, thereby making it extremely difficult to perform drawing near the critical boundary of the sound and defect zones.

In spite of inconclusive results of workability, the present investigation revealed several significant findings. In extrusion, the energy density level critical for center bursting was less for work-hardening materials when compared with that for a non-work-hardening material. This energy density level is reduced with increasing friction at the die-workpiece interface. It increases first with increasing area reduction and then decreases indicating a maximum as a function of area reduction. In drawing, the energy density level monotonically increases with the area reduction, and increases, as opposed to that in extrusion, with increasing interface friction.

Although conclusive validity of the present workability theory in extrusion and drawing awaits more extensive and systematic experimental investigations, as well as theoretical calculations, the method of computation is available and the approach has been cleared toward complete understanding of ductile fracture in metalworking processes.

REFERENCES

1. S. N. Shah, S. I. Oh, and Shiro Kobayashi, "Theories on Flow and Fracture in Metalworking Processes," USAF Technical Report AFML-TR-76-1, May 1976.
2. C. H. Lee and S. Kobayashi, "New Solutions to Rigid-plastic Deformation Problems Using a Matrix Method," Trans. ASME, J. of Engrg for Ind., vol. 95, 1973, pp. 865-873.
3. K. Washizu, Variational Methods in Elasticity and Plasticity, Pergamon Press, 1950.
4. O. C. Zeinkiewicz and Y. K. Cheung, The Finite-Element Method in Structural and Continuum Mechanics, McGraw-Hill, London, 1967.
5. G. Strang and G. J. Fix, An Analysis of the Finite-Element Method, Prentice-Hall, Englewood Cliffs, N.J., 1973.
6. S. N. Shah and Shiro Kobayashi, "A Theory on Metal Flow in Axisymmetric Piercing and Extrusion," to be published in J. Prod. Engrg, vol. 1, 1977.
7. T. Murota, T. Jimma, and K. Kato, "Analysis of Axisymmetric Extrusion," Bulletin of the JSME, vol. 13, 1970, pp. 1366-1374.
8. K. Iwata, K. Osakada, and S. Fujino, "Analysis of Hydrostatic Extrusion by the Finite-Element Method," Trans. ASME, J. of Engrg. for Ind., vol. 94, 1972, pp. 697-703.
9. C. H. Lee, H. Iwasaki, and S. Kobayashi, "Calculation of Residual Stresses in Plastic Deformation Processes," Trans. ASME, J. of Engrg. for Ind., vol. 95, 1973, pp. 283-291.
10. E. H. Lee, R. L. Mallett, and W. H. Yang, "Stress and Deformation Analysis of the Metal Extrusion Process," SUDAM No. 76-2, Stanford University, June 1976.
11. A. H. Shabaik and E. G. Thomsen, "Investigation of the Application of the Visioplasticity Methods of Analysis to Metal Deformation Processes," Final Report-Part II, Department of the Navy, 1968.
12. J. G. Wistreich, "Investigation of the Mechanics of Wire Drawing," Proc. Inst. Mech. Engrs., vol. 169, 1955, pp. 654-665.
13. F. A. McClintock, "A Criterion for Ductile Fracture by the Growth of Holes," J. Appl. Mech., 1968, p. 363.
14. F. A. McClintock, S. M. Kaplan, and C. A. Berg, "Ductile Fracture by Hole Growth in Shear Band," Int. J. of Fracture Mechanics, vol. 2, 1966, p. 614.

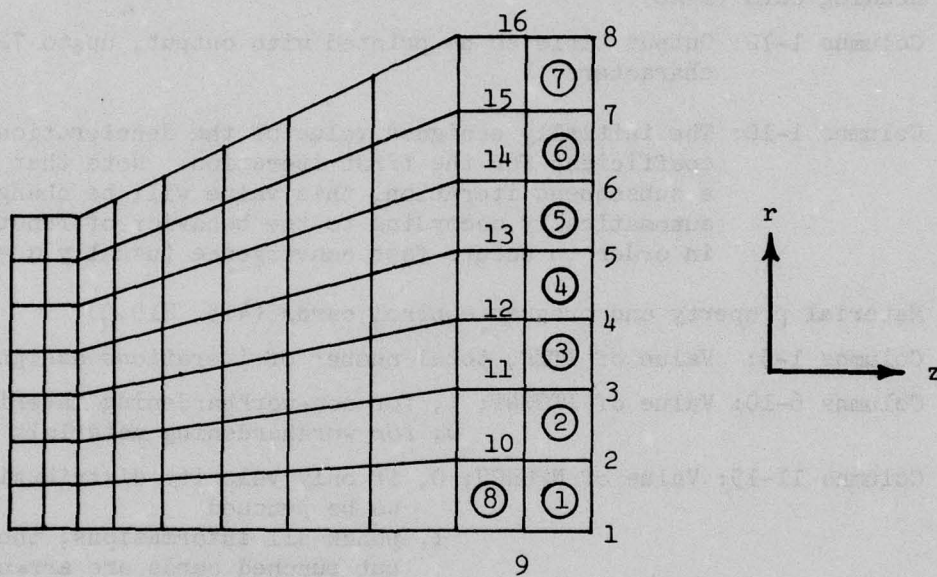
15. D. J. Latham and M. G. Cockroft, "The Effect of Stress System on the Workability of Metals," National Engineering Laboratory, Report No. 216, February 1966.
16. M. G. Cockroft and D. J. Latham, "A Simple Criterion of Fracture for Ductile Metals," National Engineering Laboratory, Report No. 240, July 1966.
17. H. Kudo and K. Aoi, "Effect of Compression Test Condition upon Fracturing of a Medium Carbon Steel--Study on Cold Forgeability Test, Part II," J. Japan Soc. for Tech. of Plasticity, vol. 8, 1967, pp. 17-27.
18. S. Kobayashi, "Deformation Characteristics and Ductile Fracture of 1040 Steel in Simple Upsetting of Solid Cylinders and Rings," Trans. ASME, J. Engrg. Ind., vol. 92, 1970, pp. 391-399.
19. Shiro Kobayashi, C. H. Lee, and S. I. Oh, "Workability Theory of Materials in Deformation Processes," USAF Technical Report AFML-TR-73-192, May 1973.
20. P. W. Lee and H. A. Kuhn, "Fracture in Metal-working Processes," Technical Report to American Iron and Steel Institute, April 1972.
21. P. W. Bridgman, Studies in Large Plastic Flow and Fracture, Harvard University Press, Cambridge, Mass., 1964, pp. 51-57.
22. B. Avitzur, "Analysis of Central Bursting Defects in Extrusion and Wire Drawing," ASME Trans. J. Engrg. Ind., vol. 90, 1968, pp. 79-91.
23. Z. Zimmerman and B. Avitzur, "Analysis of the Effect of Strain Hardening on Central Bursting Defects in Drawing and Extrusion," ASME Trans. J. Engrg. Ind., vol. 92, 1970, pp. 135-145.
24. A. L. Hoffmanner, "Workability Testing Techniques," Technical Report AFML-TR-69-174, June 1969.
25. J. J. Pepe, "Central Burst Formation During Hydrostatic Extrusion," Metals Engineering Quarterly, February 1976, pp. 46-58.
26. Z. Zimerman, H. Darlington, and E. H. Kottcamp, Jr., "Selection of Operating Parameters to Prevent Central Bursting Defects During Cold Extrusion," Metal Forming Interrelation Between Theory and Practice, edited by A. L. Hoffmanner, 1970, pp. 47-62.

APPENDIX

COMPUTER PROGRAM OF THE MATRIX METHOD
FOR THE ANALYSIS OF AXISYMMETRIC EXTRUSION AND DRAWING

I. Program Interpretation and Input Data Cards

The program was written according to the numbering system of nodal points and elements and the mesh system as shown in the figure.



The four surrounding nodal points (I, J, K, L) of an element are arranged in a clockwise direction with the lowest index assigned to I (e.g., for the first element in the figure (I, J, K, L) = (1, 9, 10, 2)).

The output values of stress and die force are all normalized by the initial yield stress and are positive in the sense of positive r or z direction.

In addition to preparing the input data cards, the following variables in program PURT need to be specified according to the mesh system and geometry considered:

THETA: Semi-included angle of conical die
 NIPTS: Number of lines in mesh system parallel to the axis of symmetry
 NJPTS: Number of lines in mesh system perpendicular to the axis of symmetry
 NTIMES: Number of flow lines to be constructed
 NMAX: Total number of increments for strain integration
 RENTER: Radius of the billet at entrance (it is convenient to choose RENTER = 1.0)
 YEXIT: z-coordinate of the billet at the die exit (YEXIT = 0.0)

A. Sequence of input data card preparation for the main program

1. Heading card (12A6)

Columns 1-72: Output title to be printed with output, up to 72 characters

2. Columns 1-10: The initially assigned value of the deceleration coefficient for the first iteration. Note that in a subsequent iteration, this value will be changed automatically according to the behavior of functions in order to ensure fast convergence (usually $\alpha = 0.5$)

3. Material property and program control cards (4I5, F10.0)

Columns 1-5: Value of ITER, total number of iterations assigned

Columns 6-10: Value of ITCONT; 1, for non-workhardening materials
0, for workhardening materials

Columns 11-15: Value of NPUNCH; 0, if only velocity distributions to be punched
1, punch all informations; the output punched cards are arranged as follows:

a. Nodal point velocity distributions (u_r, u_z) (8F10.6)

b. Total effective strain ($\bar{\epsilon}$) distribution (8F10.6)

c. Strain rate ($\dot{\epsilon}_r, \dot{\epsilon}_z, \dot{\epsilon}_\theta, \dot{\epsilon}_{rz}, \dot{\bar{\epsilon}}$) distributions (8F10.6)

d. Stress ($\sigma_r, \sigma_z, \sigma_\theta, \sigma_{rz}, \bar{\sigma}, \sigma_m$) distributions (8F10.6)

e. Boundary nodal point forces and velocities (F_r, F_z, u_r, u_z) (8F10.6)

Columns 15-20: Value of NPRINT; 1, if nodal point and element data are to be printed
0, otherwise

Columns 21-30: Value of FLIMIT, assigned value of accuracy desired ($\|\Delta u\|/\|u\|$), program will stop if this value is achieved (recommend value is 0.00008)

4. Geometry and traction boundary control card (4I5)

Columns 1-5: Value of NUMNP, total number of nodal points

Columns 6-10: Value of NUMEL, total number of elements

Columns 11-15: Value of NUMPC, number of traction boundary condition cards to be read (see Sequence 6, below)

Columns 16-20: Value of NBF, total number of nodal points along the die surface at which force calculation is required (see Sequence 6, below)

5. Nodal point data cards (I5, F5.0, 2F10.0)

The numbering system of nodal points for the boundary conditions

Columns 1-5: Nodal point number

Columns 6-10: Code for this nodal point

0.0 if R- and z-forces are specified

1.0 if R-velocity and z-force are specified

2.0 if R-force and z-velocity are specified

3.0 if R- and z-velocity are specified

5.0 for special boundary condition (nodal points on die surface)

Columns 11-20: R-coordinate of the nodal point

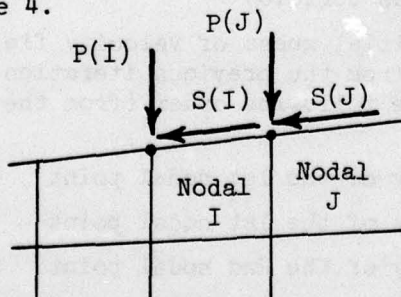
Columns 21-30: z-coordinate of the nodal point

6. Force calculation nodal points cards (16I5)

These cards provide the nodal point numbers at which the force calculations are desired. Each card provides 16 nodal points punched in every five columns. The total number of these nodal points should be the same as NBF specified in Sequence 4.

7. Traction boundary condition cards (2I5, 4F10.0)

These cards provide prescribed traction stresses along boundaries. If the prescribed stresses are all zero or no traction stresses are prescribed (e.g., for the case of extrusion (or drawing) with frictionless dies), these cards can be omitted and put NUMPC = 0 of Columns 11-15 of Sequence 4.



For the case with constant frictional stress (in terms of initial yield stress), these cards are needed. The total number of cards

AD-A048 842

CALIFORNIA UNIV BERKELEY DEPT OF MECHANICAL ENGINEERING F/G 13/8
DUCTILE FRACTURE IN AXISYMMETRIC EXTRUSION AND DRAWING. PART 1.--ETC(U).
JUN 77 C C CHEN, S I OH, S KOBAYASHI F33615-75-C-5151

UNCLASSIFIED

AFML-TR-77-96

NL

2 OF 2

AD
A048 842



END
DATE
FILMED
2-78
DDC

should be the same as the value of NUMPC. The shear stress and the normal stress are positive in the direction shown in the figure, which is opposite to the output positive stress and die force directions.

Columns 1-5: Nodal point number for point I

Columns 6-10: Nodal point number for point J

Columns 11-20: Prescribed normal stress in terms of initial yield stress at point I

Columns 21-30: Prescribed normal stress in terms of initial yield stress at point J (if normal stresses are not prescribed, put 0.0 into these two values)

Columns 31-40: Prescribed shear stress in terms of yield stress at point I

Columns 41-50: Prescribed shear stress in terms of yield stress at point J (e.g., for the case of constant friction stress with $f = 0.4Y_0$, put "-0.4" into these two values)

8. Flow line data cards (8F10.0)

Specify the R-coordinates of every flow line to be constructed before entering the die. The total number of these points should be the same as NTIMES specified in the program PURT. Each card is to be punched 8 entering points each in 10 columns.

9. Element data cards (5I5)

For each element these cards provide the four surrounding nodal point numbers (I,J,K,L) in a clockwise direction

Columns 1-5: Element number

Columns 6-10: Nodal point number of point I

Columns 11-15: Nodal point number of point J

Columns 16-20: Nodal point number of point K

Columns 21-25: Nodal point number of point L

10. Input velocity field cards (8F10.0)

These cards can be an initial guess of velocity field or a new velocity field obtained from the previous iteration. These input cards are arranged in the following order (from the nodal point to the last nodal point)

Columns 1-10: R-velocity of the 1st nodal point

Columns 11-20: z-velocity of the 1st nodal point

Columns 21-30: R-velocity of the 2nd nodal point

Columns 31-40: z-velocity of the 2nd nodal point

Each card provides four nodal point velocities

B. Sequence of input data cards for program EXDRSUM

The output stress distributions from the matrix iteration method are different from a uniform hydrostatic stress from the actual solution over all elements in extrusion or drawing.

This program calculates the average extrusion (or drawing) stress by either the energy balance method or the method of zero total axial force at the entrance boundary (for drawing) or at the exit boundary (for extrusion). After the converged solution is obtained from the main program, the output punched cards are then used in this program to calculate the correct stresses according to the following sequence of input data cards:

1. Problem control card (I5)
Columns 1-5: Value of IEXDR; 1, for the extrusion problem
0, for the drawing problem
2. Geometry control card (4I5, F10.0)
Columns 1-5: Value of NUMNP, same as in the main program
Columns 6-10: Value of NUMEL, same as in the main problem
Columns 11-15: Value of NIPTS, same as in the main problem
Columns 16-20: Value of NBF, same as in the main problem
Columns 21-30: Value of THETA, semi-included cone die angle
3. Initial yield stress card (F10.0)
Columns 1-10: Value of YIELD, initial yield stress of the material considered
4. Nodal point data cards (I5, F5.0, 2F10.0)
Same as Sequence 5 of the main program
5. Element data cards (5I5)
Same as Sequence 9 of the main program
6. Input strain-rate distribution cards
From output of the main program (Sequence 3-c)
7. Input stress distribution cards
From output of the main program (Sequence 3-d)
8. Input boundary nodal point force and velocity cards
From output of the main program (Sequence 3-e)

The output values are listed in the matrix following each of the
alternatives from a uniform experimental scheme from the actual solution over
all elements in experiment.

II. Computer program listing

This program calculates the average deviation (or average) errors by
attaching the energy balance method of the method of zero total initial force
at the entrance boundary for bending, or at the exit boundary for extension
etc. After the converged solution is obtained from the data program, the
output printed cards are used to this program to calculate the correct
answers according to the following sequence of input data cards:

1. Problem control card (P1)
Columns 1-5: Value of W_{max} , 1, for the extension program
or for the bending program

2. Geometry control card (G1, G2, G3)
Columns 1-5: Value of W_{max} , same as in the main program
Columns 6-10: Value of W_{max} , same as in the main program
Columns 11-15: Value of W_{max} , same as in the main program
Columns 16-20: Value of W_{max} , same as in the main program
Columns 21-25: Value of W_{max} , same as in the main program

3. Initial yield stress card (I1, I2)
Columns 1-10: Value of $YIELD$, Initial yield stress of the
material considered

4. Load point data card (L1, L2, L3, L4)
Same as response 2 of the main program

5. Element data card (E1)
Same as response 2 of the main program

6. Input strain-rate distribution card
From output of the main program (response 2-4)

7. Input stress distribution card
From output of the main program (response 2-4)

8. Input density model point load and velocity card
From output of the main program (response 2-4)

```

PROGRAM EXOSM1(INPUT,OUTPUT,PUNCH)
EXDRSUM 2
EXDRSUM 3 C
EXDRSUM 4 C *****
EXDRSUM 5 C SINCE FOR EXTRUSION OR DRAWING, THE OUTPUT STRESS DISTRIBUTION FROM
EXDRSUM 6 C MATRIX ITERATION METHOD ARE IN DIFFERENCE OF A UNIFORM HYDROSTATIC
EXDRSUM 7 C PRESSURE FROM THE ACTURE SOLUTION OVER ALL ELEMENTS. THIS PROGRAM
EXDRSUM 8 C CALCULATES THE AVERAGE EXTRUSION OR DRAWING PRESSURE AND THE CORREC-
EXDRSUM 9 C TION FACTOR OF THE MEAN STRESS. THE OUTPUT STRESS AND DIE PRESSURE
EXDRSUM 10 C DISTRIBUIONS OF THIS PROGRAM ARE THE ACTUAL SOLUTIONS.
EXDRSUM 11 C ***NOTE THAT ALL QUANTITIES INVOLVING VOLUMN OR SURFACE INTEGRAL ARE
EXDRSUM 12 C MEASURED PER RADIAN(I.E. QUANTITIES DIVIDED BY (2*PAI))***
EXDRSUM 13 C ***NOTE ALSO ALL OUTPUT OF STRESSES AND DIE PRESSURE ARE IN TERMS
EXDRSUM 14 C OF INITIAL YIELD STRESS *****
EXDRSUM 15 C *****
EXDRSUM 16 C
EXDRSUM 17 C DIMENSION R(242),Z(242),UR(20),UZ(20),F(20),EFSTRN(210),IEL(210,4)
EXDRSUM 18 C ,FZ(20),FR(20),STS(4,210),EFSTPS(210),ICAL(20),STSCR(4,210),
EXDRSUM 19 C 2 UDIE(20),NF(20),CODE(210)
EXDRSUM 20 C
EXDRSUM 21 C *****
EXDRSUM 22 C READ PROGRAM AND GEOMITRY CNTRL CARDS
EXDRSUM 23 C IEXDR=1...AXI-SYMMETRIC EXTRUSION PPROLEM
EXDRSUM 24 C 0...AXI-SYMETPIC DRAWING PROBLEM
EXDRSUM 25 C NUMNP=TOTAL NODAL POINTS
EXDRSUM 26 C NUMEL=TOTAL ELEMENTS
EXDRSUM 27 C NIPTS=TOTAL LINES IN MESH SYSTEM PARALLEL TO AXIS
EXDRSUM 28 C NBF=TOTAL INPUT CARDS OF SURFACE NODAL POINT FORCE FROM OUTPUT OF MAIN
EXDRSUM 29 C PROGRAM.
EXDRSUM 30 C THETA=SEMI-INCLUDED CONIC DIE ANGLE
EXDRSUM 31 C YIELD=INITIAL YIELD STRESS
EXDRSUM 32 C *****
EXDRSUM 33 C
EXDRSUM 34 C READ 2300,IEXDR
EXDRSUM 35 C READ 2311,NUMNP,NUMEL,NIPTS,NBF,THETA
EXDRSUM 36 C READ 3312, YIELD
EXDRSUM 37 C PAI=4.*ATAN(1.)
EXDRSUM 38 C ANG=PAI*THETA/180.
EXDRSUM 39 C RCOS=COS(ANG)
EXDRSUM 40 C SSIN=SIN(ANG)
EXDRSUM 41 C
EXDRSUM 42 C *****
EXDRSUM 43 C READ NODAL POINT DATA AND ELEMENT DATA CAPDS
EXDRSUM 44 C *****
EXDRSUM 45 C
EXDRSUM 46 C DO 100 I=1,NUMNP
EXDRSUM 47 C N=I
EXDRSUM 48 C 100 READ 1000,N,CODE(N),R(N),Z(N)
EXDRSUM 49 C REXIT=R(NUMNP)
EXDRSUM 50 C RENTER=R(NIPTS)
EXDRSUM 51 C VEXIT=-((RENER/REXIT)*(RENER/REXIT)
EXDRSUM 52 C N=0
EXDRSUM 53 C 130 READ 1001,M,((IEL(M,I),I=1,4)
EXDRSUM 54 C 140 N=N+1
EXDRSUM 55 C IF(M=N) 170,170,150
EXDRSUM 56 C 150 DO 160 J=1,4
EXDRSUM 57 C 160 IEL(N,J)=IEL(N-1,J)+1
EXDRSUM 58 C 170 IF(M=N) 180,180,140
EXDRSUM 59 C 180 IF(NUMEL=N) 190,190,130
EXDRSUM 60 C 190 CONTINUE
EXDRSUM 61 C
EXDRSUM 62 C *****
EXDRSUM 63 C READ INPUT DATA CARDS
EXDRSUM 64 C ALL INPUT DATAS BELOW ARE FROM THE OUTPUTS OF THE MAIN PROGRAM
EXDRSUM 65 C EFSTRN=EFFECTIVE STRAIN PATE
EXDRSUM 66 C STS(1,N)=R-STRESS OF N-TH ELEMENT
EXDRSUM 67 C STS(2,N)=Z-STRESS OF N-TH ELEMENT
EXDRSUM 68 C STS(3,N)=TH-STRESS OF N-TH ELEMENT
EXDRSUM 69 C STS(4,N)=RZ-STRESS OF N-TH ELEMENT
EXDRSUM 70 C EFSTRS=EFFECTIVE STRESS
EXDRSUM 71 C AX, AY ,AZ,AW STAND FOR INPUT DATAS WHICH ARE NOT USED IN DOING THIS
EXDRSUM 72 C PROGRAM.
EXDRSUM 73 C UR,UZ,FR,FZ ARE THE VELOCITY AND FOPCES AT NODAL POINT IN R AND Z-DIR.
EXDRSUM 74 C *****
EXDRSUM 75 C
EXDRSUM 76 C READ 1003,((AX,AY,AZ,AW,EFSTRN(N)),N=1,NUMEL)
EXDRSUM 77 C READ 1003,((STS(I,N),I=1,4),EFSTPS(N),AX),N=1,NUMEL)
EXDRSUM 78 C DO 220 I=1,NBF
EXDRSUM 79 C 220 READ 1002,NF(I),UR(I),UZ(I),FR(I),FZ(I)
EXDRSUM 80 C IF(IEXDR.EQ.1) PRINT 3303
EXDRSUM 81 C IF(IEXDR.EQ.0) PRINT 3304
EXDRSUM 82 C PRINT 2201

```



```

EXDRSUM 83      PRINT 2202,(K,CODE(K),R(K),7(K),K=1,NUMNP)
EXDRSUM 84      PRINT 2204
EXDRSUM 85      DO 250 I=1,NRF
EXDRSUM 86      FR(I)=FR(I)/YIELD
EXDRSUM 87      FZ(I)=FZ(I)/YIELD
EXDRSUM 88      J=NF(I)
EXDRSUM 89      250 PRINT 2203,NF(I),CODE(J),UP(I),U7(I),FR(I),FZ(I)
EXDRSUM 90      C
EXDRSUM 91      C *****
EXDRSUM 92      C FRTOTL=TOTAL DIE FORCE IN Z-DIRECTION BEFORE CORRECTION
EXDRSUM 93      C *****
EXDRSUM 94      C
EXDRSUM 95      FRTCTL=0.
EXDRSUM 96      DO 300 I=1,NRF
EXDRSUM 97      J=NF(I)
EXDRSUM 98      IF(CODE(J).EQ.5.0.OR.CODE(J).EQ.15.0) GO TO 301
EXDRSUM 99      GO TO 300
EXDRSUM 100     301 FRTCTL=FRTOTL+F7(I)
EXDRSUM 101     300 CONTINUE
EXDRSUM 102     C
EXDRSUM 103     C *****
EXDRSUM 104     C METHOD=1...IF ENERGY BALANCE METHOD IS USED
EXDRSUM 105     C 2...IF ZERO TOTAL Z-FORCE AT RIGID BOUNDARY METHOD IS USED
EXDRSUM 106     C *****
EXDRSUM 107     C
EXDRSUM 108     DO 900 METHOD=1,2
EXDRSUM 109     IF(METHOD.EQ.1) GO TO 901
EXDRSUM 110     IF(METHOD.EQ.2) GO TO 902
EXDRSUM 111     C
EXDRSUM 112     C *****
EXDRSUM 113     C **ENERGY BALANCE METHOD*****
EXDRSUM 114     C CALCULATE DISSIPATION ENERGY RATE OVER DIE SURFACE DUE TO FRICTION
EXDRSUM 115     C *****
EXDRSUM 116     C
EXDRSUM 117     901 CONTINUE
EXDRSUM 118     FRICTN=0.
EXDRSUM 119     DO 103 I=1,NRF
EXDRSUM 120     J=NF(I)
EXDRSUM 121     IF(CODE(J).EQ.5.0.OR.CODE(J).EQ.15.0) GO TO 102
EXDRSUM 122     GO TO 103
EXDRSUM 123     102 FRICTN=FRICTN+(FR(I)*RSIN+FZ(I)*RCOS)*(UR(I)*RSIN+U7(I)*RCOS)
EXDRSUM 124     103 CONTINUE
EXDRSUM 125     C
EXDRSUM 126     C *****
EXDRSUM 127     C CALCULATE TOTAL STRAIN ENERGY RATE OVER THE DEFORMED PORTION
EXDRSUM 128     C *****
EXDRSUM 129     C
EXDRSUM 130     DSENGY=0.
EXDRSUM 131     DO 210 N=1,NUMEL
EXDRSUM 132     EFSS=EFSTRN(N)
EXDRSUM 133     IF(EFSTRN(N).LE.0.01) EFSS=0.0
EXDRSUM 134     I1=IEL(N,1)
EXDRSUM 135     I2=IEL(N,2)
EXDRSUM 136     I3=IEL(N,3)
EXDRSUM 137     I4=IEL(N,4)
EXDRSUM 138     VOL1=(Z(I2)-Z(I1))*(R(I1)*R(I1)+R(I2)*R(I2)+R(I1)*R(I2))
EXDRSUM 139     VOL2=(Z(I4)-Z(I3))*(R(I4)*R(I4)+R(I3)*R(I3)+R(I4)*R(I3))
EXDRSUM 140     VOL3=(Z(I3)-Z(I2))*(R(I3)*R(I3)+R(I2)*R(I2)+R(I3)*R(I2))
EXDRSUM 141     VOL4=(Z(I1)-Z(I4))*(R(I4)*R(I4)+R(I1)*R(I1)+R(I1)*R(I4))
EXDRSUM 142     VOLUMN=(VOL1+VOL2+VOL3+VOL4)/6.
EXDRSUM 143     DSENGY=DSENGY+EFSTRN(N)*EFSS*VOLUMN
EXDRSUM 144     210 CONTINUE
EXDRSUM 145     C
EXDRSUM 146     C *****
EXDRSUM 147     C CALCULATE AVERAGE EXTRUSION PRESSURE OR AVERAGE DRAWING PRESSURE (EXT-
EXDRSUM 148     C PSS) AND CORRECTION HYDROSTATIC PRESSURE (ALANDA) BY ENERGY BALANCE-
EXDRSUM 149     C METHOD.
EXDRSUM 150     C *****
EXDRSUM 151     C
EXDRSUM 152     PRINT 3300
EXDRSUM 153     IF(IEKOR.EQ.1) GO TO 502
EXDRSUM 154     501 EXTPSS=(DSENGY-FRICTN)*2./(-VEXIT*REXIT*REXIT)
EXDRSUM 155     ALANDA=(2.*FRTOTL-EXTPSS*REXIT*REXIT)/(RENTOP*RENTOP-PEXIT*REXIT)
EXDRSUM 156     GO TO 503
EXDRSUM 157     502 EXTPSS=(DSENGY-FRICTN)*2./((RENTOP*RENTOP)
EXDRSUM 158     ALANDA=(2.*FRTOTL-EXTPSS)/(RENTOP*RENTOP-PEXIT*REXIT)
EXDRSUM 159     GO TO 503
EXDRSUM 160     C
EXDRSUM 161     902 CONTINUE
EXDRSUM 162     C
EXDRSUM 163     C *****
EXDRSUM 164     C *****METHOD OF ZERO TOTAL Z-FORCE OVER THE RIGID BOUNDARY*****
EXDRSUM 165     C *****

```

```

EXDRSUM 166 C
EXDRSUM 167 NI=NIPTS-1
EXDRSUM 168 IF(IEXDR.EQ.1) GO TO 705
EXDRSUM 169 C
EXDRSUM 170 C *****
EXDRSUM 171 C CHECK ELEMENTS NEXT TO RIGID BOUNDARY AT ENTRANCE FOR DRAWING
EXDRSUM 172 C *****
EXDRSUM 173 C
EXDRSUM 174 DO 706 I=1,NI
EXDRSUM 175 J=I
EXDRSUM 176 706 IF(EFSTRN(J).LE.0.01) GO TO 707
EXDRSUM 177 ICAL(I)=J
EXDRSUM 178 GO TO 709
EXDRSUM 179 707 J=J+NI
EXDRSUM 180 GO TO 706
EXDRSUM 181 708 CONTINUE
EXDRSUM 182 GO TO 400
EXDRSUM 183 C
EXDRSUM 184 C *****
EXDRSUM 185 C CHECK ELEMENTS NEXT TO RIGID BOUNDARY AT EXIT FOR EXTRUSION
EXDRSUM 186 C *****
EXDRSUM 187 C
EXDRSUM 188 705 DO 719 I=1,NI
EXDRSUM 189 J=NUMEL-NI+I
EXDRSUM 190 716 IF(EFSTRN(J).LE.0.01) GO TO 717
EXDRSUM 191 ICAL(I)=J
EXDRSUM 192 GO TO 718
EXDRSUM 193 717 J=J-NI
EXDRSUM 194 GO TO 716
EXDRSUM 195 718 CONTINUE
EXDRSUM 196 800 CONTINUE
EXDRSUM 197 C
EXDRSUM 198 C *****
EXDRSUM 199 C CALCULATE TOTAL Z-FORCE (BEFORE CORRECTION) FOR ELEMENTS NEXT TO
EXDRSUM 200 C RIGID BOUNDARY
EXDRSUM 201 C *****
EXDRSUM 202 C
EXDRSUM 203 TFCRCE=0.
EXDRSUM 204 I=1
EXDRSUM 205 INDEX=1
EXDRSUM 206 801 KK=ICAL(I)
EXDRSUM 207 I1=IEL(KK,1)
EXDRSUM 208 I2=IEL(KK,2)
EXDRSUM 209 I3=IEL(KK,3)
EXDRSUM 210 I4=IEL(KK,4)
EXDRSUM 211 Z1=0.
EXDRSUM 212 Z2=(Z(I1)-Z(I2))/2.
EXDRSUM 213 R2=(R(I3)+R(I4))/2.
EXDRSUM 214 IF(INDEX.EQ.1) GO TO 808
EXDRSUM 215 AREA1=(R2*R2-R1*R1)/2.
EXDRSUM 216 AREA2=R1*Z2
EXDRSUM 217 GO TO 809
EXDRSUM 218 809 R1=(R(I1)+R(I2))/2.
EXDRSUM 219 AREA1=(R2*R2-R1*R1)/2.
EXDRSUM 220 AREA2=0.
EXDRSUM 221 800 TFCRCE=TFCRCE+AREA1*STS(2, KK)+AREA2*STS(4, KK)
EXDRSUM 222 IF(I.EQ.NI) GO TO 810
EXDRSUM 223 R1=R2
EXDRSUM 224 KAROVE=KK+1
EXDRSUM 225 IF(KAROVE=ICAL(I+1)) 753,750,753
EXDRSUM 226 750 I=I+1
EXDRSUM 227 INDEX=1
EXDRSUM 228 GO TO 801
EXDRSUM 229 753 IF(KAROVE=LT.ICAL(I+1)) KNEXT=KAROVE+NI
EXDRSUM 230 IF(KAROVE=GT.ICAL(I+1)) KNEXT=KAROVE-NI
EXDRSUM 231 I1=IEL(KNEXT,1)
EXDRSUM 232 I2=IEL(KNEXT,2)
EXDRSUM 233 I3=IEL(KNEXT,3)
EXDRSUM 234 I4=IEL(KNEXT,4)
EXDRSUM 235 R2=(R(I1)+R(I2)+R(I3)+R(I4))/4.
EXDRSUM 236 AREA1=(R2*R2-R1*R1)/2.
EXDRSUM 237 AREA3=R1*Z1
EXDRSUM 238 AREA2=R2*Z2
EXDRSUM 239 TFCRCE=TFCRCE+STS(2, KAROVE)*(AREA1+AREA3)+STS(4, KAROVE)*AREA2
EXDRSUM 240 R1=R2
EXDRSUM 241 Z2=(Z(I1)-Z(I2))/2.
EXDRSUM 242 Z1=Z2
EXDRSUM 243 IF(KNEXT=EQ.ICAL(I+1)) GO TO 803
EXDRSUM 244 KAROVE=KNEXT
EXDRSUM 245 GO TO 753
EXDRSUM 246 803 I=I+1
EXDRSUM 247 INDEX=2
EXDRSUM 248 GO TO 801
EXDRSUM 249 C
EXDRSUM 250 C *****
EXDRSUM 251 C CALCULATE CORRECTION HYDROSTATIC PRESSURE BY REQUESTING TOTAL Z-FORCE
EXDRSUM 252 C EQUAL TO ZERO AFTER CORRECTION (ALANDA). CALCULATE AVERAGE EXTRUSION
EXDRSUM 253 C PRESSURE OR AVERAGE DRAWING PRESSURE (EXTPSS) BY FORCE BALANCING.
EXDRSUM 254 C *****

```



```

EXDRSUM 255 C
EXDRSUM 256 810 PRINT 3301
EXDRSUM 257 PRINT 2307,(ICAL(I),I=1,N1)
EXDRSUM 258 IF(IXDR.EQ.1) GO TO 811
EXDRSUM 259 ALANDA=-(TFORCE/(RENTER*RENTER))*2.
EXDRSUM 260 EXTPS1=-ALANDA*(RENTER*RENTER-REXIT*REXIT)+2.*FRTOTL
EXDRSUM 261 EXTPSS=EXTPS1/(REXIT*REXIT)
EXDRSUM 262 GO TO 503
EXDRSUM 263 811 ALANDA=-(TFORCE/(REXIT*REXIT))*2.
EXDRSUM 264 EXTPSS=-ALANDA*(RENTER*RENTER-REXIT*REXIT)+2.*FRTOTL
EXDRSUM 265 503 CONTINUE
EXDRSUM 266 PRINT 2301,EXTPSS
EXDRSUM 267 PRINT 2302,ALANDA
EXDRSUM 268 C
EXDRSUM 269 C *****
EXDRSUM 270 C CALCULATE THE ACTURE DIE PRESSURE
EXDRSUM 271 C *****
EXDRSUM 272 C
EXDRSUM 273 PRINT 3310
EXDRSUM 274 DD 400 I=1,NBF
EXDRSUM 275 J=NF(I)
EXDRSUM 276 IF(CODE(J).EQ.5.0.CR.CODE(J).EQ.15.0) GO TO 409
EXDRSUM 277 GO TO 400
EXDRSUM 278 409 J2=J-NIPTS
EXDRSUM 279 J1=J-NIPTS
EXDRSUM 280 IF(J1.LT.NIPTS) J1=J
EXDRSUM 281 IF(J2.GT.NUMNP) J2=J
EXDRSUM 282 R1=(R(J)+R(J2))/2.
EXDRSUM 283 R2=(R(J1)+R(J1))/2.
EXDRSUM 284 H=(Z(J1)-Z(J2))/2.
EXDRSUM 285 AREA=(R1+R2)*SQRT((R2-R1)*(R2-R1)+H*H)/2.
EXDRSUM 286 P=(1/FR(I)*RCOS-FZ(I)*BSINI)/AREA+ALANDA
EXDRSUM 287 PRINT 2303,J.CODE(J),R(J),Z(J),AREA,P
EXDRSUM 288 400 CONTINUE
EXDRSUM 289 C
EXDRSUM 290 C *****
EXDRSUM 291 C CALCULATE THE ACTUAL STRESS DISTRIBUTION
EXDRSUM 292 C *****
EXDRSUM 293 C
EXDRSUM 294 IF(METHOD.EQ.1) PRINT 3300
EXDRSUM 295 IF(METHOD.EQ.2) PRINT 3301
EXDRSUM 296 PRINT 2304
EXDRSUM 297 DD 405 N=1,NUMEL
EXDRSUM 298 STSCR(4,N)=STS(4,N)
EXDRSUM 299 DD 406 I=1,3
EXDRSUM 300 406 STSCR(I,N)=STS(I,N)+ALANDA
EXDRSUM 301 AVES=(STSCR(1,N)+STSCR(2,N)+STSCP(3,N))/3.
EXDRSUM 302 405 PRINT 2305,N,(STSCR(I,N),I=1,4),AVES,EFSTRS(N),EFSTRN(N)
EXDRSUM 303 900 CONTINUE
EXDRSUM 304 C
EXDRSUM 305 1000 FORMAT(15,F5.0,5F10.0)
EXDRSUM 306 1001 FORMAT(16I5)
EXDRSUM 307 1002 FORMAT(19,4F17.0)
EXDRSUM 308 1003 FORMAT(8F10.0)
EXDRSUM 309 2201 FORMAT(/,5X,*NODAL*,5X,*CODE*,5X,*R-COORD...*,5X,*Z-COORD...*,1
EXDRSUM 310 2202 FORMAT(5X,15,5X,F5.2,5X,F10.6,5X,F10.6)
EXDRSUM 311 2203 FORMAT(2X,15,(2X,F10.6))
EXDRSUM 312 2204 FORMAT(///,5X,*INPUT DATA*,2X,*NODAL* ,6X,*CODE*,8X,*R-VELOCITY*
EXDRSUM 313 1,2X,*Z-VELOCITY*,2X,*R-FORCE...*,2X,*Z-FORCE*)
EXDRSUM 314 2300 FORMAT(15)
EXDRSUM 315 2301 FORMAT(///,5X,*AVERAGE EXTRUSION( OR DRAWING) PRESSURE=*,F12.6)
EXDRSUM 316 2302 FORMAT(///,5X,*THE CORRECTION HYDROSTATIC PRESSURE=*,F12.6)
EXDRSUM 317 2303 FORMAT(2X,*NODAL POINT=*,14,2X,*CODE=*,F5.2,2X,*R-COORD=*,F10.6,
EXDRSUM 318 1 2X,*Z-COORD=*,F10.6,2X,*APEA=*,F10.6,2X,*DIE PRESSURE=*,F15.8)
EXDRSUM 319 2304 FORMAT(/,10X,*ACTUAL STRESS DISTRIBUTION**
EXDRSUM 320 1,5X,*ELE.NO.* ,5X,*R-STRESS*,5X,*7-STRESS*,5X,*TH-STRESS*,
EXDRSUM 321 2 5X,*RZ-STRESS*,*..MEAN STRESS..EF-STRESS*,3X,*EFF-STRAIN RATE*)
EXDRSUM 322 2305 FORMAT(7X,16,7F13.6)
EXDRSUM 323 2307 FORMAT(///,5X,*ELEMENTS NEXT TO RIGID BOUNDARY=*,/,6X,16I5)
EXDRSUM 324 2311 FORMAT(4I5,F10.0)
EXDRSUM 325 3300 FORMAT(1H1,5X,*ENERGY BALANCE METHOD*)
EXDRSUM 326 3301 FORMAT(1H1,5X,*TOTAL ZERO Z-FORCE AT RIGID BOUNDARY METHCD*)
EXDRSUM 327 3303 FORMAT(1H1,*...EXTRUSION PROBLEM...*)
EXDRSUM 328 3304 FORMAT(1H1,*...DRAWING PROBLEM...*)
EXDRSUM 329 3310 FORMAT(///,5X,*THE ACTUAL DIE PRESSURE DISTRIBUTION*)
EXDRSUM 330 3312 FORMAT(F10.0)
EXDRSUM 331 STOP
EXDRSUM 332 END

```

```

EXTRUDE 2      PROGRAM PURT(TAPE1,INPUT,OUTPUT,TAPE5=INPUT,TAPE6=OUTPUT,PUNCH)
EXTRUDE 3      C
EXTRUDE 4      C *****
EXTRUDE 5      C PROGRAM FOR STEADY STATE EXTRUSION OR DRAWING BY MATRIX METHOD.
EXTRUDE 6      C NOTE THAT THE FOLLOWING PROGRAM IS WRITING ACCORDING TO THE RIGHT
EXTRUDE 7      C ORDERING OF NODAL POINTS AND ELEMENT NUMBERS (SEE EXPLANATION)
EXTRUDE 8      C *****
EXTRUDE 9      C
EXTRUDE 10     COMMON/GENCON/NUMNP,NUMEL,HED(12),VOL,NEG,NS,ITERNO,ISTOP,
EXTRUDE 11     1YIELD,MBAND,TEST,MDIAG,NBF,NUMPC,ITER,NRF2,NSCALE,NPUNCH,NPRINT,
EXTRUDE 12     2 NCHECK,ACFINI
EXTRUDE 13     COMMON /WALL/ THETA,FT,TANTH
EXTRUDE 14     COMMON /STRPATH/ STEP,YSTART,YDIF,YEXIT,YMIN,PENTER,REXIT,VEXIT
EXTRUDE 15     COMMON /DIMEN/ M1,M2,M3,M4,M5,M6,M7,M8,M9,M10,M11,M12,M13,M14
EXTRUDE 16     C
EXTRUDE 17     C *****
EXTRUDE 18     C PROGRAM PURT IS FOR CONTROLLING THE DIMENSION OF THE COMPLETE PROGRAM
EXTRUDE 19     C ITS PURPOSE IS TO PREVENT ASSIGNING A LARGER THAN NECESSARY DIMENSION
EXTRUDE 20     C FOR ANY ARRAY THROUGH THE USE OF FOLLOWING STATEMENT..
EXTRUDE 21     C *****
EXTRUDE 22     C
EXTRUDE 23     COMMON A(24650)
EXTRUDE 24     C
EXTRUDE 25     C *****
EXTRUDE 26     C NFIELD IS THE DIMENSION OF ARRAY A. ITS VALUE CAN BE DETERMINED
EXTRUDE 27     C PRECISELY BY RUNNING THE PROGRAM ONCE.
EXTRUDE 28     C *****
EXTRUDE 29     C
EXTRUDE 30     NFIELD=24650
EXTRUDE 31     PAI=4.*ATAN(1.0)
EXTRUDE 32     C
EXTRUDE 33     C *****
EXTRUDE 34     C THETA          SEMI-INCLUDED CONIC DIE ANGLE.
EXTRUDE 35     C YSTART        Z-COORDINATE OF STARTING POINT TO CALCULATE TOTAL
EXTRUDE 36     C              EFFECTIVE STRAIN AND IS SETTING SLIGHTLY LESS THAN
EXTRUDE 37     C              THE CENTER OF FIRST ELEMENT.
EXTRUDE 38     C STEP          THE INCREMENT SIZE FOR STRAIN-RATE INTEGRATION
EXTRUDE 39     C YDIE         Z-COORDINATE AT ENTRANCE TO THE DIE
EXTRUDE 40     C YEXIT        Z-COORDINATE AT EXIT FROM DIE
EXTRUDE 41     C YMIN         MINIMUM Z-COORDINATE OF THE CONTROL VOLUME
EXTRUDE 42     C PENTER      RADIUS OF BILLET BEFORE EXTRUSION
EXTRUDE 43     C REXIT       RADIUS OF BILLET AFTER EXTRUSION
EXTRUDE 44     C VEXIT       EXIT VELOCITY OF THE PRODUCT
EXTRUDE 45     C NTIMES     NUMBER OF FLOW LINES TO BE CONSTRUCTED
EXTRUDE 46     C NIPTS      NUMBER OF LINES IN MESH SYSTEM PARALLEL TO AXIS
EXTRUDE 47     C NJPTS      NUMBER OF LINES IN MESH SYSTEM PERPENDICULAR TO AXIS
EXTRUDE 48     C NMAX       TOTAL NUMBER OF INCREMENTS FOR INTEGRATION
EXTRUDE 49     C *****
EXTRUDE 50     C
EXTRUDE 51     THETA=4.
EXTRUDE 52     THETA=THETA*PAI/180.
EXTRUDE 53     TANTH=TAN(THETA)
EXTRUDE 54     YEXIT=0.
EXTRUDE 55     PENTER=1.0
EXTRUDE 56     NTIMES=11
EXTRUDE 57     NIPTS=7
EXTRUDE 58     NJPTS=15
EXTRUDE 59     NMAX=350
EXTRUDE 60     C
EXTRUDE 61     C *****
EXTRUDE 62     C READ THE INPUT DATA CONTROL CARDS
EXTRUDE 63     C HED=OUTPUT TITLE UP TO 72 CHARACTERS.
EXTRUDE 64     C ACFINI=INITIAL DECELERATION COEFFICIENTS, FOR FIRST ITERATION ONLY.
EXTRUDE 65     C ITER=TOTAL NUMBER OF ITERATIONS ASSIGNED.
EXTRUDE 66     C ITCONT=1, FOR NONWORKHARDENING MATERIALS
EXTRUDE 67     C 0, FOR WORK-HARDENING MATERIALS.
EXTRUDE 68     C NPUNCH=0, IF NOTHING OTHER THAN VELOCITIES TO BE PUNCHED.
EXTRUDE 69     C 1, OTHERWISE.
EXTRUDE 70     C NPRINT=1, IF THE NODAL POINT DATAS TO BE PRINTED.
EXTRUDE 71     C 0, OTHERWISE.
EXTRUDE 72     C FLIMIT=VALUE OF (ERROR NORM)/(SOLUTION NORM) REQUIRED FOR FINAL RESULT
EXTRUDE 73     C NUMNP=NUMBER OF NODAL POINTS(TOTAL).
EXTRUDE 74     C NUMEL=NUMBER OF ELEMENTS(TOTAL)
EXTRUDE 75     C NUMPC=NUMBER OF TRACTION BOUNDARY CONDITIONS CARDS TO BE READ.
EXTRUDE 76     C NBF=NUMBER OF NODAL POINTS AT WHICH FORCE CALCULATIONS ARE REQUIRED.
EXTRUDE 77     C *****
EXTRUDE 78     C
EXTRUDE 79     READ(5,1000) HED
EXTRUDE 80     READ(5,1004)ACFINI
EXTRUDE 81     READ(5,1003) ITER,ITCONT,NPUNCH,NPRINT,FLIMIT
EXTRUDE 82     READ(5,1005) NUMNP,NUMEL,NUMPC,NBF

```



```

EXTRUDE 83      NIPTS=NIPTS+1
EXTRUDE 84      NRF2=NRF*2
EXTRUDE 85      NR=NRF
EXTRUDE 86      NB2=NRF*2
EXTRUDE 87      NEL=NUMEL
EXTRUDE 88      NPC=NUMPC
EXTRUDE 89      NEQ=3*NUMNP
EXTRUDE 90      NO=NEQ
EXTRUDE 91      NI=NIPTS
EXTRUDE 92      NJ=NJPTS
EXTRUDE 93      C
EXTRUDE 94      C *****
EXTRUDE 95      C DETERMINE THE LOCATION OF THE STARTING POINTS OF DIFFERENT ARRAYS ON
EXTRUDE 96      C ARRAY A
EXTRUDE 97      C *****
EXTRUDE 98      C
EXTRUDE 99      N1=1
EXTRUDE 100     N2=N1+NUMNP
EXTRUDE 101     N3=N2+NUMNP
EXTRUDE 102     N4=N3+NUMNP
EXTRUDE 103     N5=N4+NUMNP
EXTRUDE 104     N6=N5+NUMNP
EXTRUDE 105     N7=N6+4*NUMEL
EXTRUDE 106     N8=N7+NUMEL
EXTRUDE 107     N9=N8+6*NUMEL
EXTRUDE 108     N10=N9+5*NUMEL
EXTRUDE 109     N11=N10+5*NUMEL
EXTRUDE 110     N12=N11+NBF
EXTRUDE 111     N13=N12+NBF2
EXTRUDE 112     N14=N13+2*NUMEC
EXTRUDE 113     N15=N14+4*NUMPC
EXTRUDE 114     N16=N15+NBF
EXTRUDE 115     N17=N16+NBF
EXTRUDE 116     N18=N17+NBF
EXTRUDE 117     N19=N18+NTIMES
EXTRUDE 118     C
EXTRUDE 119     C *****
EXTRUDE 120     C READ THE INPUT DATA
EXTRUDE 121     C *****
EXTRUDE 122     C
EXTRUDE 123     CALL PRELIM (A(N1),A(N2),A(N3),A(N4),A(N5),A(N6),A(N11),A(N13),
EXTRUDE 124     1 A(N14),A(N18),NEL,NPC,NTIMES,NIPTS,YSTART,YMIN,REXIT)
EXTRUDE 125     YDIE=(PENTER-REXIT)/TANTH
EXTRUDE 126     VEXIT=- (RENTER/REXIT)**2
EXTRUDE 127     STEP=(YSTART-YMIN)/(NMAX*1.15)
EXTRUDE 128     WRITE(6,1007) ACFINI,ITCONT,FLIMIT
EXTRUDE 129     WRITE(6,1008) STEP,YSTART,YDIE,VEXIT,YMIN,RENTER,REXIT,VEXIT,
EXTRUDE 130     1 NTIMES,NIPTS,NJPTS,NMAX
EXTRUDE 131     C
EXTRUDE 132     N20=N19+NEQ
EXTRUDE 133     C
EXTRUDE 134     C
EXTRUDE 135     C *****
EXTRUDE 136     C SINCE AFTER THE SOLUTION OF STIFFNESS EQUATIONS, THE STIFFNESS MATRIX
EXTRUDE 137     C IS NOT NEEDED FOR THAT ITERATION, THE SPACE PROVIDED FOR STIFFNESS
EXTRUDE 138     C MATRIX WILL BE USED FOR CONSTRUCTION OF FLOW LINES AND FOR STRAIN-
EXTRUDE 139     C RATE INTEGRATION. THE NUMBERS M1 TO M14 ARE FOR DETERMINING THE
EXTRUDE 140     C LOCATION OF PROPER ARRAY
EXTRUDE 141     C *****
EXTRUDE 142     C
EXTRUDE 143     M1=1
EXTRUDE 144     M2=M1+NI*NJ
EXTRUDE 145     M3=M2+NI*NJ
EXTRUDE 146     M4=M3+NJ
EXTRUDE 147     M5=M4+NI
EXTRUDE 148     M6=M5+NI*NJ
EXTRUDE 149     M7=M6+NI*NJ
EXTRUDE 150     M8=M7+NTIMES*NMAX
EXTRUDE 151     M9=M8+NTIMES*NMAX
EXTRUDE 152     M10=M9+NUMEL
EXTRUDE 153     M11=M10+NUMEL
EXTRUDE 154     M12=M11+NI*NJ
EXTRUDE 155     M13=M12+NJ
EXTRUDE 156     M14=M13+NTIMES*NMAX
EXTRUDE 157     C
EXTRUDE 158     C *****
EXTRUDE 159     C HOWEVER, IF THE SPACE OF STIFFNESS MATRIX IS NOT ENOUGH FOR STRAIN RATE
EXTRUDE 160     C INTEGRATION, CREATES MORE SPACE AS REQUIRED.
EXTRUDE 161     C *****
EXTRUDE 162     C
EXTRUDE 163     NNN=MBAND*NEQ
EXTRUDE 164     N21=N20+NNN
EXTRUDE 165     IF (M14.GE.NNN) N21=N20+M14
EXTRUDE 166     N22=N21+NRF*2*(2*MBAND-1)
EXTRUDE 167     N23=N22+NEQ
EXTRUDE 168     N24=N23+NEQ

```

```

EXTRUDE 169 C
EXTRUDE 170 C *****
EXTRUDE 171 C N24 IS TOTAL SPACE REQUIRED, IF NFIELD , THE INITIAL ASSIGNED SPACE,
EXTRUDE 172 C IS NOT ENOUGH, STOP THE PROGRAM.
EXTRUDE 173 C *****
EXTRUDE 174 C
EXTRUDE 175 C IF(N24.LE.NFIELD) GO TO 100
EXTRUDE 176 C WRITE(6,1001) N24
EXTRUDE 177 C STOP
EXTRUDE 178 C 100 CONTINUE
EXTRUDE 179 C WRITE(6,1002) N24
EXTRUDE 180 C
EXTRUDE 181 C *****
EXTRUDE 182 C THE FOLLOWING SUBROUTINE PLAST DOING THE MAIN PART OF MATRIX ITERATION
EXTRUDE 183 C METHOD OF PRESENT PROBLEM.
EXTRUDE 184 C *****
EXTRUDE 185 C
EXTRUDE 186 C CALL PLAST(A(N1),A(N2),A(N3),A(N4),A(N5),A(N6),A(N7),A(N8),A(N9),
EXTRUDE 187 C 1A(N10),A(N11),A(N12),A(N13),A(N14),A(N15),A(N16),A(N17),A(N18),
EXTRUDE 188 C 2A(N19),A(N20),A(N21),A(N22),A(N23),NO,NEL,NPC,NB2,
EXTRUDE 189 C 3PLIMIT,ITCONT,NTIMES,NIPTS,NJPTS,NMAX)
EXTRUDE 190 C
EXTRUDE 191 C 1000 FORMAT(12A6)
EXTRUDE 192 C 1001 FORMAT(/** THE DIMENSION OF THE ARRAY (A) IS TOO SMALL*/
EXTRUDE 193 C 1* THE SIZE OF THE ARRAY (A) MUST BE *, I7)
EXTRUDE 194 C 1002 FORMAT(/** THE NECESSARY SIZE OF THE ARRAY (A) IS*, I7)
EXTRUDE 195 C 1003 FORMAT(4I5,F10.0)
EXTRUDE 196 C 1004 FORMAT(8F10.0)
EXTRUDE 197 C 1005 FORMAT(4I5)
EXTRUDE 198 C 1007 FORMAT(/** ACOEF = *,F8.5,10X,* ITCONT = *,I2,
EXTRUDE 199 C 1 10X,* FLIMIT=*,F10.6,/)
EXTRUDE 200 C 1008 FORMAT(/** STEP SIZE = *,F8.4,10X,* YSTART = *,F8.4,10X,* YDIE = *
EXTRUDE 201 C 1 F8.4,10X,* YEXIT = *,F8.4,/** YMIN = *,F8.4,10X,* RENTER = *,
EXTRUDE 202 C 2 F8.4,10X,* REXIT = *,F8.4,10X,* VEXIT = *,F8.4,/** NTIMES = *,
EXTRUDE 203 C 3 I4,10X,* NIPTS = *,I3,10X,* NJPTS = *,I3,10X,* NMAX = *,I4,/)
EXTRUDE 204 C 1009 FORMAT(/ * STORAGE SPACE AVAILABLE FOR THE STRAIN CALCULATIONS IS
EXTRUDE 205 C 1 NOT ENOUGH*/)
EXTRUDE 206 C
EXTRUDE 207 C STOP
EXTRUDE 208 C END

```

```

EXTRUDE 210 SUBROUTINE PRELIM (R,Z,UR,UZ,CODE,IEL,NF,IJBC,PSBC,RR,NEL,NPC,
EXTRUDE 211 1 NTIMES,NIPTS,YSTART,YMIN,REXIT)
EXTRUDE 212 COMMON/GENCON/NUMNP,NUMEL,HED(12),VOL,NEQ,NS,ITERNO,ISTOP,
EXTRUDE 213 1YIELD,MBAND,TEST,MDIAG,NBF,NUMPC,ITER,NBF2,NSCALE,NPUNCH,NPRINT,
EXTRUDE 214 2 NCHECK,ACFINI
EXTRUDE 215 DIMENSION R(1),Z(1),CODE(1),UR(1),UZ(1),IEL( NEL ,1),NF(1),
EXTRUDE 216 1 IJBC(NPC,1),PSBC(NPC,1),RR(1)
EXTRUDE 217 C
EXTRUDE 218 C *****
EXTRUDE 219 C THIS SUBROUTINE READS AND PRINTS ALL CONTROL INFORMATIONS AND
EXTRUDE 220 C NODAL POINT DATAS AND BOUNCARY CONDITIONS.
EXTRUDE 221 C *****
EXTRUDE 222 C
EXTRUDE 223 C WRITE(6,1000)
EXTRUDE 224 C WRITE(6,2000) HED,NUMNP,NUMEL
EXTRUDE 225 C
EXTRUDE 226 C *****
EXTRUDE 227 C CALCULATE INITIAL YIELD STRESS.
EXTRUDE 228 C *****
EXTRUDE 229 C
EXTRUDE 230 C CALL HARD(0.,YIELD)
EXTRUDE 231 C WRITE(6,2010) YIELD
EXTRUDE 232 C WRITE(6,2011) ITER
EXTRUDE 233 C
EXTRUDE 234 C *****
EXTRUDE 235 C READ AND PRINT OF NODAL POINT DATA
EXTRUDE 236 C *****
EXTRUDE 237 C
EXTRUDE 238 C L=0
EXTRUDE 239 C IF(NPRINT.EQ.0) GO TO 60
EXTRUDE 240 C WRITE(6,1114)
EXTRUDE 241 C WRITE(6,2004)
EXTRUDE 242 C 60 READ(5,1002) N,CODE(N),R(N),Z(N)
EXTRUDE 243 C 90 IF(NUMNP-N) 100,110,60
EXTRUDE 244 C 100 WRITE(6,2009) N
EXTRUDE 245 C CALL EXIT
EXTRUDE 246 C 110 CONTINUE
EXTRUDE 247 C YSTART=(Z(1)+Z(NIPTS+2))/2.-0.001
EXTRUDE 248 C YMIN=Z(NUMNP)
EXTRUDE 249 C REXIT=(NUMNP)
EXTRUDE 250 C IF(NPRINT.EQ.0) GO TO 120
EXTRUDE 251 C WRITE(6,2002) (K,CODE(K),R(K),Z(K),K=1,NUMNP)

```



```

EXTRUDE 252 C
EXTRUDE 253 C *****
EXTRUDE 254 C READ AND PRINT SPECIAL CONDITIONS ALONG BOUNDARY
EXTRUDE 255 C NPF = TOTAL NUMBER OF NODAL POINTS AT WHICH FORCES ARE DESIRED
EXTRUDE 256 C NPF(I) = SEQUENTIAL NUMBER OF NODAL POINTS AT WHICH FORCES ARE DESIRED
EXTRUDE 257 C RR(I)=R-COORDINATE OF FLOW LINES TO BE CONSTRUCTED AT ENTRANCE.
EXTRUDE 258 C *****
EXTRUDE 259 C
EXTRUDE 260 C 120 READ(5,1003) (NPF(I),I=1,NPF)
EXTRUDE 261 C IF(NUMPC .LE. 0) GO TO 440
EXTRUDE 262 C WRITE(6,1007)
EXTRUDE 263 C
EXTRUDE 264 C *****
EXTRUDE 265 C SEE EXPLANATION OF INPUT DATA CARDS PREPARATION
EXTRUDE 266 C *****
EXTRUDE 267 C
EXTRUDE 268 C DO 441 I=1, NUMPC
EXTRUDE 269 C READ(5,1005) IJRC(I,1),IJRC(I,2),(PSRC(I,J),J=1,4)
EXTRUDE 270 C 441 WRITE(5,1008)IJRC(I,1),IJRC(I,2),(PSRC(I,J),J=1,4)
EXTRUDE 271 C 440 CONTINUE
EXTRUDE 272 C WRITE(6,1006) (NPF(I),I=1,NPF)
EXTRUDE 273 C READ (5,1001) (RR(I),I=1,NTIMES)
EXTRUDE 274 C WRITE(6,1013) (RR(I),I=1,NTIMES)
EXTRUDE 275 C
EXTRUDE 276 C *****
EXTRUDE 277 C READ AND PRINT OF ELEMENT PROPERTIES
EXTRUDE 278 C *****
EXTRUDE 279 C
EXTRUDE 280 C N=0
EXTRUDE 291 C 170 READ (5,1003) M,(IEL(N,I),I=1,4)
EXTRUDE 282 C 140 N=N+1
EXTRUDE 293 C IF (M=N) 170,170,150
EXTRUDE 284 C 150 DO 160 J=1,4
EXTRUDE 285 C 160 IEL(N,J)=IEL(N-1,J)+1
EXTRUDE 286 C 170 IF (M=N) 180,180,140
EXTRUDE 287 C 190 IF (NUMEL-N) 190,190,130
EXTRUDE 288 C 190 CONTINUE
EXTRUDE 289 C
EXTRUDE 290 C IF(NPRINT.EQ.0) GO TO 210
EXTRUDE 291 C WRITE (6,2001)
EXTRUDE 292 C DO 205 N=1,NUMEL
EXTRUDE 293 C 205 WRITE (6,2003) N,(IEL(N,I),I=1,4)
EXTRUDE 294 C
EXTRUDE 295 C *****
EXTRUDE 296 C DETERMINE BAND WIDTH
EXTRUDE 297 C *****
EXTRUDE 298 C
EXTRUDE 299 C 210 J=0
EXTRUDE 300 C DO 240 N=1,NUMEL
EXTRUDE 301 C DO 240 I=1,4
EXTRUDE 302 C DO 230 L=1,4
EXTRUDE 303 C KK=ABS( IEL(N,I)-IEL(N,L) )
EXTRUDE 304 C IF(KK-J) 230,230,220
EXTRUDE 305 C 220 J=KK
EXTRUDE 306 C 230 CONTINUE
EXTRUDE 307 C 240 CONTINUE
EXTRUDE 308 C MBAND=3*J+3
EXTRUDE 309 C MDIAG=1
EXTRUDE 310 C 250 WRITE (6,1122) NEQ,MBAND,MDIAG
EXTRUDE 311 C
EXTRUDE 312 C *****
EXTRUDE 313 C FOR EACH ELEMENT, ASSIGN THE MEAN PRESSURE VALUE TO THE NODAL POINT
EXTRUDE 314 C OF THE HIGHEST NUMBER AMONG THE FOUR CORNER NODAL POINTS.
EXTRUDE 315 C *****
EXTRUDE 316 C
EXTRUDE 317 C NSTOP=0
EXTRUDE 318 C DO 370 J=1,NUMEL
EXTRUDE 319 C MID=MAX0( IEL(J,1), IEL(J,2), IEL(J,3), IEL(J,4) )
EXTRUDE 320 C CODE(MID)=CODE(MID)+10.
EXTRUDE 321 C IF(CODE(MID).LT.20.) GO TO 370
EXTRUDE 322 C WRITE(6,1012) MID
EXTRUDE 323 C NSTOP=1
EXTRUDE 324 C 370 CONTINUE
EXTRUDE 325 C IF(NSTOP.EQ.1) STOP
EXTRUDE 326 C
EXTRUDE 327 C
EXTRUDE 328 C 1000 FORMAT(1H1)
EXTRUDE 329 C 1001 FORMAT(8F10.0)
EXTRUDE 330 C 1002 FORMAT (15,F5.0,5F10.0)
EXTRUDE 331 C 1003 FORMAT(16I5)
EXTRUDE 332 C 1005 FORMAT(2I5,4F10.0)
EXTRUDE 333 C 1006 FORMAT(// * THE NODAL POINTS AT WHICH FORCE CALCULATIONS ARE DESIR
EXTRUDE 334 C 1ED* // 2015)
EXTRUDE 335 C 1007 FORMAT(1H1,15X, 39H LINEARLY DISTRIBUTED BOUNDARY STRESSES/
EXTRUDE 336 C 1 / * NODE-I...NODE-J...PRESSURE-I...PRESSURE-J*
EXTRUDE 337 C 2 * SHEAR I SHEAR J*)
EXTRUDE 338 C 1008 FORMAT(1H ,2I5,4E15.5)

```

```

EXTRUDE 338 1012 FORMAT(/ * NODAL POINT ERROR FOR POINT NO. *,I5,*.....IT CONTAINS
EXTRUDE 339 1 MORE THAN ONE ELEMENT INFORMATION#/)
EXTRUDE 340 1013 FORMAT(/ * THE STARTING R-COORDINATES FOR STRAIN CALCULATIONS,*/
EXTRUDE 341 1 11F9.4,/)
EXTRUDE 342 1114 FORMAT(1H1, * NODAL POINT INFORMATION*,//)
EXTRUDE 343 1122 FORMAT(/// * NNUMBER OF EQUATIONS =*, I4/
EXTRUDE 344 1 * BANDWIDTH =*, I4/
EXTRUDE 345 2 * DIAGONAL ELEMENTS =*, I4 )
EXTRUDE 346 2000 FORMAT(1H 12A6/
EXTRUDE 347 1 30H0 NUMBER OF NODAL PCINTS----- I3 /
EXTRUDE 348 2 30H0 NUMBER OF ELEMENTS----- I3 /)
EXTRUDE 349 2001 FORMAT (1H1,40H ELEMENT NO. I J K L )
EXTRUDE 350 2002 FORMAT (112,F12.2,2F12.3)
EXTRUDE 351 2003 FORMAT (1113,8I6,1112)
EXTRUDE 352 2004 FORMAT (/ ,* NODAL POINT TYPE R-ORDINATE Z-ORDINATE*)
EXTRUDE 353 2009 FORMAT (26H NODAL POINT CARD ERROR N= I5)
EXTRUDE 354 2010 FORMAT(// * INITIAL YIELD STRESS = *, F15.2//)
EXTRUDE 355 2011 FORMAT(/// * MAXIMUM NUMBER OF ITERATIONS ALLOWED=*, I3)
EXTRUDE 356 RETURN
EXTRUDE 357 END

```

```

EXTRUDE 359 SUBROUTINE PLAST(R,Z,UR,UZ,CODE,IEL,YY,STS,TEPS,EPS,NF,FPUR,
EXTRUDE 360 11JBC,PSBC,FR,FZ,SDIE,RR,B,A,FST,ALANDA,GVCTR,NQ,NEL,NPC,
EXTRUDE 361 1NB2,FLIMIT,ITCNT,NTIMES,NIPTS,NJPTS,NMAX)
EXTRUDE 362 C
EXTRUDE 363 C *****
EXTRUDE 364 C PLAST IS THE CONTROLLING SUBROUTINE OF THE MATRIX METHOD
EXTRUDE 365 C *****
EXTRUDE 366 C
EXTRUDE 367 COMMON/GENCON/NUMNP,NUMEL,HED(12),VOL,NEQ,NS,ITERNO,ISTOP,
EXTRUDE 368 1YIELD,MBAND,TEST,MDIAG,NBF,NUMPC,ITER,NBF2,NSCALE,NPUNCH,NPRINT,
EXTRUDE 369 2 NCHECK,ACFINI
EXTRUDE 370 COMMON /WALL/ THETA,FT,TANTH
EXTRUDE 371 COMMON /DIMEN/ M1,M2,M3,M4,M5,M6,M7,M8,M9,M10,M11,M12,M13,M14
EXTRUDE 372 DIMENSION R(1),Z(1),UR(1),UZ(1),CODE(1),IEL( NEL ,1),YY(1)
EXTRUDE 373 1,STS(6,1),TEPS(5,1),EPS(5,1),NF(1),FPUR(1),JBC(NPC,1),RR(1),
EXTRUDE 374 2PSBC( NPC ,1),FR(1),FZ(1),SDIE(1),B(1),A( NO,1),FST(NB2 ,1)
EXTRUDE 375 DIMENSION ALANDA(1),GVCTR(1)
EXTRUDE 376 C
EXTRUDE 377 C*****
EXTRUDE 378 C INITIALIZED ALL VARIABLES
EXTRUDE 379 C GVCTR(N) IS USED FOR STORING THE AMOUNT OF VELOCITY AND MEAN STRESS
EXTRUDE 380 C TO BE MODIFIED FROM THE RESULT OF ITERATION,THESE VALUES
EXTRUDE 381 C ARE REDUCED BY DECELERATION COEFFICIENT IN ORDER TO ENSURE
EXTRUDE 382 C THE CONVERGENCE OF THE SOLUTION.
EXTRUDE 383 C TEPS(5,N)=TOTAL EFFECTIVE STRAIN
EXTRUDE 384 C A, B, STAND FOR MATRICES IN EQUATION AX=B, AFTER SOLVING THIS EQUATION
EXTRUDE 385 C THE X VECTOR IS THEN STORED IN B
EXTRUDE 386 C YY(N)= EFFECTIVE STRESS
EXTRUDE 387 C TEPS(I,N)= TO STORE THE PREVIOUS VALUE OF YY(N) FOR CHECKING
EXTRUDE 388 C CONVERGENCE FOR WORK-HARDENING MATERIAL
EXTRUDE 389 C TEPS(2,N)=DIFFERENCE OF EFFECTIVE STRESS BETWEEN THE PREVIOUS AND NEW
EXTRUDE 390 C SOLUTIONS.(FOR WORK-HARDENING MATERIALS)
EXTRUDE 391 C ITST= INDEX FOR CONVERGENCE OF SOLUTIONS(ITST=2 INDICATES THE ITERATION
EXTRUDE 392 C DOES NOT CONVERGENT)
EXTRUDE 393 C FSORI,FF= TOTAL SQUARE NORM OF EQUATIONS IN MINIMIZATION
EXTRUDE 394 C FSQRS,FFFF= SQUARE NORM OF EQUATIONS CORRESPONDING TO
EXTRUDE 395 C INCOMPRESSIBILITY CONDITIONS(VOLUMN CONSISTANCE)
EXTRUDE 396 C DIFF=FF-FSORI, DIFFERENCE OF TOTAL SQUARE NORMS OF PREVIOUS AND
EXTRUDE 397 C PRESENT ITERATIONS
EXTRUDE 398 C*****
EXTRUDE 399 C
EXTRUDE 400 DO 998 I=1,M14
EXTRUDE 401 998 A(I)=0.0
EXTRUDE 402 DO 999 N=1,NEQ
EXTRUDE 403 ALANDA(N)=0.
EXTRUDE 404 999 GVCTR(N)=0.
EXTRUDE 405 DO 442 N=1, NUMEL
EXTRUDE 406 YY(N)=1.0
EXTRUDE 407 DO 442 I=1, 5
EXTRUDE 408 442 TEPS(I,N)=0.
EXTRUDE 409 FSORI=0.
EXTRUDE 410 FSQRS=0.
EXTRUDE 411 FFFF=0.
EXTRUDE 412 ITST=1
EXTRUDE 413 FF=0.
EXTRUDE 414 DIFF=0.
EXTRUDE 415 C
EXTRUDE 416 C*****
EXTRUDE 417 C READ THE INPUT VELOCITY FIELD
EXTRUDE 418 C*****
EXTRUDE 419 C
EXTRUDE 420 READ(5,1017) (UR(I), UZ(I), I=1, NUMNP)

```



```

EXTRUDE 421 C
EXTRUDE 422 C*****
EXTRUDE 423 C DOUBLE CHECK THE INPUT DATA
EXTRUDE 424 C*****
EXTRUDE 425 C
EXTRUDE 426 DO 9889 I=1,NUMNP
EXTRUDE 427 IF(CODE(I).EQ.1..OR.CODE(I).EQ.11..OR.CODE(I).EQ.3..OR.CODE(I)
EXTRUDE 428 1 .EQ.13.) UR(I)=0.0
EXTRUDE 429 IF(CODE(I).EQ.5..OR.CODE(I).EQ.15.) UR(I)=UZ(I)*TANTH
EXTRUDE 430 9889 CONTINUE
EXTRUDE 431 WRITE(6,1020)
EXTRUDE 432 WRITE(6,1017) (UR(I), UZ(I), I=1, NUMNP)
EXTRUDE 433 C
EXTRUDE 434 C*****
EXTRUDE 435 C ITER=TOTAL NUMBER OF ITERATIONS ASSIGNED.
EXTRUDE 436 C ITERNO = AN INDEX FOR QUAD1(SEE SUBROUTINE STIFF AND COMMENT BELOW)
EXTRUDE 437 C*****
EXTRUDE 438 C
EXTRUDE 439 ITERNO=1
EXTRUDE 440 DO 2000 KIT=1,ITER
EXTRUDE 441 INDCON=KIT
EXTRUDE 442 C
EXTRUDE 443 C*****
EXTRUDE 444 C CHECK IF IT IS FIRST ITERATION
EXTRUDE 445 C IF FIRST ITERATION, ITERNO=1,PERFORM QUAD1. OTHERWISE JUST READ
EXTRUDE 446 C RESULTS OF QUAD1 FROM TAPE 1.
EXTRUDE 447 C*****
EXTRUDE 448 C
EXTRUDE 449 579 IF(KIT-1) 599,599,598
EXTRUDE 450 C
EXTRUDE 451 C*****
EXTRUDE 452 C NWKHRD IS AN INDEX TO SUBROUTINE STIFF
EXTRUDE 453 C NWKHRD=1 JUST CALCULATE STRAIN RATE IN SUBROUTINE STIFF
EXTRUDE 454 C NWKHRD=0 DOING WHOLE THING IN SUBROUTINE STIFF
EXTRUDE 455 C*****
EXTRUDE 456 C
EXTRUDE 457 599 NWKHRD=0
EXTRUDE 458 IF(ITCONT.NE.1) NWKHRD=1
EXTRUDE 459 CALL STIFF (R,Z,UR,UZ, CODE, IEL, YV, STS, EPS, NF, FPUR, FST,
EXTRUDE 460 1 IJBC, PSBC, A, B, NEL, NO, NPC, NB2, ALANDA, NWKHRD)
EXTRUDE 461 ITERNO=2
EXTRUDE 462 IF(ITCONT.EQ.1) GO TO 593
EXTRUDE 463 C
EXTRUDE 464 C*****
EXTRUDE 465 C UNNECESSARY TO CALCULATE TOTAL EFFECTIVE STRAIN FOR NON-HARDENING
EXTRUDE 466 C MATERIALS EXCEPT AT FINAL OUTPUT
EXTRUDE 467 C*****
EXTRUDE 468 C
EXTRUDE 469 CALL STRAINSTR, Z, UR, UZ, IEL, EPS, TEPS, A(M1), A(M2), A(M3), A(M4), A(M5),
EXTRUDE 470 1 A(M6), A(M7), A(M8), A(M9), A(M10), A(M11), A(M12), RR, A(M13), NIPTS,
EXTRUDE 471 2 NJPTS, NTIMES, NEL, NUMNP, NMAX)
EXTRUDE 472 C
EXTRUDE 473 C*****
EXTRUDE 474 C CALCULATE NORMALIZED EFFECTIVE STRESS (FOR WORK-HARDENING)
EXTRUDE 475 C*****
EXTRUDE 476 C
EXTRUDE 477 DO 220 N=1, NUMEL
EXTRUDE 478 CALL HARD(TEPS(S,N), YV(N))
EXTRUDE 479 YV(N)=YV(N)/YIELD
EXTRUDE 480 220 TEPS(1,N)=YV(N)
EXTRUDE 481 NWKHRD=0
EXTRUDE 482 CALL STIFF (R,Z,UR,UZ, CODE, IEL, YV, STS, EPS, NF, FPUR, FST,
EXTRUDE 483 1 IJBC, PSBC, A, B, NEL, NO, NPC, NB2, ALANDA, NWKHRD)
EXTRUDE 484 593 CALL MODIFY (CODE, A, B, NUMNP, NEO, MBAND)
EXTRUDE 485 598 CONTINUE
EXTRUDE 486 C
EXTRUDE 487 C*****
EXTRUDE 488 C SOLUTION FOR BANDED SYMMETRIC MATRIX
EXTRUDE 489 C*****
EXTRUDE 490 C
EXTRUDE 491 CALL TRIA(NEO, MBAND, A)
EXTRUDE 492 CALL BACKS(NEO, MBAND, A, B)
EXTRUDE 493 C
EXTRUDE 494 C*****
EXTRUDE 495 C SET CORRESPONDING VALUE FOR INCLINED SPECIAL BOUNDARY CONDITIONS
EXTRUDE 496 C*****
EXTRUDE 497 C
EXTRUDE 498 DO 769 N=1, NUMNP
EXTRUDE 499 IZ=3*N-1
EXTRUDE 500 IR=IZ-1
EXTRUDE 501 769 IF(CODE(N).EQ.5..OR.CODE(N).EQ.15.) B(IR)=B(IZ)*TAN(THETA)
EXTRUDE 502 C
EXTRUDE 503 C*****
EXTRUDE 504 C IF FIRST ITERATION, SET INITIAL STEP LENGTH ACCORDING TO
EXTRUDE 505 C DECELERATION COEFF. ASSIGNED. OTHERWISE FIND THE BEST DECELERATION
EXTRUDE 506 C COEFF. FROM INFORMATION OF PREVIOUS ITERATION.
EXTRUDE 507 C*****
EXTRUDE 508 C

```

```

EXTRUDE 509      507 C4=0.0
EXTRUDE 510      DO 509 I=1,NUMNP
EXTRUDE 511      IZ=3*I-1
EXTRUDE 512      IR=IZ-1
EXTRUDE 513      509 C4=C4+B(IZ)*B(IZ)+B(IR)*B(IR)
EXTRUDE 514      CORNOM=SQRT(C4)
EXTRUDE 515      IF(KIT.EQ.1) GO TO 551
EXTRUDE 516      67 ACDEF=1.0
EXTRUDE 517      510 IF((ACDEF*CORNOM).LT.STEPLM) GO TO 550
EXTRUDE 518      522 ACDEF=0.9*ACDEF
EXTRUDE 519      GO TO 510
EXTRUDE 520      551 ACDEF=ACFINI
EXTRUDE 521      STEPLM=ACDEF*CORNOM
EXTRUDE 522      STEPOR=STEPLM
EXTRUDE 523      550 FF=FSOR1
EXTRUDE 524      FFFF=FSORS
EXTRUDE 525      C
EXTRUDE 526      C*****
EXTRUDE 527      C CALCULATE FORCES AT NODAL POINTS
EXTRUDE 528      C*****
EXTRUDE 529      C
EXTRUDE 530      CALL CFORCE(NP,FR,FZ,FST,FPUR,B,MBAND,NBF,NBF2)
EXTRUDE 531      WRITE(6,1007)
EXTRUDE 532      WRITE(6,1016) KIT
EXTRUDE 533      C
EXTRUDE 534      C*****
EXTRUDE 535      C STS(6,N)=MEAN STRESS AT PRESENT SOLUTION.
EXTRUDE 536      C ALANDA(IR)=MEAN STRESS FROM PREVIOUS SOLUTION. IF FIRST ITERATION,
EXTRUDE 537      C THESE VALUES ARE THE SAME AS STS(6,N)
EXTRUDE 538      C*****
EXTRUDE 539      C
EXTRUDE 540      DO 133 N=1, NUMEL
EXTRUDE 541      I=MAX0(IEL(N,1), IEL(N,2), IEL(N,3), IEL(N,4))
EXTRUDE 542      IR=3*I
EXTRUDE 543      112 STS(6,N)=B(IR)
EXTRUDE 544      IF(KIT.EQ.1) ALANDA(IR)=B(IR)
EXTRUDE 545      GVECTR(IR)=B(IR)-ALANDA(IR)
EXTRUDE 546      133 B(IR)=0.
EXTRUDE 547      C
EXTRUDE 548      C*****
EXTRUDE 549      C CALCULATION OF SOLUTION NORM FOR VELOCITIES
EXTRUDE 550      C SNORM= NORM OF SOLUTION VECTOR OF VELOCITIES
EXTRUDE 551      C ENORM= NORM OF ERROR VECTOR OF VELOCITIES
EXTRUDE 552      C*****
EXTRUDE 553      C
EXTRUDE 554      SNORM = 0.
EXTRUDE 555      DO 134 I=1, NUMNP
EXTRUDE 556      IZ=3*I-1
EXTRUDE 557      IR=IZ-1
EXTRUDE 558      IN=IZ+1
EXTRUDE 559      GVECTR(IR)=B(IR)
EXTRUDE 560      GVECTR(IZ)=B(IZ)
EXTRUDE 561      SNORM = SNORM + UR(I)*UR(I) + UZ(I)*UZ(I)
EXTRUDE 562      C
EXTRUDE 563      C*****
EXTRUDE 564      C MODIFY THE VELOCITY FIELDS AND MEAN STRESSES
EXTRUDE 565      C*****
EXTRUDE 566      C
EXTRUDE 567      ALANDA(IN)=ALANCA(IN)+GVECTR(IN)*ACDEF
EXTRUDE 568      UR(I)=UR(I)+B(IR)*ACDEF
EXTRUDE 569      UZ(I)=UZ(I)+B(IZ)*ACDEF
EXTRUDE 570      134 CONTINUE
EXTRUDE 571      ENORM=CORNOM
EXTRUDE 572      SNORM = SQRT(SNORM)
EXTRUDE 573      ESNORM=ENORM/SNORM
EXTRUDE 574      C
EXTRUDE 575      C *****
EXTRUDE 576      C PRINT SOLUTION NORM OF VELOCITIES, VELOCITY DISTRIBUTIONS AND NODAL-
EXTRUDE 577      C POINT FORCES
EXTRUDE 578      C *****
EXTRUDE 579      C
EXTRUDE 580      IF(NBF .LE. 0) GO TO 125
EXTRUDE 581      DO 123 I=1, NBF
EXTRUDE 582      FR(I)=FR(I)*YIELD
EXTRUDE 583      FZ(I)=FZ(I)*YIELD
EXTRUDE 584      123 CONTINUE
EXTRUDE 585      125 CONTINUE
EXTRUDE 586      WRITE(6,1015) SNORM,ENORM,ESNORM
EXTRUDE 587      WRITE(6,1006) KIT,ACDEF
EXTRUDE 588      DO 439 I=1, NUMNP
EXTRUDE 589      IZ=3*I-1
EXTRUDE 590      IR=IZ-1
EXTRUDE 591      WRITE(6,1002) I,B(IR),B(IZ),UR(I),UZ(I),R(I),Z(I)
EXTRUDE 592      439 CONTINUE
EXTRUDE 593      WRITE(6,1010)
EXTRUDE 594      DO 140 I=1, NBF
EXTRUDE 595      SHEAR=FZ(I)*COS(THETA) + FR(I)*SIN(THETA)
EXTRUDE 596      140 WRITE(6,1012) NP(I),FR(I),FZ(I) ,SHEAR

```



```

EXTRUDE 597 C
EXTRUDE 598 C *****
EXTRUDE 599 C CONSTRUCT THE FLOW LINES AND CARRY OUT THE INTEGRATION OF THE STRAIN
EXTRUDE 600 C RATES TO DETERMINE THE TOTAL STRAIN DISTRIBUTION FOR WORK-HARDENING
EXTRUDE 601 C MATERIAL. THIS STEP IS PERFORMED ONLY AT FINAL ITERATION FOR NON-
EXTRUDE 602 C WORKHARDENING MATERIAL
EXTRUDE 603 C *****
EXTRUDE 604 C
EXTRUDE 605 563 IF(ESNORM.LE.FLIMIT.OR.KIT.EO.ITER) GO TO 56
EXTRUDE 606 IF(ITCONT.EO.1) GO TO 55
EXTRUDE 607 56 IF(ITCONT.EO.1) GO TO 58
EXTRUDE 608 NWKHRD=1
EXTRUDE 609 CALL STIFF (R,Z,UR,UZ,CCDE,IEL,YY,STS,EPS,NF,FPUR,FST,
EXTRUDE 610 IJBC,PS9C,A,B,NEL,NO,NPC,NB2,ALANDA,NWKHRD)
EXTRUDE 611 5A CALL STRAINS(R,Z,UR,UZ,IEL,EPS,TEPS,A(M1),A(M2),A(M3),A(M4),A(M5),
EXTRUDE 612 1 A(M6),A(M7),A(M8),A(M9),A(M10),A(M11),A(M12),RR,A(M13),NIPTS,
EXTRUDE 613 2 NJPTS,NTIMES,NEL,NUMNP,NMAX)
EXTRUDE 614 IF(ITCONT.EO.1) GO TO 55
EXTRUDE 615 DD 230 N=1,NUMEL
EXTRUDE 616 CALL HARD(TEPS(5,N),YY(N))
EXTRUDE 617 YY(N)=YY(N)/YIELD
EXTRUDE 618 C
EXTRUDE 619 C *****
EXTRUDE 620 C TEPS(1,N)= PREVIOUS EFFECTIVE STRESS
EXTRUDE 621 C TEPS(2,N)=DIFFERENCE OF EFFECTIVE STRESS BETWEEN THE PREVIOUS AND NEW
EXTRUDE 622 C SOLUTIONS.(FOR WORK-HARDENING MATERIALS)
EXTRUDE 623 C *****
EXTRUDE 624 C
EXTRUDE 625 TEPS(2,N)=YY(N)-TEPS(1,N)
EXTRUDE 626 230 TEPS(1,N)=YY(N)
EXTRUDE 627 C
EXTRUDE 628 C *****
EXTRUDE 629 C PRINT THE STRESS AND STRAIN-RATE DISTRIBUTIONS AND THE EFFECTIVE
EXTRUDE 630 C STRAIN DISTRIBUTION.
EXTRUDE 631 C *****
EXTRUDE 632 C
EXTRUDE 633 55 CONTINUE
EXTRUDE 634 WRITE(6,1007)
EXTRUDE 635 WRITE(6,1005) KIT
EXTRUDE 636 DD 222 N=1, NUMEL
EXTRUDE 637 CONST=2.*YY(N)/(3.*EPS(5,N))
EXTRUDE 638 STS(1,N)=EPS(1,N)*CONST
EXTRUDE 639 STS(2,N)=EPS(2,N)*CONST
EXTRUDE 640 STS(3,N)=EPS(3,N)*CONST
EXTRUDE 641 STS(4,N)=EPS(4,N)*CONST/2.
EXTRUDE 642 DD 132 J=1, 3
EXTRUDE 643 132 STS(J,N)=STS(J,N)+STS(6,N)
EXTRUDE 644 STS(5,N)=EFSTRS(STS(1,N),STS(2,N),STS(3,N),STS(4,N))
EXTRUDE 645 WRITE(6,1004) N, ( EPS(I,N),I=1,5),TEPS(5,N),(STS(I,N),I=1,6)
EXTRUDE 646 222 CONTINUE
EXTRUDE 647 C
EXTRUDE 648 C *****
EXTRUDE 649 C CHECK THE CONVERGENCE OF NEW SOLUTION, IF IT IS NOT, THEN REDUCE
EXTRUDE 650 C ACCEL. COEFF. AND CORRESPONDING STEP LENGTH AND CHECK IT AGAIN
EXTRUDE 651 C FOR FIRST ITERATION, THIS STEP IS OMITTED AND JUST COMPUTE THE TOTAL
EXTRUDE 652 C SQUARE NORM OF EQUATIONS AND INCOMPRESSIBILITY CONDITIONS
EXTRUDE 653 C *****
EXTRUDE 654 C
EXTRUDE 655 564 NWKHRD=0
EXTRUDE 656 CALL STIFF (R,Z,UR,UZ,CCDE,IEL,YY,STS,EPS,NF,FPUR,FST,
EXTRUDE 657 IJBC,PS9C,A,B,NEL,NO,NPC,NB2,ALANDA,NWKHRD)
EXTRUDE 658 CALL MODIFY (CODE,A,B,NUMNP,NEG,MBAND)
EXTRUDE 659 C
EXTRUDE 660 C *****
EXTRUDE 661 C COMPUTE TOTAL SQUARE NORM OF EQUATIONS(FSQR1) AND SQUARE NORM OF
EXTRUDE 662 C INCOMPRESSIBILITY CONDITIONS(FSQRS)
EXTRUDE 663 C *****
EXTRUDE 664 C
EXTRUDE 665 FSQR5=0.0
EXTRUDE 666 FSQR1=0.0
EXTRUDE 667 DD 501 N=1,NUMNP
EXTRUDE 668 II=3*N
EXTRUDE 669 FSQR1=FSQR1+B(II)*B(II)
EXTRUDE 670 FSQR5=FSQR5+B(II)*R(II)
EXTRUDE 671 DD 591 JJ=2,3
EXTRUDE 672 II=II-1
EXTRUDE 673 BLANII=B(II)
EXTRUDE 674 JA=JJ
EXTRUDE 675 JK=II+JA-1
EXTRUDE 676 889 IF(JA.GT.MBAND) GO TO 889
EXTRUDE 677 BLANII=BLANII-A(II,JA)*ALANDA(JK)
EXTRUDE 678 JA=JA+3
EXTRUDE 679 JK=JK+3
EXTRUDE 680 GO TO 889
EXTRUDE 681 889 IF(N.GT.1) GO TO 792
EXTRUDE 682 GO TO 891

```

```

EXTRUDE 683 792 DO 893 J=3,11,3
EXTRUDE 684 KK=I+1-J
EXTRUDE 685 IF(KK.GT.MBRAND) GO TO 891
EXTRUDE 686 893 BLANII=PLANII-A(I,J,KK)=ALANDA(J)
EXTRUDE 687 891 FSQR1=FSQR1+BLANII*BLANII
EXTRUDE 688 501 CONTINUE
EXTRUDE 689 IF(KIT.EQ.1) GO TO 788
EXTRUDE 690 C
EXTRUDE 691 C *****
EXTRUDE 692 C COMPARE SQUARE NORM OF FUNCTIONS WITH PREVIOUS ONE.
EXTRUDE 693 C *****
EXTRUDE 694 C
EXTRUDE 695 DIFF=FF-FSQR1
EXTRUDE 696 IF(FSQR1-FF) 571,571,572
EXTRUDE 697 C
EXTRUDE 698 C *****
EXTRUDE 699 C CASE FOR SQUARE NORM OF NEW SOLUTION LARGER THAN PREVIOUS ONE, REDUCE
EXTRUDE 700 C ACCEL. COEFF. BY HALF AND COMPARE AGAIN.
EXTRUDE 701 C *****
EXTRUDE 702 C
EXTRUDE 703 572 IF((ABS(DIFF)/FF).LE.1.E-3) GO TO 444
EXTRUDE 704 STEPLM=0.5*STEPLM
EXTRUDE 705 ACCEF=ACCEF*0.5
EXTRUDE 706 INOCON=INOCON+1
EXTRUDE 707 IF(INOCON-(KIT+5))581,581,592
EXTRUDE 708 581 DO 595 I=1,NUMNP
EXTRUDE 709 IZ=3*I-1
EXTRUDE 710 IR=IZ-1
EXTRUDE 711 IN=IZ+1
EXTRUDE 712 ALANDA(IN)=ALANDA(IN)-GVECTR(IN)*ACCEF
EXTRUDE 713 UR(I)=UR(I)-GVECTR(IR)*ACCEF
EXTRUDE 714 595 UZ(I)=UZ(I)-GVECTR(IZ)*ACCEF
EXTRUDE 715 WRITE(6,1155) STEPLM,FSQR1,FF,DIFF,FSQRS,FFFF
EXTRUDE 716 WRITE(6,1030) ACCEF
EXTRUDE 717 DO 772 I=1,NUMNP
EXTRUDE 718 IZ=3*I-1
EXTRUDE 719 IR=IZ-1
EXTRUDE 720 WRITE(6,1002)I,B(IP),B(IZ),UR(I),UZ(I)
EXTRUDE 721 772 CONTINUE
EXTRUDE 722 IF(ITCONT.EQ.1) GO TO 564
EXTRUDE 723 DO 561 N=1,NUMEL
EXTRUDE 724 561 VV(N)=TEPS(1,N)-TEPS(2,N)*0.5
EXTRUDE 725 GO TO 564
EXTRUDE 726 C
EXTRUDE 727 C *****
EXTRUDE 728 C IF CONTINUOUS REDUCING DECEL. COEFF. OF FIVE TIMES, THE SOLUTION
EXTRUDE 729 C STILL NOT CONVERGENT, THEN PUNCH AND PRINT THE RESULT AND STOP THE
EXTRUDE 730 C PROGRAM.
EXTRUDE 731 C *****
EXTRUDE 732 C
EXTRUDE 733 582 WRITE(6,1135) STEPLM,FSQR1,FF,DIFF,FSQRS,FFFF
EXTRUDE 734 WRITE(6,1056)
EXTRUDE 735 ITST=2
EXTRUDE 736 GO TO 600
EXTRUDE 737 C
EXTRUDE 738 C *****
EXTRUDE 739 C CASE FOR SQUARE NORM OF NEW SOLUTION LESS THAN PREVIOUS ONE, IF
EXTRUDE 740 C CONVERGENCE CHARACTER IS IN GOOD SITUATION, THEN INCREASE STEP
EXTRUDE 741 C LENGTH FOR NEXT ITERATION.
EXTRUDE 742 C *****
EXTRUDE 743 C
EXTRUDE 744 571 FSQR2=(STEPOR/STEPLM)*(FSQR1-FF)+FF
EXTRUDE 745 IF(FSQR2-0.965*FF) 574,574,575
EXTRUDE 746 575 STEPLM=0.8*STEPLM
EXTRUDE 747 GO TO 444
EXTRUDE 748 574 IF(FSQR2-0.900*FF) 576,576,444
EXTRUDE 749 576 STEPLM=1.2*STEPLM
EXTRUDE 750 444 CONTINUE
EXTRUDE 751 STEPOR=STEPLM
EXTRUDE 752 WRITE(6,1155) STEPLM,FSQR1,FF,DIFF,FSQRS,FFFF
EXTRUDE 753 788 CONTINUE
EXTRUDE 754 C
EXTRUDE 755 C *****
EXTRUDE 756 C STOP ITERATIONS AND PUNCH RESULTS IF (ERROR NORM)/(SOLUTION NORM)
EXTRUDE 757 C REACH THE ASSIGNED ACCUPACY.
EXTRUDE 758 C *****
EXTRUDE 759 C
EXTRUDE 760 IF(ESNORM.LE.FLIMIT) GO TO 600
EXTRUDE 761 C
EXTRUDE 762 C *****
EXTRUDE 763 C PUNCH SOLUTIONS AT EVERY FIFTH ITERATION BUT DOES NOT STOP THE
EXTRUDE 764 C ITERATIONS. PUNCH SOLUTIONS AT FINAL ITERATION.
EXTRUDE 765 C *****
EXTRUDE 766 C
EXTRUDE 767 K1=KIT/5
EXTRUDE 768 K2=K1*5

```



```

EXTRUDE 769      IF(K2.GE.KIT) GO TO 600
EXTRUDE 770      IF(KIT.EQ.ITER) GO TO 600
EXTRUDE 771      GO TO 660
EXTRUDE 772      600 PUNCH 1017, (UR(I),UZ(I), I=1, NUMNP)
EXTRUDE 773      NN=3*NUMNP
EXTRUDE 774      IF(NPUNCH .EQ. 0) GO TO 660
EXTRUDE 775      PUNCH 1017, (TEPS(5,N),N=1,NUMEL)
EXTRUDE 776      PUNCH 1017, ( (EPS(I,N),I=1,5), N=1,NUMEL)
EXTRUDE 777      PUNCH 1017,((STS(I,N),I=1,6),N=1,NUMEL)
EXTRUDE 778      DD 100 I=1,NBF
EXTRUDE 779      K=NF(I)
EXTRUDE 780      100 PUNCH 1012,K,UR(K),UZ(K),FR(I),FZ(I)
EXTRUDE 781      660 CONTINUE
EXTRUDE 782      IF(ITST.EQ.2) GO TO 2205
EXTRUDE 783      IF(ESNORM.LE.FLIMIT) GO TO 2205
EXTRUDE 784      2000 CONTINUE
EXTRUDE 785      C
EXTRUDE 786      C *****
EXTRUDE 787      C PRINT THE FINAL STRAIN-RATES, THE INCOMPRESSIBILITY AND THE
EXTRUDE 788      C INTEGRATED EFFECTIVE STRAIN DISTRIBUTION.
EXTRUDE 789      C *****
EXTRUDE 790      C
EXTRUDE 791      2205 CONTINUE
EXTRUDE 792      WRITE(6,1019) KIT
EXTRUDE 793      DD 500 N=1,NUMEL
EXTRUDE 794      SUM=EPS(1,N)+EPS(2,N)+EPS(3,N)
EXTRUDE 795      500 WRITE(6,1003) N,(EPS(I,N),I=1,5),SUM,TEPS(5,N)
EXTRUDE 796      WRITE(6,2222) STEPLM
EXTRUDE 797      C
EXTRUDE 798      1002 FORMAT(I10,2F13.7,10X, 2F13.7, 10X, 2F13.7)
EXTRUDE 799      1003 FORMAT(I7,11F11.6)
EXTRUDE 800      1004 FORMAT(I7,12F10.6)
EXTRUDE 801      1005 FORMAT(1H1,* STRAIN RATE-STRESS SOLUTION AT ITER. NUMBER =*,I4//
EXTRUDE 802      1 * EL. NO..R-STRAIN..Z-STRAIN..TH-STRAIN..RZ-STRAIN..EF-STRAIN..TOT.E
EXTRUDE 803      2FF...R-STRESS..Z-STRESS..TH-STRESS..RZ-STRESS..EF-STRESS..AVG-STRESS.
EXTRUDE 804      3.*,/,11X,*RATE*,6X,*RATE*,6X,*RATE*,6X,*RATE*,6X,*RATE*,6X,*RATE*,8X,*STRAIN
EXTRUDE 805      4*/)
EXTRUDE 806      1006 FORMAT(/// 30X, * VELOCITY SOLUTION AT ITERATION NUMBER =*,I4
EXTRUDE 807      1/,30X,* DECELERATION COEFFICIENT=* F13.8,
EXTRUDE 808      1/// 15X,*CORRECTED AMOUNT OF VEL.*,15X,*NEW SOLUTION*,21X,*COORDIN
EXTRUDE 809      1ATES*/.24X,*IN..*,29X,*OF*
EXTRUDE 810      2 /* NODAL NO. R-VELOCITY Z-VELOCITY R-VELOCITY
EXTRUDE 811      3 Z-VELOCITY R-COORD Z-COORD*)
EXTRUDE 812      1007 FORMAT(1H1)
EXTRUDE 813      1010 FORMAT( // * NODAL POINT FORCE**//
EXTRUDE 814      1*.....N.P.....R-FORCE.....Z-FORCE.....SHEAR FORCE ON DIE
EXTRUDE 815      2 SURFACE...*)
EXTRUDE 816      1012 FORMAT(I9,4F17.5)
EXTRUDE 817      1015 FORMAT( // 50X, * NORM OF SOLUTION VECTOR =*, F13.8
EXTRUDE 818      1 / 50X, * NORM OF ERROR VECTOR =*, F13.8
EXTRUDE 819      2 / 50X, * FRACTIONAL NODM =*, F13.8)
EXTRUDE 820      1016 FORMAT(/// 65X, * VELOCITY SOLUTION AT ITERATION NUMBER =*,I4)
EXTRUDE 821      1017 FORMAT(8F10.6)
EXTRUDE 822      1019 FORMAT(1H1,*FINAL STRAIN RATE SOLUTION AT ITER.NUMBER = *,I4,//
EXTRUDE 823      1 * EL. NO..R-STRAIN..Z-STRAIN..TH-STRAIN..RZ-STRAIN..EF-STRAIN..
EXTRUDE 824      2.....SUM.....TOT-EF-STRAIN*/.12X,*RATE*,7X,*RATE*7X,*RATE*
EXTRUDE 825      3,7X,*RATE*,7X,*RATE*//)
EXTRUDE 826      1020 FORMAT(///,* THE INITIAL GUESS( OR INPUT DATA) OF VELOCIT DISTRIBU
EXTRUDE 827      1TION*,/,* FROM FIRST NODAL POINT(R-VEL., Z-VEL.) TO LAST NODAL
EXTRUDE 828      2 POINT(R-VEL., Z-VEL.)*
EXTRUDE 829      1030 FORMAT(///,25X,*THE ABOVE VELOCITY DISTRIBUTION DOES NOT CONVERGE*
EXTRUDE 830      1/,25X,*REDUCE DECELERATION COEFF. WITH THE FOLLOWING VELOCITY DIS
EXTRUDE 831      1TRIBUTIONS*/.25X,*AND CALCULATE ALL NORMS AGAIN*
EXTRUDE 832      1/,25X,*NEW DECELERATION COEFFICIENT=*F13.8,
EXTRUDE 833      1 // 15X,*CORRECTED AMOUNT OF VEL.*,15X,*NEW SOLUTION*/.24X,*IN..*,
EXTRUDE 834      129X,*OF*/.
EXTRUDE 835      2 * NODAL NO. R-VELOCITY Z-VELOCITY R-VELOCITY
EXTRUDE 836      3 Z-VELOCITY*)
EXTRUDE 837      1056 FORMAT(///,20X,*SOLUTION DOES NOT CONVERGENT*)
EXTRUDE 838      1155 FORMAT(///,25X,*STEP LENGTH FOR NEXT ITERATION=*F13.8,
EXTRUDE 839      1 /,25X,*TOTAL SQUARE NORM OF ALL EQUATIONS AT PRESENT SOL
EXTRUDE 840      1UTION=*E16.8,
EXTRUDE 841      1 /,25X,*TOTAL SQUARE NORM OF ALL EQUATIONS FROM PREVIOUS
EXTRUDE 842      1SOLUTION=*E16.8,
EXTRUDE 843      1 /,25X,*DIFFERENCE=*E16.8,
EXTRUDE 844      1//,25X,*SQUARE NORM OF PRESENT VALUE IN VOL.CONSTISTANCE=*E16.8,
EXTRUDE 845      1 /,25X,*SQUARE NORM OF PREVIOUS VALUE IN VOL.CONSTISTANCE=*E16.8)
EXTRUDE 846      2222 FORMAT(///,20X,*FINAL STEPLM=* F14.6)
EXTRUDE 847      C
EXTRUDE 848      RETURN
EXTRUDE 849      END

```

```

EXTRUDE 851          SUBROUTINE HARD(STRAIN,YIELD)
EXTRUDE 852          C
EXTRUDE 853          C *****
EXTRUDE 854          C SPECIFY THE MATERIAL PROPERTIES FOR WORK-HARDENING MATERIAL (STRESS-
EXTRUDE 855          C STRAIN RELATIONSHIP) FOR NON-HARDENING MATERIAL. REPLACE #YIELD# CARD
EXTRUDE 856          C AND SET YIELD=THE CONSTANT YIELD STRESS.
EXTRUDE 857          C *****
EXTRUDE 858          C
EXTRUDE 859          B=0.262E-4
EXTRUDE 860          AN=0.06
EXTRUDE 861          YIELD=(1.+STRAIN/B)**AN
EXTRUDE 862          RETURN
EXTRUDE 863          END

```

```

EXTRUDE 865          SUBROUTINE STIFF (R,7,UR,UZ,CODE,IEL,VY,STS,EPS,NF,FPUR,FST,
EXTRUDE 866          IJBC,PSBC,A,B,NEL,NO,NPC,NR2,ALANDA,NWKHPD)
EXTRUDE 867          C
EXTRUDE 868          C *****
EXTRUDE 869          C CALCULATION STIFFNESS MATRIX FOR ENTIRE SYSTEM.
EXTRUDE 870          C *****
EXTRUDE 871          C
EXTRUDE 872          COMMON /GENCON/NUMNP,NUMEL,HED(12),VOL,NEG,NS,ITERNO,ISTOP,
EXTRUDE 873          IYIELD,MRAND,TEST,WDIAG,NBF,NUMPC,ITER,NPF2,NSCALE,NPUNCH,NPRINT,
EXTRUDE 874          2 NCHECK,ACFINI
EXTRUDE 875          COMMON /WALL/ THETA,FT,TANTH
EXTRUDE 876          COMMON /STFNAT/ P(9,9),H(9)
EXTRUDE 877          DIMENSION ALANDA(1)
EXTRUDE 878          DIMENSION R(1),Z(1),CODE(1),UR(1),UZ(1),IEL( NEL ,1),P(1),A( NO,1)
EXTRUDE 879          1,EPS(5,1),STS(6,1),NF(1),FST( NR2 ,1),FPUR(1),IJBC( NPC ,1),
EXTRUDE 880          2 PSBC(NPC,1),RR(4),ZZ(4),IXY(9),UU(6),VY(1),ID(2)
EXTRUDE 881          C
EXTRUDE 882          C *****
EXTRUDE 883          C INITIALIZED A AND B MATRICES (FOR EQUATION AX=R)
EXTRUDE 884          C BECAUSE BANDED SYMMETRIC PROPERTY OF THE STIFFNESS MATRIX A, THE
EXTRUDE 885          C STORAGE OF A IS IN A SQUIRE ARRAY.
EXTRUDE 886          C *****
EXTRUDE 887          C
EXTRUDE 888          NSTOP=0
EXTRUDE 889          DO 50 N=1, NEG
EXTRUDE 890          B(N)=0.
EXTRUDE 891          DO 50 M=1, MBAND
EXTRUDE 892          50 A(N,M)=0.
EXTRUDE 893          C
EXTRUDE 894          C *****
EXTRUDE 895          C CONSTRUCT ELEMENT LEVEL MATRICES FOR STIFFNESS
EXTRUDE 896          C IF ITERNO.GT.1 MEANS SUBROUTINE QIAD1 HAS BEEN PERFORMED ONCE BEFORE
EXTRUDE 897          C AND IS STORED IN TAPE 1.
EXTRUDE 898          C *****
EXTRUDE 899          C
EXTRUDE 900          IF(ITERNO.GT.1) GO TO 20
EXTRUDE 901          REWIND 1
EXTRUDE 902          DO 510 N=1,NUMEL
EXTRUDE 903          DO 100 I=1,4
EXTRUDE 904          II=IEL(N,I)
EXTRUDE 905          RR(I)=R(II)
EXTRUDE 906          100 ZZ(I)=Z(II)
EXTRUDE 907          CALL QUAD1(RR,ZZ,VOL)
EXTRUDE 908          42 IF(VOL.GT.0.) GO TO 510
EXTRUDE 909          WRITE(6,1005) N
EXTRUDE 910          NSTCP=1
EXTRUDE 911          510 CONTINUE
EXTRUDE 912          20 REWIND 1
EXTRUDE 913          IF(NSTOP .EQ. 1) STOP
EXTRUDE 914          C
EXTRUDE 915          C *****
EXTRUDE 916          C CONSTRUCT P AND M MATRICES AT ELEMENT LEVEL.
EXTRUDE 917          C *****
EXTRUDE 918          C
EXTRUDE 919          DO 1000 N=1, NUMEL
EXTRUDE 920          DO 60 I=1,4
EXTRUDE 921          II=IEL(N,I)
EXTRUDE 922          I2=2*I
EXTRUDE 923          I1=I2-1
EXTRUDE 924          IXV(I1)=3*II-2
EXTRUDE 925          IXV(I2)=3*II-1
EXTRUDE 926          UU(I2)=U7(II)
EXTRUDE 927          50 UU(I1)=UR(II)
EXTRUDE 928          II=MAX0( IEL(N,1),IEL(N,2),IEL(N,3),IEL(N,4) )
EXTRUDE 929          IXV(9)=3*II
EXTRUDE 930          CALL QUAD2(UU,IPLNAX,TEX,TEY,TEZ,TEXY)

```



```

EXTRUDE 931 C
EXTRUDE 932 C *****
EXTRUDE 933 C NWKHRD IS AN INDEX TO INDICATE WHETHER ONLY STRAIN RATE CALCULATION IS
EXTRUDE 934 C REQUIRED OR THE WHOLE STIFFNESS MATRIX NEED TO BE CONSTRUCTED.
EXTRUDE 935 C *****
EXTRUDE 936 C
EXTRUDE 937 IF(NWKHRD.EQ.1) GO TO 201
EXTRUDE 938 C
EXTRUDE 939 C *****
EXTRUDE 940 C PERFORM THE ASSEMBLY OPERATION. BECAUSE MATRIX A IS SYMMETRIC, ONLY
EXTRUDE 941 C UPPER HALF OF THE MATRIX IS CREATED. AND THE STORAGE FOR MATRIX A IS
EXTRUDE 942 C A SQUARE ARRAY BECAUSE OF PANDED SYMMETRIC PROPERTY.
EXTRUDE 943 C *****
EXTRUDE 944 C
EXTRUDE 945 DO 62 I=1,8
EXTRUDE 946 M(I)=M(I)+VY(N)
EXTRUDE 947 DO 62 J=1,8
EXTRUDE 948 62 P(I,J)=P(I,J)+VY(N)
EXTRUDE 949 DO 200 I=1, 9
EXTRUDE 950 II=IXY(I)
EXTRUDE 951 B(II)=B(II)-M(I)
EXTRUDE 952 DO 200 J=1, 9
EXTRUDE 953 JJ=IXY(J)-II+1
EXTRUDE 954 IF(IJ .LT. 1) GO TO 200
EXTRUDE 955 A(II,JJ)=A(II,JJ)+P(I,J)
EXTRUDE 956 200 CONTINUE
EXTRUDE 957 201 CONTINUE
EXTRUDE 958 EPS(1,N)=TEX
EXTRUDE 959 EPS(2,N)=TEY
EXTRUDE 960 EPS(3,N)=TEZ
EXTRUDE 961 EPS(4,N)=TEXY
EXTRUDE 962 1000 CONTINUE
EXTRUDE 963 563 DO 150 N=1,NUMEL
EXTRUDE 964 150 EPS(5,N)=RBAR(EPS(1,N),EPS(2,N),EPS(3,N),EPS(4,N))
EXTRUDE 965 IF(NWKHRD.EQ.1) RETURN
EXTRUDE 966 C
EXTRUDE 967 C *****
EXTRUDE 968 C PREPARATION FOR FORCE CALCULATION
EXTRUDE 969 C *****
EXTRUDE 970 C
EXTRUDE 971 IF(NBF .LE. 0) GO TO 402
EXTRUDE 972 MBAND2=2*MBAND-1
EXTRUDE 973 DO 330 I=1, NBF
EXTRUDE 974 IZ=2*I
EXTRUDE 975 IR=IZ-1
EXTRUDE 976 DO 330 J=1, MBAND2
EXTRUDE 977 FST(IR,J)=0.
EXTRUDE 978 330 FST(IZ,J)=0.
EXTRUDE 979 DO 400 I=1, NBF
EXTRUDE 980 II=NF(I)
EXTRUDE 981 I7=3*II-1
EXTRUDE 982 IR=IZ-1
EXTRUDE 983 IIZ=2*I
EXTRUDE 984 IIR=II7-1
EXTRUDE 985 DO 401 J=MBAND, MBAND2
EXTRUDE 986 JJ=J-MBAND+1
EXTRUDE 987 FST(IIR,J)=A(IR,JJ)
EXTRUDE 988 401 FST(IIZ,J)=A(IZ,JJ)
EXTRUDE 989 DO 403 J=1, MBAND
EXTRUDE 990 NP=IR-J+1
EXTRUDE 991 N7=I7-J+1
EXTRUDE 992 JJ=MBAND-J+1
EXTRUDE 993 IF(NR .LE. 0) GO TO 404
EXTRUDE 994 FST(IIR,JJ)=A(NR,J)
EXTRUDE 995 404 IF(NZ .LE. 0) GO TO 403
EXTRUDE 996 FST(IIZ,JJ)=A(NZ,J)
EXTRUDE 997 403 CONTINUE
EXTRUDE 998 FPUR(IIR)=B(IR)
EXTRUDE 999 400 FPUR(IIZ)=B(IZ)
EXTRUDE 1000 402 CONTINUE
EXTRUDE 1001 C
EXTRUDE 1002 C *****
EXTRUDE 1003 C ADD PRESSURE BOUNDARY CONDITION. (FOR CONSTANT FRICTIONAL STRESS DIES,
EXTRUDE 1004 C THE SHEAR TRACTIONAL STRESS (FRICTIONAL STRESS) IS ADDING HERE).
EXTRUDE 1005 C *****
EXTRUDE 1006 C
EXTRUDE 1007 IF ( NUMPC .EQ. 0 ) GO TO 410
EXTRUDE 1008 ID(1)=2
EXTRUDE 1009 ID(2)=1
EXTRUDE 1010 RI=1.0
EXTRUDE 1011 RJ=1.0
EXTRUDE 1012 DO 420 L=1,NUMPC
EXTRUDE 1013 I=JBC(L,1)
EXTRUDE 1014 J=JBC(L,2)
EXTRUDE 1015 DR=R(I)-R(J)
EXTRUDE 1016 DZ=Z(I)-Z(J)

```

```

EXTRUDE 1017 DO 290 M=1,2
EXTRUDE 1018 N=10(M)
EXTRUDE 1019 I=JRC(L,M)
EXTRUDE 1020 J=JRC(L,N)
EXTRUDE 1021 R1=R(I)
EXTRUDE 1022 RJ=R(J)
EXTRUDE 1023 I2=I+1
EXTRUDE 1024 I1=I2-1
EXTRUDE 1025 P1=PSBC(L,M)
EXTRUDE 1026 PJ=PSBC(L,N)
EXTRUDE 1027 S1=PSBC(L,M+2)
EXTRUDE 1028 SJ=PSBC(L,N+2)
EXTRUDE 1029 PM=(R1*(3.0*P1+PJ)+RJ*(P1+PJ))/12.0
EXTRUDE 1030 SM=(R1*(3.0*S1+SJ)+RJ*(S1+SJ))/12.0
EXTRUDE 1031 R1=DZ*PM+DR*SM
EXTRUDE 1032 R2=-DR*PM+DZ*SM
EXTRUDE 1033 B(I1)=B(I1)+R1
EXTRUDE 1034 B(I2)=B(I2)+R2
EXTRUDE 1035 290 CONTINUE
EXTRUDE 1036 420 CONTINUE
EXTRUDE 1037 410 CONTINUE
EXTRUDE 1038 C
EXTRUDE 1039 C 1005 FORMAT(// 29H ELEMENT WITH NEGATIVE AREA =, IS)
EXTRUDE 1040 C
EXTRUDE 1041 C RETURN
EXTRUDE 1042 C END

```

```

EXTRUDE 1044 SUBROUTINE QUAD(RR,ZZ,VOL)
EXTRUDE 1045 C
EXTRUDE 1046 C *****
EXTRUDE 1047 C CONSTRUCT B MATRIX AND K MATRIX (K=(TRANPOSE(B))(D)(B)), AND Q VECTOR
EXTRUDE 1048 C AT ELEMENT LEVEL FOR ALL ELEMENTS AND WRITE THESE MATRIX ON TAPE 1.
EXTRUDE 1049 C *****
EXTRUDE 1050 C
EXTRUDE 1051 COMMON /QUAD/ B(4,8),XX(8,8),C(B)
EXTRUDE 1052 DIMENSION RR(4),ZZ(4),SS(4),TT(4)
EXTRUDE 1053 DATA SS/-1.,+1.,+1.,-1./, TT/-1.,-1.,+1.,+1./
EXTRUDE 1054 SORT2=1.414213562373092
EXTRUDE 1055 DO 1 I=1,8
EXTRUDE 1056 Q(I)=0.
EXTRUDE 1057 DO 1 J=1,4
EXTRUDE 1058 1 B(J,I)=0.
EXTRUDE 1059 R1=RR(1)
EXTRUDE 1060 R2=RR(2)
EXTRUDE 1061 R3=RR(3)
EXTRUDE 1062 R4=RR(4)
EXTRUDE 1063 Z1=ZZ(1)
EXTRUDE 1064 Z2=ZZ(2)
EXTRUDE 1065 Z3=ZZ(3)
EXTRUDE 1066 Z4=ZZ(4)
EXTRUDE 1067 R12=R1-R2
EXTRUDE 1068 R13=R1-R3
EXTRUDE 1069 R14=R1-R4
EXTRUDE 1070 R23=R2-R3
EXTRUDE 1071 R24=R2-R4
EXTRUDE 1072 R34=R3-R4
EXTRUDE 1073 Z12=Z1-Z2
EXTRUDE 1074 Z13=Z1-Z3
EXTRUDE 1075 Z14=Z1-Z4
EXTRUDE 1076 Z23=Z2-Z3
EXTRUDE 1077 Z24=Z2-Z4
EXTRUDE 1078 Z34=Z3-Z4
EXTRUDE 1079 VOL=R13*Z24-R24*Z13
EXTRUDE 1080 IF(VOL.LE.0.) RETURN
EXTRUDE 1081 C
EXTRUDE 1082 C *****
EXTRUDE 1083 C CALCULATION OF TOTAL VOLUME PER RADIAN OF THE ELEMENT.
EXTRUDE 1084 C *****
EXTRUDE 1085 C
EXTRUDE 1086 VOL1=(Z1-Z4)*(R1*R1+R4*R4+P1*R4)
EXTRUDE 1087 VOL2=(Z3-Z2)*(R3*R3+R2*R2+R3*R2)
EXTRUDE 1088 VOL3=(Z2-Z1)*(R1*R1+R2*R2+R1*R2)
EXTRUDE 1089 VOL4=(Z4-Z3)*(R3*R3+R4*R4+R3*R4)
EXTRUDE 1090 VOLL=(VOL1+VOL2+VOL3+VOL4)/6.
EXTRUDE 1091 C
EXTRUDE 1092 C *****
EXTRUDE 1093 C THE FOLLOWING CONSTRUCT B AND K MATRIX BY TAKING FOUR INTEGRATION
EXTRUDE 1094 C POINTS OF THE ELEMENT.
EXTRUDE 1095 C *****
EXTRUDE 1096 C

```



```

EXTRUDE 1097      DO 15 I1=1,4
EXTRUDE 1098      S=S(I1)*0.577350269189626
EXTRUDE 1099      T=TT(I1)*0.577350269189626
EXTRUDE 1100      XJB=V/L+S*(R34*Z12-R12*Z34)+T*(R23*Z14-R14*Z23)
EXTRUDE 1101      XJ=XJB/R.
EXTRUDE 1102      C
EXTRUDE 1103      SM4=1.-S
EXTRUDE 1104      SP=1.+S
EXTRUDE 1105      TM=1.-T
EXTRUDE 1106      TP=1.+T
EXTRUDE 1107      H1=0.25*SM*TM
EXTRUDE 1108      H2=0.25*SP*TM
EXTRUDE 1109      H3=0.25*SP*TP
EXTRUDE 1110      H4=0.25*SM*TP
EXTRUDE 1111      R=H1*R1+H2*R2+H3*R3+H4*R4
EXTRUDE 1112      G1=H1/R
EXTRUDE 1113      G2=H2/R
EXTRUDE 1114      G3=H3/R
EXTRUDE 1115      G4=H4/R
EXTRUDE 1116      C
EXTRUDE 1117      C *****
EXTRUDE 1118      C CONSTRUCT R MATRIX AT EACH POINT
EXTRUDE 1119      C *****
EXTRUDE 1120      C
EXTRUDE 1121      X1=(-R24+R34*S+R23*T)/XJB
EXTRUDE 1122      X2=(R13-R34*S-R14*T)/XJB
EXTRUDE 1123      X3=(R24-R12*S+R14*T)/XJB
EXTRUDE 1124      X4=(-R13+R12*S-R23*T)/XJB
EXTRUDE 1125      Y1=(Z24-Z34*S-Z23*T)/XJB
EXTRUDE 1126      Y2=(-Z13+Z34*S+Z14*T)/XJB
EXTRUDE 1127      Y3=(-Z24+Z12*S-Z14*T)/XJB
EXTRUDE 1128      Y4=(Z13-Z12*S+Z23*T)/XJB
EXTRUDE 1129      B(1, 1)=Y1
EXTRUDE 1130      B(1, 3)=Y2
EXTRUDE 1131      B(1, 5)=Y3
EXTRUDE 1132      B(1, 7)=Y4
EXTRUDE 1133      B(2, 2)=X1
EXTRUDE 1134      B(2, 4)=X2
EXTRUDE 1135      B(2, 6)=X3
EXTRUDE 1136      B(2, 8)=X4
EXTRUDE 1137      B(3, 1)=G1
EXTRUDE 1138      B(3, 3)=G2
EXTRUDE 1139      B(3, 5)=G3
EXTRUDE 1140      B(3, 7)=G4
EXTRUDE 1141      B(4, 1)=X1/SORT2
EXTRUDE 1142      B(4, 2)=Y1/SORT2
EXTRUDE 1143      B(4, 3)=X2/SORT2
EXTRUDE 1144      B(4, 4)=Y2/SORT2
EXTRUDE 1145      B(4, 5)=X3/SORT2
EXTRUDE 1146      B(4, 6)=Y3/SORT2
EXTRUDE 1147      B(4, 7)=X4/SORT2
EXTRUDE 1148      B(4, 8)=Y4/SORT2
EXTRUDE 1149      C
EXTRUDE 1150      C *****
EXTRUDE 1151      C CONSTRUCT K MATRIX AT EACH POINT (IE. XX(I,J))
EXTRUDE 1152      C *****
EXTRUDE 1153      C
EXTRUDE 1154      DO 6 I=1,8
EXTRUDE 1155      DO 6 J=1,8
EXTRUDE 1156      DUM1=0.
EXTRUDE 1157      DO 5 K=1,4
EXTRUDE 1158      5 DUM1=DUM1+B(K,J)*B(K,I)
EXTRUDE 1159      XX(I,J)=DUM1
EXTRUDE 1160      XX(J,I)=DUM1
EXTRUDE 1161      6 CONTINUE
EXTRUDE 1162      C
EXTRUDE 1163      C *****
EXTRUDE 1164      C CONSTRUCT Q VECTOR AT EACH POINT, AND ADD ALL FOUR INTEGRATION POINTS
EXTRUDE 1165      C *****
EXTRUDE 1166      C
EXTRUDE 1167      XJR=XJ*R
EXTRUDE 1168      Q(1)=Q(1)+(Y1+G1)*XJR
EXTRUDE 1169      Q(2)=Q(2)+ X1 *XJR
EXTRUDE 1170      Q(3)=Q(3)+(Y2+G2)*XJR
EXTRUDE 1171      Q(4)=Q(4)+ X2 *XJR
EXTRUDE 1172      Q(5)=Q(5)+(Y3+G3)*XJR
EXTRUDE 1173      Q(6)=Q(6)+ X3 *XJR
EXTRUDE 1174      Q(7)=Q(7)+(Y4+G4)*XJR
EXTRUDE 1175      Q(8)=Q(8)+ X4 *XJR
EXTRUDE 1176      C
EXTRUDE 1177      C *****
EXTRUDE 1178      C WRITE K AND B MATRICES AT EACH INTEGRATION POINT ON TAPE 1
EXTRUDE 1179      C *****
EXTRUDE 1180      C

```

```

EXTRUDE 1181      WRITE(1) XJR
EXTRUDE 1182      WRITE(1)((XX(I,J),J=1,8 ),I=1,8 )
EXTRUDE 1183      WRITE(1)((P(I,J),J=1,8 ),I=1,4)
EXTRUDE 1184      16 CONTINUE
EXTRUDE 1185      C
EXTRUDE 1186      C *****
EXTRUDE 1187      C WRITE 0 VECTOR (AFTER INTEGRATION, I.E. ADDING FOUR POINTS) AND THE
EXTRUDE 1188      C TOTAL VOLUMN OF THE ELEMENT ON TAPE 1.
EXTRUDE 1189      C *****
EXTRUDE 1190      C
EXTRUDE 1191      WRITE(1)(O(I),I=1,8)
EXTRUDE 1192      VOL=VOLL
EXTRUDE 1193      WRITE(1) VOL
EXTRUDE 1194      C
EXTRUDE 1195      RETURN
EXTRUDE 1196      END

```

```

EXTRUDE 1198      SUBROUTINE QUAD2(UU,IPLNAX,TEX,TEY,TEZ,TEXY)
EXTRUDE 1199      C
EXTRUDE 1200      C *****
EXTRUDE 1201      C READ INFORMATION FROM TAPE1 REGARDING B, K AND O, AND CONSTRUCT P AND
EXTRUDE 1202      C H MATRICES AT ELEMENT LEVEL (I.E.P(I,J) AND H(I))
EXTRUDE 1203      C *****
EXTRUDE 1204      C
EXTRUDE 1205      COMMON /QUAD/ B(4,8),XX(8,8),BZERO(8)
EXTRUDE 1206      COMMON /STFNAT/ P(9,9),H(9)
EXTRUDE 1207      DIMENSION E(4),UU(8)
EXTRUDE 1208      DO 1 I=1,9
EXTRUDE 1209      H(I)=0.
EXTRUDE 1210      DO 1 J=1,9
EXTRUDE 1211      1 P(I,J) = 0.
EXTRUDE 1212      SORT2 = 1.414212562373092
EXTRUDE 1213      SORT1 = 1.224744871301586
EXTRUDE 1214      C
EXTRUDE 1215      C *****
EXTRUDE 1216      C TEX= R-STRAIN RATE
EXTRUDE 1217      C TEY= ?-STRAIN RATE
EXTRUDE 1218      C TEZ= TM-STRAIN RATE
EXTRUDE 1219      C TEXP= RZ-STRAIN RATE
EXTRUDE 1220      C *****
EXTRUDE 1221      C
EXTRUDE 1222      TEX = 0.
EXTRUDE 1223      TEY = 0.
EXTRUDE 1224      TEZ = 0.
EXTRUDE 1225      TEXP=0.
EXTRUDE 1226      DO 16 I=1,4
EXTRUDE 1227      READ(1)XJR
EXTRUDE 1228      READ(1)((XX(I,J),J=1,8 ),I=1,8 )
EXTRUDE 1229      READ(1)((B(I,J),J=1,8 ),I=1,4)
EXTRUDE 1230      DO 8 I=1,8
EXTRUDE 1231      DUMI=0.
EXTRUDE 1232      DO 7 J=1,8
EXTRUDE 1233      7 DUMI=DUMI+XX(I,J)*UU(J)
EXTRUDE 1234      8 BZERO(I)=DUMI
EXTRUDE 1235      PZERO=0.
EXTRUDE 1236      DO 9 I=1,8
EXTRUDE 1237      9 PZERO=PZERO+UU(I)*BZERO(I)
EXTRUDE 1238      C
EXTRUDE 1239      C *****
EXTRUDE 1240      C PZERO=(3/2) * SQUARE OF (EFF. STRINT RATE),
EXTRUDE 1241      C IF PZERO IS TOO SMALL CORRESPONDING TO RIGID ELEMENT, SET PZERO AS A
EXTRUDE 1242      C LIMITING VALUE IN ORDER NOT TO BREAK THE STIFFNESS MATRIX
EXTRUDE 1243      C P1=(2/3)/(SQUARE OF (EFFECTIVE STRAIN RATE))
EXTRUDE 1244      C P2=(2/3)/(EFFECTIVE STRAIN RATE)
EXTRUDE 1245      C *****
EXTRUDE 1246      C
EXTRUDE 1247      IF(PZERO.LE.1.E-08) PZERO=1.E-08
EXTRUDE 1248      P1=1./PZERO
EXTRUDE 1249      PZERO=SQRT(PZERO)
EXTRUDE 1250      P2=PZERO*SORT1
EXTRUDE 1251      DO 13 I=1,8
EXTRUDE 1252      DO 12 J=1,8
EXTRUDE 1253      12 P(I,J)=P(I,J)+(XX(I,J)-P1*BZERO(I)+BZERO(J))*XJR/P2
EXTRUDE 1254      13 H(I)=H(I)+BZERO(I)*XJR/P2
EXTRUDE 1255      DO 14 I=1,4
EXTRUDE 1256      E(I)=0.
EXTRUDE 1257      DO 14 J=1,8
EXTRUDE 1258      14 E(I)=E(I)+B(I,J)*UU(J)
EXTRUDE 1259      TEX=TEX+E(1)*XJR
EXTRUDE 1260      TEY=TEY+E(2)*XJR
EXTRUDE 1261      TEZ=TEZ+E(3)*XJR
EXTRUDE 1262      TEXP=TEXP+E(4)*SORT2*XJR
EXTRUDE 1263      16 CONTINUE

```



```

EXTRUDE 1264 C
EXTRUDE 1265 READ(1)(P(J,9),J=1,8)
EXTRUDE 1266 DO 17 J=1,8
EXTRUDE 1267 17 M(9)=M(9)+P(J,9)*UU(J)
EXTRUDE 1268 READ(1) VOL
EXTRUDE 1269 DO 18 I=1,9
EXTRUDE 1270 DO 18 J=1,9
EXTRUDE 1271 18 P(J,I)=P(I,J)
EXTRUDE 1272 TEX=TEX/VOL
EXTRUDE 1273 TEY=TEY/VOL
EXTRUDE 1274 TEZ=TEZ/VOL
EXTRUDE 1275 TEXY=TEXY/VOL
EXTRUDE 1276 C
EXTRUDE 1277 RETURN
EXTRUDE 1278 END

```

```

EXTRUDE 1280 FUNCTION RBAR (RX,RV,RZ,RXY)
EXTRUDE 1281 C
EXTRUDE 1282 C *****
EXTRUDE 1283 C CALCULATE THE EFFECTIVE STRAIN RATE
EXTRUDE 1284 C *****
EXTRUDE 1285 C
EXTRUDE 1286 RBAR=(RX-RV)**2+(RV-RZ)**2+(RZ-RX)**2
EXTRUDE 1287 RBAR=2.*SQRT(0.5*RBAR+3.*RXY**2/4.)/3.
EXTRUDE 1288 C
EXTRUDE 1289 C *****
EXTRUDE 1290 C IF THE EFFECTIVE STRAIN RATE IS TOO SMALL CORRESPONDING TO A RIGID
EXTRUDE 1291 C ELEMENT, SET IT TO A LIMITING VALUE.
EXTRUDE 1292 C *****
EXTRUDE 1293 C
EXTRUDE 1294 IF(RBAR.LT.1.E-04) RBAR=1.E-04
EXTRUDE 1295 RETURN
EXTRUDE 1296 END

```

```

EXTRUDE 1298 FUNCTION EFSTRS(SR,SZ,ST,SRZ)
EXTRUDE 1299 C
EXTRUDE 1300 C *****
EXTRUDE 1301 C CALCULATION OF EFFECTIVE STRESS.
EXTRUDE 1302 C *****
EXTRUDE 1303 C
EXTRUDE 1304 EFSTRS=(SR-SZ)**2+(SZ-ST)**2+(ST-SR)**2
EXTRUDE 1305 EFSTRS=SQRT(0.5*EFSTRS+3.*SRZ**2)
EXTRUDE 1306 RETURN
EXTRUDE 1307 END

```

```

EXTRUDE 1309 SUBROUTINE MODIFY (CODE,A,B,NUMNP,NEQ,MBAND)
EXTRUDE 1310 C
EXTRUDE 1311 C *****
EXTRUDE 1312 C DETERMINE THE POINTS FOR WHICH CORRESPONDING COMPONENT OF X IS
EXTRUDE 1313 C SPECIFIED EQUAL TO ZERO IN AX=B, AND CALL CONDEN FOR MATRIX
EXTRUDE 1314 C CONDENSATION
EXTRUDE 1315 C *****
EXTRUDE 1316 C
EXTRUDE 1317 COMMON /WALL/ THETA,PT,TANTH
EXTRUDE 1318 DIMENSION CODE(1),A(NEQ,1),B(1)
EXTRUDE 1319 DO 121 I=1, NUMNP
EXTRUDE 1320 IL=3*I
EXTRUDE 1321 IZ=IL-1
EXTRUDE 1322 IP=IZ-1
EXTRUDE 1323 C=CODE(I)
EXTRUDE 1324 C
EXTRUDE 1325 C *****
EXTRUDE 1326 C CHECK IF THIS POINT CONTAINS NO INFORMATION ABOUT MEAN STRESS
EXTRUDE 1327 C *****
EXTRUDE 1328 C
EXTRUDE 1329 IF(C.LT.10.) CALL CONDENA,B,NEQ,MBAND,IL,0.1
EXTRUDE 1330 C
EXTRUDE 1331 C *****
EXTRUDE 1332 C CHECK IF THE R-VELOCITY IS SPECIFIED
EXTRUDE 1333 C *****
EXTRUDE 1334 C
EXTRUDE 1335 IF(C.EQ.1..OR.C.EQ.11..OR.C.EQ.3..OR.C.EQ.13.)
EXTRUDE 1336 1 CALL CONDEN(A,B,NEQ,MBAND,IP,0.1)

```

```

EXTRUDE 1337 C
EXTRUDE 1338 C *****
EXTRUDE 1339 C CHECK IF THE Z-VELOCITY IS SPECIFIED
EXTRUDE 1340 C *****
EXTRUDE 1341 C
EXTRUDE 1342 IF (C.EQ.2..OR.C.EQ.12..OR.C.EQ.3..OR.C.EQ.13.)
EXTRUDE 1343 1 CALL CONDEN(A,B,NEQ,MBAND,IZ,0.)
EXTRUDE 1344 C
EXTRUDE 1345 C *****
EXTRUDE 1346 C CHECK IF THE POINT IS ALONG THE INCLINED BOUNDARY
EXTRUDE 1347 C *****
EXTRUDE 1348 C
EXTRUDE 1349 IF (C.EQ.5..OR.C.EQ.15.) CALL BCMIX(A,B,NEQ,MBAND,I,THETA)
EXTRUDE 1350 121 CONTINUE
EXTRUDE 1351 C
EXTRUDE 1352 RETURN
EXTRUDE 1353 END

```

```

EXTRUDE 1355 SUBROUTINE CONDEN(A,B,NEQ,MBAND,N,U)
EXTRUDE 1356 C
EXTRUDE 1357 C *****
EXTRUDE 1358 C PERFORM THE MATRIX CONDENSATION WHEN THE VALUE OF A COMPONENT X IN
EXTRUDE 1359 C AX=R IS SPECIFIED EQUAL TO ZERO.
EXTRUDE 1360 C *****
EXTRUDE 1361 C
EXTRUDE 1362 DIMENSION B(NEQ),A(NEQ,1)
EXTRUDE 1363 DO 235 M=2,MBAND
EXTRUDE 1364 K=N-M+1
EXTRUDE 1365 IF(K) 235,235,230
EXTRUDE 1366 230 A(K,M)=0.0
EXTRUDE 1367 235 A(N,M)=0.0
EXTRUDE 1368 A(N,1)=1.0
EXTRUDE 1369 B(N)=U
EXTRUDE 1370 RETURN
EXTRUDE 1371 END

```

```

EXTRUDE 1373 SUBROUTINE BCMIX(A,B,NEQ,MBAND,N,THETA)
EXTRUDE 1374 C
EXTRUDE 1375 C *****
EXTRUDE 1376 C THIS SUBROUTINE IS TO ENSURE THAT THE VELOCITY ALONG THE DIE IS
EXTRUDE 1377 C TANGENTIAL TO THE DIE FOR CONICAL DIES
EXTRUDE 1378 C *****
EXTRUDE 1379 C
EXTRUDE 1380 DIMENSION B(NEQ),A(NEQ,1)
EXTRUDE 1381 C
EXTRUDE 1382 C *****
EXTRUDE 1383 C SINCE UR=UZ*TAN(THETA) ALONG THE DIE, A CORRESPONDING CHANGE IS MADE
EXTRUDE 1384 C IN THE STIFFNESS EQUATIONS FOR ROWS AND COLUMNS CORRESPONDING TO
EXTRUDE 1385 C THESE COMPONENTS...THEN THE EQUATIONS CONTAINING UR ARE ELIMINATED
EXTRUDE 1386 C *****
EXTRUDE 1387 C
EXTRUDE 1388 NZ=3*N-1
EXTRUDE 1389 NR=NZ-1
EXTRUDE 1390 ALPA= TAN(THETA)
EXTRUDE 1391 DO 350 M=1,MBAND
EXTRUDE 1392 350 A(NR,M)=A(NR,M)*ALPA
EXTRUDE 1393 A(NR,1)=A(NR,1)*ALPA
EXTRUDE 1394 A(NR,2)=A(NR,2)*2.
EXTRUDE 1395 DO 340 M=2,MBAND
EXTRUDE 1396 KR=NR-M+1
EXTRUDE 1397 IF(KR.LE.0) GO TO 341
EXTRUDE 1398 340 A(KR,M)=A(KR,M)*ALPA
EXTRUDE 1399 341 CONTINUE
EXTRUDE 1400 B(NR) = B(NR)*ALPA
EXTRUDE 1401 DO 351 M=2,MBAND
EXTRUDE 1402 KZ=NZ-M+1
EXTRUDE 1403 IF(KZ.LE.0) GO TO 352
EXTRUDE 1404 A(KZ,M)=A(KZ,M)+A(KZ,M-1)
EXTRUDE 1405 352 CONTINUE
EXTRUDE 1406 IF(N.EQ.MBAND) GO TO 353
EXTRUDE 1407 KZ=NZ+M-1
EXTRUDE 1408 IF(KZ.GT.NEQ) GO TO 353
EXTRUDE 1409 A(NZ,M)=A(NZ,M)+A(NR,M+1)
EXTRUDE 1410 353 CONTINUE
EXTRUDE 1411 351 CONTINUE
EXTRUDE 1412 A(NZ,1)=A(NZ,1)+A(NR,2)
EXTRUDE 1413 A(NR,1)=1.0

```



```

EXTRUDE 1414      DO 355 M=2,MBAND
EXTRUDE 1415      KR=NR-M+1
EXTRUDE 1416      IF(KR.LE.0) GC TO 360
EXTRUDE 1417      A(KR,M)=0.0
EXTRUDE 1418      360 CONTINUE
EXTRUDE 1419      A(NR,M)=0.0
EXTRUDE 1420      355 CONTINUE
EXTRUDE 1421      B(NZ)=B(NR)+B(NZ)
EXTRUDE 1422      S(NR)=0.0
EXTRUDE 1423      C
EXTRUDE 1424      RETURN
EXTRUDE 1425      END

```

```

EXTRUDE 1427      SUBROUTINE TRIA(NN,MM,A)
EXTRUDE 1428      C
EXTRUDE 1429      C *****
EXTRUDE 1430      C TRIANGULARIZATION OF GUASSIAN ELIMINATION FOR THE SOLUTION OF BANDED
EXTRUDE 1431      C SYMMETRIC MATRIX.
EXTRUDE 1432      C *****
EXTRUDE 1433      C
EXTRUDE 1434      DIMENSION A(NN,1)
EXTRUDE 1435      1000 N=0
EXTRUDE 1436      100 N=N+1
EXTRUDE 1437      IF(N.EQ.NN)RETURN
EXTRUDE 1438      IF(A(N,1).EQ.0.0)GO TO 100
EXTRUDE 1439      I=N
EXTRUDE 1440      MB=M/NO(MM,NN-N+1)
EXTRUDE 1441      DO 260 L=2,MB
EXTRUDE 1442      I=I+1
EXTRUDE 1443      C=A(N,L)/A(N,1)
EXTRUDE 1444      IF(C.EQ.0.0)GG TO 260
EXTRUDE 1445      J=0
EXTRUDE 1446      DO 250 K=L,MB
EXTRUDE 1447      J=J+1
EXTRUDE 1448      250 A(I,J)=A(I,J)-C*A(N,K)
EXTRUDE 1449      A(N,L)=C
EXTRUDE 1450      260 CONTINUE
EXTRUDE 1451      GO TO 100
EXTRUDE 1452      END

```

```

EXTRUDE 1454      SUBROUTINE BACKS(NN,MM,A,R)
EXTRUDE 1455      C
EXTRUDE 1456      C *****
EXTRUDE 1457      C BACK SUBSTITUTION FOR SOLUTION OF BANDED SYMMETRIC MATRIX
EXTRUDE 1458      C *****
EXTRUDE 1459      C
EXTRUDE 1460      DIMENSION A(1),B(1)
EXTRUDE 1461      MM=MM-1
EXTRUDE 1462      N=0
EXTRUDE 1463      270 N=N+1
EXTRUDE 1464      C=B(N)
EXTRUDE 1465      IF(A(N).NE.0.0)R(N)=B(N)/A(N)
EXTRUDE 1466      IF(A(N.EQ.NN)GO TO 300
EXTRUDE 1467      IL=N+1
EXTRUDE 1468      IH=M/NO(NN,N+MM)
EXTRUDE 1469      M=N
EXTRUDE 1470      DO 285 I=IL,IH
EXTRUDE 1471      M=M+NN
EXTRUDE 1472      285 B(I)=R(I)-A(M)*C
EXTRUDE 1473      GO TO 270
EXTRUDE 1474      300 IL=N
EXTRUDE 1475      N=N-1
EXTRUDE 1476      IF(N.EQ.0) RETURN
EXTRUDE 1477      IH=M/NO(NN,N+MM)
EXTRUDE 1478      M=N
EXTRUDE 1479      DO 400 I=IL,IH
EXTRUDE 1480      M=M+NN
EXTRUDE 1481      400 R(N)=B(N)-A(M)*B(I)
EXTRUDE 1482      GO TO 300
EXTRUDE 1483      C
EXTRUDE 1484      END

```

```

EXTRUDE 1485          SUBROUTINE CFORCE(NF,FR,FZ,FST,FPUR,B,MBAND,NBF,NBF2)
EXTRUDE 1487          C
EXTRUDE 1488          C *****
EXTRUDE 1489          C CALCULATION OF FORCES ON BOUNDARY NODAL POINTS
EXTRUDE 1490          C *****
EXTRUDE 1491          C
EXTRUDE 1492          DIMENSION NF(1),FST(NBF2,1),FPUR(NBF2),FR(1),FZ(1),B(1)
EXTRUDE 1493          IF(NBF .LE. 0) GO TO 124
EXTRUDE 1494          MEAND2=2*MBAND-1
EXTRUDE 1495          DO 121 I=1, NBF
EXTRUDE 1496          IZ=3*NF(I)-1
EXTRUDE 1497          IR=I7-1
EXTRUDE 1498          IIZ=2*I
EXTRUDE 1499          IIR=I17-1
EXTRUDE 1500          SUMR=0.
EXTRUDE 1501          SUMZ=0.
EXTRUDE 1502          DO 122 J=1, MEAND2
EXTRUDE 1503          JR=IR+J-MBAND
EXTRUDE 1504          JZ=JR+1
EXTRUDE 1505          IF(JR .LE. 0) GO TO 120
EXTRUDE 1506          SUMR=SUMR+FST(IIR,J)*B(JR)
EXTRUDE 1507          126 IF(JZ .LE. 0) GO TO 122
EXTRUDE 1508          SUMZ=SUMZ+FST(IIZ,J)*B(JZ)
EXTRUDE 1509          122 CONTINUE
EXTRUDE 1510          FR(I)=SUMR-FPUR(IIR)
EXTRUDE 1511          121 FZ(I)=SUMZ-FPUR(IIZ)
EXTRUDE 1512          124 CONTINUE
EXTRUDE 1513          RETURN
EXTRUDE 1514          END

```

```

EXTRUDE 1516          SUBROUTINE INTRPOL (X,Y,U,XX,YY,UU,IFLAG)
EXTRUDE 1517          C
EXTRUDE 1518          C *****
EXTRUDE 1519          C INTERPOLATE THE VALUE OF UU AT COORDINATES (XX,YY) BY KNOWING THE
EXTRUDE 1520          C VALUES OF U AT FOUR SURROUNDING POINTS.
EXTRUDE 1521          C *****
EXTRUDE 1522          C
EXTRUDE 1523          DIMENSION X(4),Y(4),U(4),A(4,4),COEF(4)
EXTRUDE 1524          C
EXTRUDE 1525          C *****
EXTRUDE 1526          C DETERMINE THE MATRIX A, THE INVERSE OF THE INTERPOLATION MATRIX...
EXTRUDE 1527          C IF IFLAG=1, THE A MATRIX IS ALREADY KNOWN
EXTRUDE 1528          C *****
EXTRUDE 1529          C
EXTRUDE 1530          IF(IFLAG.EC.1) GO TO 100
EXTRUDE 1531          X1=X(1)
EXTRUDE 1532          X2=X(2)
EXTRUDE 1533          X3=X(3)
EXTRUDE 1534          X4=X(4)
EXTRUDE 1535          Y1=Y(1)
EXTRUDE 1536          Y2=Y(2)
EXTRUDE 1537          Y3=Y(3)
EXTRUDE 1538          Y4=Y(4)
EXTRUDE 1539          X12=X1-X2
EXTRUDE 1540          X13=X1-X3
EXTRUDE 1541          X14=X1-X4
EXTRUDE 1542          X23=X2-X3
EXTRUDE 1543          X24=X2-X4
EXTRUDE 1544          X34=X3-X4
EXTRUDE 1545          Y12=Y1-Y2*X12
EXTRUDE 1546          Y13=Y1-Y3*X13
EXTRUDE 1547          Y14=Y1-Y4*X14
EXTRUDE 1548          Y23=Y2-Y3*X23
EXTRUDE 1549          Y24=Y2-Y4*X24
EXTRUDE 1550          Y34=Y3-Y4*X34
EXTRUDE 1551          A(1,1)=X2*Y34-X3*Y24+X4*Y23
EXTRUDE 1552          A(1,2)=-X1*Y34+X3*Y14-X4*Y13
EXTRUDE 1553          A(1,3)=X1*Y24-X2*Y14+X4*Y12
EXTRUDE 1554          A(1,4)=-X1*Y23+X2*Y13-X3*Y12
EXTRUDE 1555          A(2,1)=-Y23+Y24-Y34
EXTRUDE 1556          A(2,2)=Y13-Y14+Y34
EXTRUDE 1557          A(2,3)=-Y12+Y14-Y24
EXTRUDE 1558          A(2,4)=Y12-Y13+Y23
EXTRUDE 1559          Z11=Y1*X23
EXTRUDE 1560          Z12=Y1*X24
EXTRUDE 1561          Z13=Y1*X34
EXTRUDE 1562          Z21=Y2*X13
EXTRUDE 1563          Z22=Y2*X14
EXTRUDE 1564          Z23=Y2*X34
EXTRUDE 1565          Z31=Y3*X12
EXTRUDE 1566          Z32=Y3*X14
EXTRUDE 1567          Z33=Y3*X24
EXTRUDE 1568          Z41=Y4*X12
EXTRUDE 1569          Z42=Y4*X13
EXTRUDE 1570          Z43=Y4*X23

```



```

EXTRUDE 1571      A(3,1)=+X2*Z23-X3*Z33+X4*Z43
EXTRUDE 1572      A(3,2)=-X1*Z13+X3*Z22-X4*Z42
EXTRUDE 1573      A(3,3)=+X1*Z12-X2*Z22+X4*Z41
EXTRUDE 1574      A(3,4)=-X1*Z11+X2*Z21-X3*Z31
EXTRUDE 1575      A(4,1)=-Z23+Z33-Z43
EXTRUDE 1576      A(4,2)=+Z13-Z22+Z42
EXTRUDE 1577      A(4,3)=-Z12+Z22-Z41
EXTRUDE 1578      A(4,4)=+Z11-Z21+Z31
EXTRUDE 1579      DETER=A(1,1)+A(1,2)+A(1,3)+A(1,4)
EXTRUDE 1580      100 CONTINUE
EXTRUDE 1581      IFLAG=0
EXTRUDE 1582      IF(DETER.EQ.0.) GO TO 150
EXTRUDE 1583      DO 130 J=1,4
EXTRUDE 1584      COEF(J)=0.
EXTRUDE 1585      DO 120 I=1,4
EXTRUDE 1586      120 COEF(J)=COEF(J)+A(J,I)*U(I)
EXTRUDE 1587      130 COEF(J)=COEF(J)/DETER
EXTRUDE 1588      UU=COEF(1)+COEF(2)*XX+COEF(3)*YY+COEF(4)*XX*YY
EXTRUDE 1589      RETURN
EXTRUDE 1590      150 UU=(U(1)*(YY-Y(2))+U(2)*Y(1)-YY)/(Y(1)-Y(2))
EXTRUDE 1591      RETURN
EXTRUDE 1592      END

```

```

EXTRUDE 1594      SUBROUTINE SYRANS (R,Z,UR,UZ,IEL,EPS,TEPS,STR,X,Y,XARB,U,V,XX,YY,
EXTRUDE 1595      1 A,B,AA,BB,C,EE,NI,NJ,NTIMES,NEL,NNP,NMAX)
EXTRUDE 1596      C
EXTRUDE 1597      C *****
EXTRUDE 1598      C SUBROUTINE FOR DETERMINATION OF FLOW PATTERN, NETWORK OF GRID
EXTRUDE 1599      C DISTORTIONS, THE EFFECTIVE STRAIN DISTRIBUTION AND THE VALUES OF
EXTRUDE 1600      C EFFECTIVE STRAIN FOR EACH ELEMENT.
EXTRUDE 1601      C *****
EXTRUDE 1602      C
EXTRUDE 1603      DIMENSION R(1),Z(1),UR(1),UZ(1),IEL(NEL,1),EPS(5,1),TEPS(5,1),
EXTRUDE 1604      1 STR(NI,1),X(NI,1),Y(1),XARB(1),U(NI,1),V(NI,1),XX(NTIMES,1),
EXTRUDE 1605      2 YY(NTIMES,1),A(1),B(1),AA(NI,1),BB(1),C(1),EE(NTIMES,1)
EXTRUDE 1606      DIMENSION RR(4),ZZ(4),URR(4),UZZ(4)
EXTRUDE 1607      COMMON /STRPATH/ STEP,YSTART,YDIE,YEXIT,YMIN,REITER,REXIT,VEXIT
EXTRUDE 1608      COMMON /WALL/ THETA,FT,TANTH
EXTRUDE 1609      NIM1=NI-1
EXTRUDE 1610      NJM1=NJ-1
EXTRUDE 1611      C
EXTRUDE 1612      C *****
EXTRUDE 1613      C FIRST ARRANGE THE AVAILABLE INFORMATION IN PROPER FORM
EXTRUDE 1614      C *****
EXTRUDE 1615      C
EXTRUDE 1616      K=1
EXTRUDE 1617      L=0
EXTRUDE 1618      100 L=L+1
EXTRUDE 1619      Y(L)=Z(K)
EXTRUDE 1620      DO 110 I=1,NIM1
EXTRUDE 1621      X(I,L)=R(K)
EXTRUDE 1622      U(I,L)=UR(K)
EXTRUDE 1623      V(I,L)=UZ(K)
EXTRUDE 1624      110 K=K+1
EXTRUDE 1625      X(NI,L)=X(NIM1,L)
EXTRUDE 1626      U(NI,L)=U(NIM1,L)
EXTRUDE 1627      V(NI,L)=V(NIM1,L)
EXTRUDE 1628      IF (K.GE.NNP) 150,100
EXTRUDE 1629      C
EXTRUDE 1630      C *****
EXTRUDE 1631      C DETERMINE THE COORDINATES OF THE CENTERS OF THE ELEMENTS
EXTRUDE 1632      C *****
EXTRUDE 1633      C
EXTRUDE 1634      150 DO 160 N=1,NEL
EXTRUDE 1635      I1=IEL(N,1)
EXTRUDE 1636      I2=IEL(N,2)
EXTRUDE 1637      I3=IEL(N,3)
EXTRUDE 1638      I4=IEL(N,4)
EXTRUDE 1639      A(N)=(R(I1)+R(I2)+R(I3)+R(I4))/4.
EXTRUDE 1640      160 B(N)=(Z(I1)+Z(I2)+Z(I3)+Z(I4))/4.
EXTRUDE 1641      C
EXTRUDE 1642      C *****
EXTRUDE 1643      C ARRANGE THE NEWLY DETERMINED VALUES IN A PROPER FORM
EXTRUDE 1644      C *****
EXTRUDE 1645      C
EXTRUDE 1646      K=1
EXTRUDE 1647      L=0
EXTRUDE 1648      165 L=L+1
EXTRUDE 1649      BB(L)=B(K)
EXTRUDE 1650      AA(I,L)=0.
EXTRUDE 1651      STR(I,L)=EPS(5,K)
EXTRUDE 1652      DO 170 I=2,NIM1
EXTRUDE 1653      AA(I,L)=A(K)
EXTRUDE 1654      STR(I,L)=EPS(5,K)

```

```

EXTRUDE 1655      170 K=K+1
EXTRUDE 1656      AA(NI,L)=REXIT+BB(L)*TANTH
EXTRUDE 1657      IF(BB(L).GT.VDIE) AA(NI,L)=1.
EXTRUDE 1658      IF(BB(L).LT.VEXIT) AA(NI,L)=REXIT
EXTRUDE 1659      STR(NI,L)=EPS(5,K-1)
EXTRUDE 1660      IF(K.LT.NEL) GO TO 165
EXTRUDE 1661      C
EXTRUDE 1662      C *****
EXTRUDE 1663      C NOW DO THE INTERPOLATION AND DETERMINE THE FLOW PATTERN
EXTRUDE 1664      C *****
EXTRUDE 1665      C
EXTRUDE 1666      DO 500 N=1,NTIMES
EXTRUDE 1667      C
EXTRUDE 1668      C *****
EXTRUDE 1669      C SET THE COORDINATES OF THE STARTING POINT
EXTRUDE 1670      C *****
EXTRUDE 1671      C
EXTRUDE 1672      XX(N,1)=C(N)
EXTRUDE 1673      YY(N,1)=VSTART
EXTRUDE 1674      C
EXTRUDE 1675      C *****
EXTRUDE 1676      C DETERMINE THE LOCATION OF THE PRESENT COORDINATES OF THE POINT IN
EXTRUDE 1677      C TERMS OF THE FOUR SURROUNDING NODAL POINTS
EXTRUDE 1678      C *****
EXTRUDE 1679      C
EXTRUDE 1680      IFLAG=0
EXTRUDE 1681      NCOUNT=0
EXTRUDE 1682      MOLD=1
EXTRUDE 1683      LOLD=1
EXTRUDE 1684      210 NCOUNT=NCOUNT+1
EXTRUDE 1685      XXX=XX(N,NCOUNT)
EXTRUDE 1686      YYY=YY(N,NCOUNT)
EXTRUDE 1687      IF(N.EQ.NTIMES.AND.YYY.LE.VEXIT) GO TO 300
EXTRUDE 1688      IF(YYY.LE.YMIN) GO TO 300
EXTRUDE 1689      DO 220 I=MOLD,NJM
EXTRUDE 1690      220 IF(YYY.LE.V(I).AND.YYY.GE.V(I+1)) M=I
EXTRUDE 1691      DO 230 I=1,M
EXTRUDE 1692      230 XARB(I)=X(I,M)-(X(I,M)-X(I,M+1))*(Y(M)-YYY)/(Y(M)-Y(M+1))
EXTRUDE 1693      DO 240 I=1,NIM
EXTRUDE 1694      240 IF(XXX.GE.XARB(I).AND.XXX.LE.XARB(I+1)) L=I
EXTRUDE 1695      IF(NCOUNT.EQ.1) GO TO 250
EXTRUDE 1696      IF(M.EQ.MOLD.AND.L.EQ.LOLD) GO TO 260
EXTRUDE 1697      250 RR(1)=X(L,M)
EXTRUDE 1698      RR(2)=X(L,M+1)
EXTRUDE 1699      RR(3)=X(L+1,M+1)
EXTRUDE 1700      RR(4)=X(L+1,M)
EXTRUDE 1701      ZZ(1)=ZZ(4)=V(M)
EXTRUDE 1702      ZZ(2)=ZZ(3)=V(M+1)
EXTRUDE 1703      URR(1)=U(L,M)
EXTRUDE 1704      URR(2)=U(L,M+1)
EXTRUDE 1705      URR(3)=U(L+1,M+1)
EXTRUDE 1706      URR(4)=U(L+1,M)
EXTRUDE 1707      UZZ(1)=V(L,M)
EXTRUDE 1708      UZZ(2)=V(L,M+1)
EXTRUDE 1709      UZZ(3)=V(L+1,M+1)
EXTRUDE 1710      UZZ(4)=V(L+1,M)
EXTRUDE 1711      GO TO 270
EXTRUDE 1712      C
EXTRUDE 1713      C *****
EXTRUDE 1714      C THE POINT IS LOCATED IN THE SAME ELEMENT AS IT WAS FOR THE LAST STEP.
EXTRUDE 1715      C HENCE THE INVERSE OF THE INTERPOLATION MATRIX IS ALREADY KNOWN
EXTRUDE 1716      C *****
EXTRUDE 1717      C
EXTRUDE 1718      260 IFLAG=1
EXTRUDE 1719      C
EXTRUDE 1720      C *****
EXTRUDE 1721      C DETERMINE U AND V AT THE POINT ON FLOW LINE BY INTERPOLATION.
EXTRUDE 1722      C *****
EXTRUDE 1723      C
EXTRUDE 1724      270 CALL INTRPOL(RR,ZZ,URR,XXX,YYY,UU,IFLAG)
EXTRUDE 1725      IFLAG=1
EXTRUDE 1726      CALL INTRPOL(PP,ZZ,UZZ,XXX,YYY,VV,IFLAG)
EXTRUDE 1727      C
EXTRUDE 1728      C *****
EXTRUDE 1729      C DETERMINE THE NEXT LOCATION OF POINT ON FLOW LINE
EXTRUDE 1730      C *****
EXTRUDE 1731      C
EXTRUDE 1732      XX(N,NCOUNT+1)=XXX+UU*STEP
EXTRUDE 1733      YY(N,NCOUNT+1)=YYY+VV*STEP
EXTRUDE 1734      LOLD=L
EXTRUDE 1735      MOLD=M
EXTRUDE 1736      IF(N.EQ.NTIMES) GO TO 310
EXTRUDE 1737      XXX=REXIT+YY(N,NCOUNT+1)*TANTH
EXTRUDE 1738      IF(XXX.LT.XX(N,NCOUNT+1)) XX(N,NCOUNT+1)=XXX
EXTRUDE 1739      IF(XX(N,NCOUNT+1).GT.1.) XX(N,NCOUNT+1)=1.
EXTRUDE 1740      GO TO 310

```



```

EXTRUDE 1741 C
EXTRUDE 1742 C *****
EXTRUDE 1743 C THE POINT IS MOVING WITH EXIT VELOCITY
EXTRUDE 1744 C *****
EXTRUDE 1745 C
EXTRUDE 1746 300 XX(N,NCOUNT+1)=XXX
EXTRUDE 1747 YY(N,NCOUNT+1)=YYY+VEXIT*STEP
EXTRUDE 1748 310 IF(NCOUNT.LT.NMAX-1) GC TO 210
EXTRUDE 1749 C
EXTRUDE 1750 C *****
EXTRUDE 1751 C DETERMINE THE VALUES OF EFFECTIVE STRAIN AT EACH POINT FOR ALL FLOW
EXTRUDE 1752 C LINES
EXTRUDE 1753 C *****
EXTRUDE 1754 C
EXTRUDE 1755 NCCUNT=0
EXTRUDE 1756 EE(N,1)=0.
EXTRUDE 1757 MOLD=LOLD=1
EXTRUDE 1758 400 NCCUNT=NCOUNT+1
EXTRUDE 1759 YYY=YY(N,NCOUNT)
EXTRUDE 1760 XXX=XX(N,NCOUNT)
EXTRUDE 1761 IF(YYY.LE.VEXIT) GO TO 480
EXTRUDE 1762 C
EXTRUDE 1763 C *****
EXTRUDE 1764 C DETERMINE THE LOCATION OF FOUR SURROUNDING ELEMENT CENTERS.
EXTRUDE 1765 C *****
EXTRUDE 1766 C
EXTRUDE 1767 NJM11=NJM1-1
EXTRUDE 1768 DO 410 I=MOLD,NJM11
EXTRUDE 1769 410 IF(YYY.LE.RB(I).AND.YYY.GE.RB(I+1)) M=I
EXTRUDE 1770 DO 420 I=1,N1
EXTRUDE 1771 420 XARB(I)=AA(I,M)-(AA(I,M)-AA(I,M+1))*(RB(M)-YYY)/(RB(M)-RB(M+1))
EXTRUDE 1772 DO 430 I=1,N1M1
EXTRUDE 1773 430 IF(XXX.GE.XARB(I).AND.XXX.LE.XARB(I+1)) L=I
EXTRUDE 1774 IF(NCCUNT.EQ.1) GO TO 450
EXTRUDE 1775 IF(M.EQ.MOLD.ANC.L.EQ.LOLD) GO TO 460
EXTRUDE 1776 C
EXTRUDE 1777 C *****
EXTRUDE 1778 C INTERPOLATE THE VALUES OF STRAIN-RATES.
EXTRUDE 1779 C *****
EXTRUDE 1780 C
EXTRUDE 1781 450 RR(1)=AA(L,M)
EXTRUDE 1782 RR(2)=AA(L,M+1)
EXTRUDE 1783 RR(3)=AA(L+1,M+1)
EXTRUDE 1784 RR(4)=AA(L+1,M)
EXTRUDE 1785 ZZ(1)=ZZ(4)=RB(M)
EXTRUDE 1786 ZZ(2)=ZZ(3)=RB(M+1)
EXTRUDE 1787 URR(1)=STR(L,M)
EXTRUDE 1788 URR(2)=STR(L,M+1)
EXTRUDE 1789 URR(3)=STR(L+1,M+1)
EXTRUDE 1790 UPR(4)=STR(L+1,M)
EXTRUDE 1791 GO TO 470
EXTRUDE 1792 460 IFLAG=1
EXTRUDE 1793 470 CALL INTRPOL(FR,ZZ,URR,XXX,YYY,ESTEP,IFLAG)
EXTRUDE 1794 C
EXTRUDE 1795 C *****
EXTRUDE 1796 C ADD THE INTERPOLATED STRAIN-RATE INCREMENTALLY TO THE VALUE OF
EXTRUDE 1797 C EFFECTIVE STRAIN AT PREVIOUS LOCATION TO DETERMINE THE EFFECTIVE
EXTRUDE 1798 C STRAIN AT NEW LOCATION.
EXTRUDE 1799 C *****
EXTRUDE 1800 C
EXTRUDE 1801 EE(N,NCOUNT+1)=EE(N,NCCUNT)+ESTEP*STEP
EXTRUDE 1802 LOLD=L
EXTRUDE 1803 MOLD=M
EXTRUDE 1804 GO TO 490
EXTRUDE 1805 480 EE(N,NCOUNT+1)=EE(N,NCOUNT)
EXTRUDE 1806 490 IF(NCOUNT.LT.NMAX-1) GC TO 400
EXTRUDE 1807 500 CONTINUE
EXTRUDE 1808 C
EXTRUDE 1809 C *****
EXTRUDE 1810 C INTERPOLATE THE EFFECTIVE STRAIN DISTRIBUTION FOR ELEMENTS FROM VALUE
EXTRUDE 1811 C OF EFFECTIVE STRAINS ALONG FLOW LINES.
EXTRUDE 1812 C *****
EXTRUDE 1813 C
EXTRUDE 1814 DO 700 N=1,NEL
EXTRUDE 1815 IF(R(N).GT.YY(1,1)) GC TO 550
EXTRUDE 1816 DO 550 J=2,NTIMES
EXTRUDE 1817 DO 520 I=1,NMAX
EXTRUDE 1818 IF(B(N).LT.YY(J,1)) GO TO 520
EXTRUDE 1819 L=I
EXTRUDE 1820 GO TO 530
EXTRUDE 1821 520 CONTINUE
EXTRUDE 1822 530 IF(XX(J,L).LT.A(N)) GO TO 550
EXTRUDE 1823 K=J
EXTRUDE 1824 GO TO 540
EXTRUDE 1825 550 CONTINUE

```

```

EXTRUDE 1826      560 IFLAG=0
EXTRUDE 1827      RR(1)=XX(K-1,L)
EXTRUDE 1828      RR(2)=XX(K-1,L-1)
EXTRUDE 1829      RR(3)=XX(K,L-1)
EXTRUDE 1830      RR(4)=XX(K,L)
EXTRUDE 1831      ZZ(1)=YY(K-1,L)
EXTRUDE 1832      ZZ(2)=YY(K-1,L-1)
EXTRUDE 1833      ZZ(3)=YY(K,L-1)
EXTRUDE 1834      ZZ(4)=YY(K,L)
EXTRUDE 1835      URR(1)=EE(K-1,L)
EXTRUDE 1836      URR(2)=EE(K-1,L-1)
EXTRUDE 1837      URR(3)=EE(K,L-1)
EXTRUDE 1838      URR(4)=EE(K,L)
EXTRUDE 1839      CALL INTRPOL (RR,ZZ,URR,A(N),B(N),TEPS(S,N),IFLAG)
EXTRUDE 1840      GO TO 700
EXTRUDE 1841      650 TEPS(S,N)=0.
EXTRUDE 1842      700 CONTINUE
EXTRUDE 1843      C
EXTRUDE 1844      RETURN
EXTRUDE 1845      END

```